



Ngowo, Halfan (2023) *Quantifying the ecology of Anopheles funestus and its implications for improved malaria control*. PhD thesis.

<https://theses.gla.ac.uk/83371/>

Copyright and moral rights for this work are retained by the author

A copy can be downloaded for personal non-commercial research or study, without prior permission or charge

This work cannot be reproduced or quoted extensively from without first obtaining permission in writing from the author

The content must not be changed in any way or sold commercially in any format or medium without the formal permission of the author

When referring to this work, full bibliographic details including the author, title, awarding institution and date of the thesis must be given

Enlighten: Theses

<https://theses.gla.ac.uk/>
research-enlighten@glasgow.ac.uk



College of Medical, Veterinary and Life Science

School of Life Sciences

School of Biodiversity, One Health & Veterinary Medicine

**Quantifying the ecology of *Anopheles funestus* and its
implications for improved malaria control**

Submitted in fulfillment of the requirements for the degree of

Doctor of Philosophy

By

Halfan Ngowo

Submitted on 8th July, 2020 to University of Glasgow

Abstract

The malaria burden is highest in African countries where more than 95% of deaths and cases occur. There was a consistent decline in malaria deaths and cases in Africa between 2000 and 2015 but progress has since stalled. Due to biological changes in vector populations, notably insecticide resistance and behavioral adaptations such as outdoor-biting, the primary vector control measures are no longer as successful as they once were. In recent years, mosquito species considered to be the primary vector of malaria, (e.g. *Anopheles gambiae* s.s) have declined, and even disappeared from some communities. In settings such as rural south-eastern Tanzania, the residual transmission is now being maintained by *An. funestus* followed by *An. arabiensis*.

Currently, *An. funestus* mediates a high proportion of malaria transmission events in east and southern Africa. The resilience of this vector may be linked to its high insecticide resistance; though recent evidence suggests that it may also be capable of shifting its biting behaviors to avoid contact with insecticidal interventions. Yet, our ability to tackle this vector species is impeded by the limited knowledge of its basic ecology and population dynamics, the difficulties in colonizing it under laboratory conditions and the many uncertainties about appropriate surveillance approaches.

The overall aim of this PhD project was to quantify the ecology of *An. funestus* mosquitoes in Tanzania and assess the implications of its key attributes for improved malaria control in settings such as Tanzania where the vector species dominates. The work involved the following steps: 1) quantifying the fitness and behavioral attributes of wild *An. funestus* and their offspring during repeated colonization attempts under standard laboratory conditions, 2) developing and validating a framework for predicting human biting exposures from different exposure-free sampling methods, 3) developing and testing a population dynamics model to describe the ecology of the wild *An. funestus* populations, and 4) assessing the generalizability of the population dynamics model and its ability to reconstruct missing data.

To achieve the first objective, I attempted to colonize a local population of *An. funestus* s.s. from southeastern Tanzania and assessed the key barriers which

hinder laboratory establishment. Adult females (F_0) from three wild *An. funestus* populations were brought into the laboratory for rearing. Their fecundity, and the development, survival, body size and mating success of their F_1 offspring were measured to evaluate their fitness under laboratory conditions. While adult survival was relatively high, the mating success, poor hatching rate and poor larval survival and extended larval development periods were identified as key barriers to establishing a colony in the laboratory. Due to these factors, this colony was not sustained beyond the F_1 generation in the laboratory, but the lessons were deployed for a subsequent and more successful colonization effort.

To address the second objective, I analyzed data comparing the outdoor catch rates of *An. funestus* using six exposure-free trapping methods relative to the human landing catches (HLC), the gold standard method for estimating human exposures to mosquito bites. I tested different models for the relationship between HLC and other trapping methods while allowing flexibility for associations to be impacted by interspecific and intraspecific density dependence. This analysis indicated that the association between catches in alternative traps and the HLC can best be explained by simple linear models; with minimal impact of intra and inter specific density dependence. A shiny app interface was developed to allow expanded use of this statistical calibration framework for future estimations of malaria vector biting risk in communities.

For the third objective, I used the demographic parameters generated from the colonization attempt (described above) and published literature, to develop the first population dynamics model of wild *An. funestus* in Tanzania. I used a Bayesian framework to develop a state-space model and reconstruct the observed population dynamics of this species. I then used this model to assess the strength of evidence for intrinsic (density dependence) and extrinsic (environmental covariates) drivers of *An. funestus* population dynamics and how they drive seasonality in abundance and demographic variables (development periods and survival). This analysis indicated that density dependence has a minimal contribution on the overall dynamics of *An. funestus* in these settings. Daily larval and adult survival probabilities were marginally affected by changes in environmental covariates (temperature and rainfall), suggesting there is little seasonality in these fitness parameters. This study also revealed that *An.*

funestus may be essential for sustaining year-round malaria transmission in settings such as rural south-eastern Tanzania.

Finally, I interrogated the generalizability and sensitivity of this modelling framework for *An. funestus* by assessing its ability to predict missing time series data. Here, I refitted the model to a single population and assessed any unexplained features of population dynamics which is causing the density dependence to have small contributions. I also omitted portions of the time series data to assess model prediction capability. For example I first removed 25% and then 50% of the data, then reconstructed the missing sections. The single population model indicated that *An. funestus* demographic variables were much more sensitive to changes in environmental covariates compared to the preceding hierarchical model; suggesting that clear signals of environmental drivers may be lost by fitting the model to multiple populations that may have distinct drivers. The model was able to reconstruct the observed population trajectory poorly when 50% of the data was removed as compared to when 25% was removed. Overall, the model was only able to predict for the missing data if the training set included some representation of data from both dry and wet seasons.

In conclusion, this PhD work contributes to a general understanding of the key barriers to colonization and the population dynamics of *An. funestus*. While *An. funestus* was not successfully colonised in this study, the lessons learned by documenting which fitness traits are impeded in the laboratory led to progress in further work at the Ifakara Health Institute, where a stable colony of *An. funestus* has now been established. Additionally, the model of *An. funestus* dynamics and demography developed here will underpin further research to evaluate and select optimal vector control packages for crashing these populations in southern Tanzania and other settings where they are the major source of residual malaria transmission.

Table of Contents

Abstract	2
Table of Contents	5
List of Tables.....	9
List of Figures	11
Acknowledgements.....	14
Author’s Declaration	16
List of Abbreviations	17
1.0 Chapter 1: General Introduction.....	18
1.0 Global burden	18
1.1 Malaria biology and pathology	19
1.2 Mosquito life cycle	20
1.3 African malaria vectors	22
1.4 Vector Surveillance.....	25
1.5 Population dynamics model of malaria vectors	26
1.6 Vector control interventions.....	29
1.7 Research focus	31
1.8 Objectives and outline.....	32
2.0 Chapter 2: Fitness characteristics of the malaria vector <i>Anopheles funestus</i> during an attempted laboratory colonization	35
Abstract	35
2.0 Background	37
2.1 Methods	39
2.1.1 Study area	39
2.1.2 Mosquito sampling.....	40
2.1.3 Laboratory maintenance and fitness measurements for FUTAZ mosquitoes	40
2.1.4 Laboratory maintenance and fitness measurements for FUMUZ mosquitoes	42
2.1.5 Mosquito wing size measurements	43
2.1.6 Statistical analysis.....	45
2.2 Results	46
2.2.1 Mosquito wing lengths, mating status, fecundity and pupation	46
2.2.2 Adult survival.....	49

2.3	Discussion	51
2.4	Conclusions	55
3.0	Chapter 3: A statistical calibration tool for methods used to sample outdoor-biting mosquitoes	56
	Abstract	56
3.0	Background	58
3.1	Methods	60
3.1.1	Study area and vector species	60
3.1.2	Data collection.....	60
3.1.3	Model fitting.....	61
3.1.4	Interactive calibration tool	64
3.2	Results	65
3.2.1	<i>Anopheles arabiensis</i>	68
3.2.2	<i>Anopheles funestus</i>	70
3.2.3	<i>Culex</i> species.....	73
3.2.4	Interactive calibration tool	73
3.3	Discussion	74
3.4	Conclusion	77
4.0	Chapter 4: Using Bayesian state-space models to understand the population dynamics of the dominant malaria vector, <i>Anopheles funestus</i> in rural Tanzania	78
	Abstract	78
4.1	Background	80
4.2	Methods	82
4.2.1	Time series data on wild <i>An. funestus</i> populations	82
4.2.2	Prior information on life-history and gonotrophic cycle stages.....	84
4.2.3	Biological process components of the Bayesian SSMs	85
4.2.4	Observation-derived components of the Bayesian SSMs	90
4.2.5	Model selection, model fitting and outputs	92
4.3	Results	92
4.3.1	Population trajectories and seasonal trends	92
4.3.2	Survival and fecundity	93
4.3.3	Effects of density dependence	97
4.4	Discussion	104
4.5	Conclusions	108

5.0	Chapter 5: Density dependence and demography alone cannot explain explosive dynamics in <i>Anopheles funestus</i>	109
	Abstract	109
5.1	Background	111
5.2	Methods	113
5.2.1	Population dynamic model	113
5.2.2	Model fitting and diagnosis.....	115
5.3	Results	115
5.3.1	Generalizability of inferences from a single population and hierarchical model	115
5.3.2	Unexplained drivers of population dynamics	120
5.3.3	Ability of the model to predict missing seasonal data	121
5.4	Discussion	124
5.5	Conclusion:	127
6.0	Chapter 6: General Discussion	128
6.1	Overview of the main findings.....	128
6.1.1	Fitness characteristics and colonization barriers	128
6.1.2	Surveillance methods of outdoor vectors of malaria transmission .	129
6.1.3	Drivers of population dynamics of wild <i>Anopheles funestus</i>	130
6.1.4	Generalizability of population dynamics models	132
6.2	Questions arising.....	133
6.3	Implications of the findings	135
6.3.1	<i>Anopheles funestus</i> colonization bottlenecks	135
6.3.2	Reliability of the mosquito sampling tools.....	136
6.3.3	Model parameterization and validation	137
6.3.4	Selection of optimal vector control package	138
6.4	Limitations of the study	138
6.5	Further work	140
6.6	Conclusions	141
7.0	Chapter 7: Addendum of Chapter 3	143
7.1	Rationale	143
7.2	Model fitting	143
7.3	Interactive calibration tool	146
7.4	Results summary.....	146
7.5	Conclusion	154

8.0	Appendices.....	155
8.1	Appendix 1: Shiny App Interfaces.....	155
8.1.1	Shiny App dashboard showing one example of a linear relationship (model 1) between HLC and an alternative trap (i.e., MTC) for <i>Culex</i> spp ...	155
8.1.2	Shiny App dashboard showing one example of a saturation effect (model 2) between HLC and an alternative trap (i.e., MTC) for <i>Culex</i> spp ...	156
8.1.3	Shiny App dashboard showing one example of a model which account for other species (model 3) between HLC and an alternative trap (i.e., MTC) for <i>Culex</i> spp	157
9	References.....	158

List of Tables

Table 2.1: Descriptions of terms used and strains compared as used in this study	44
Table 2.2: Relative odds (OR) and means of insemination, sex ratio, pupation and adult emergence for different strains of <i>Anopheles funestus</i> , number in brackets are 95% confidence intervals with their respective p-values.	48
Table 2.3: Relative rate (RR) and means of fecundity for different strains of <i>Anopheles funestus</i> , number in brackets are 95% confidence intervals.	48
Table 2.4: Hazard Ratio and median values of the adult survival between males and females of the F ₁ -FUTAZ and FUMOZ, associated p-values indicate the significance difference of sex and species on the number of days survived by F ₁ -FUTAZ and FUMOZ strains.	50
Table 3.1: Description of models used to investigate the relationships between female mosquito catches by human landing catch and the alternative traps. ...	63
Table 3.2: Summary of all other mosquitoes collected for each trap type including the Human Landing Catches (HLC)	66
Table 3.3: Summary (R ² and DIC values) of models used to investigate the relationship between the numbers of female mosquitoes collected with human landing catch (HLC) and the six alternative outdoor traps. See Table 1 for description of models.	69
Table 3.4: Predicted values for estimating the expected mosquito catches by human landing catch and alternative traps, according to the linear model (Model 1). Numbers in the first column refer to the mosquitoes collected with a given trap. To obtain the estimate of the equivalent number that one would collect with HLC, refer to the column corresponding to the trap itself. Numbers in brackets are (95% credible intervals).	71
Table 4.1: Priors as used in the state-space population models of <i>Anopheles funestus</i> and the estimated posteriors mean and 95% credible intervals. Day $d - 1$ was considered as a unit of time in this modelling development.	94
Table 4.2: Priors for the intrinsic and extrinsic drivers of the population dynamic as used in the state-space model of <i>Anopheles funestus</i> and the estimated posteriors mean and 95% credible intervals.	100

Table 4.3: Model selection: Description of all models fitted with and without environmental covariates and their corresponding delta-Deviance Information Criterion Δ DIC102

Table 5.1: Posterior means for the intrinsic and extrinsic drivers of the population dynamic as estimated by the state space model in [153] and the refitted single population model for *Anopheles funestus* and their respective means and 95% credible intervals.118

Table 7.1: Description of models used to investigate the relationships between female mosquito catches by human landing catch and alternative traps. 145

Table 7.2: Coefficients of each parameter (β_1, β_2) used to explain the relationship between HLC catches and alternative traps for all the four models.148

Table 7.3: Summary (R^2 , DIC and RMSE values) of models used to investigate the relationship between the numbers of female mosquitoes collected with human landing catch (HLC) and the six alternative outdoor traps. See Table 6.1 for description and models formulation.149

Table 7.4: Predicted values for estimating the expected mosquito catches by human landing catch and alternative traps, according to the linear model (Model 1). Numbers in the first column refer to the mosquitoes collected with a given trap. To obtain the estimate of the equivalent number that one would collect with HLC, refer to the column corresponding to the trap itself. Numbers in brackets are (95% credible intervals).....150

List of Figures

- Figure 1.1:** A global map of dominant vectors of malaria transmission [69]. 23
- Figure 2.1:** A map of study area showing the location of the villages where *Anopheles funestus* females (wild-FUTAZ) were sampled for colonization experiments. 39
- Figure 2.2:** Images of laboratory set-up for the colonization process: 41
- Figure 2.3:** Microscopic images of different parts of *Anopheles funestus*: 45
- Figure 3.1:** Illustration of models used to investigate the relationship between number of female mosquitoes collected with human landing catch and six alternative traps..... 64
- Figure 3.2:** Expected number of female *Culex spp.* mosquitoes collected with HLC (y-axis), given the number of females collected with alternative traps (x-axis). Continuous line is the prediction of a Gamma-Poisson model assuming a linear relationship; dashed lines are 95% credible intervals. 66
- Figure 3.3:** Expected number of female *Anopheles arabiensis* mosquitoes collected with HLC (y-axis), given the number of females collected with alternative traps (x-axis). Continuous line is the prediction of a Gamma-Poisson model assuming a linear relationship; dashed lines are 95% credible intervals. . 67
- Figure 3.4:** Expected number of female *Anopheles funestus* mosquitoes collected with HLC (y-axis), given the number of females collected with alternative traps (x-axis). Continuous line is the prediction of a Gamma-Poisson model assuming a linear relationship; dashed lines are 95% credible intervals. . 68
- Figure 4.1:** A map depicting the locations of various study villages where mosquito sampling was carried out in 2015-2016 and 2018-2019. 83
- Figure 4.2:** Schematic representation of the state-space population model showing different life stages compartment (circles) and flows (arrows) of *Anopheles funestus*. 85
- Figure 4.3:** Reconstruction of the abundance trajectories for all the six life-stages. The red line indicates the mean posterior values and the respective 95% confidence intervals are shown in “sky-blue”. Left column (a,c,e,g,i,k) is data collected from June 2018 to May 2019 and right column (b,d,f,h,j,l) is data collected from Jan-Dec 2015. The grey area indicates the period with rainfall. 96
- Figure 4.4:** Observed vs. model estimated values for the three adult stages with data collected using CDC light trap both in May 2018 -June 2019 (left column-

a,c,d) and Jan-Dec 2015 (right column- b,d,e). Red lines are the model estimated trajectories with “sky-blue” showing their 95% credible intervals. The blue circles are the observed values from the Light trap catches. Grey areas are the periods with rainfalls episodes. 97

Figure 4.5: Reconstruction of the survival trajectories for all the four stages (larvae, unfed, bloodfed, and gravid) which were affected by the environmental covariates. The two bottom rows show the larval development period and fecundity trends. Left column (a,c,e,g,i,k) is trajectories from June 2018 to May 2019 and right column (b,d,f,h,j,l) is from Jan-Dec 2015. Grey area is the period with rainfall. Y-axis shows the survival rates of different life stages and the bottom row (k&l) shows per-capita fecundity 98

Figure 4.6: Relationship between environmental covariates and fitness parameters as estimated from the SSMs of population dynamic of *Anopheles funestus*..... 99

Figure 4.7: Goodness of fit: Observed versus predicted unfed, bloodfed and gravid densities across all populations. Adjusted R-squared, intercept and slope values are from a linear model of the predicted against observed values. Dotted lines correspond to 1:1 line. Left column (a,c,d) is data collected from June 2018 to May 2019 and right column (b,d,e) is data from Jan-Dec 2015. 103

Figure 5.1: Reconstruction of the abundance trajectories of the six mosquito life-stages (eggs, larvae, pupae, unfed, bloodfed and gravid) from the SSM fitted to a single population. The red line indicates the mean posterior values and the respective 95% credible intervals are shown in “sky-blue”. The grey-shaded region indicates periods with rainfall. 116

Figure 5.2: The survival trajectories of *An. funestus* from a wild population in Tanzania as estimated by the SSM model for the four life stages (larvae, unfed, blood-fed and gravid) mosquitoes. The bottom row shows the larval development rate and fecundity trends over time. The red line indicates the mean posterior values and the respective 95% credible intervals are shown in “sky-blue”. The grey shaded region indicates periods with rainfall. 119

Figure 5.3: The influence of environmental covariates on the demographic parameters as estimated from the single population dynamics model of wild *An. funestus*..... 120

Figure 5.4: Abundance trajectories showing the prediction of the 25% missing data at the end. The vertical red dotted lines corresponds to missing data (25%)

which were removed during model fitting and allow the model to predict. The red line indicates the mean posterior values and the respective 95% credible intervals are shown in “sky-blue”. The grey shaded region indicates periods with rainfall.122

Figure 5.5: Abundance trajectories showing the prediction of the 50% missing data at the end. The vertical red dotted lines corresponds to missing data (50%) which were removed during model fitting and allow the model to predict. The red line indicates the mean posterior values and the respective 95% credible intervals are shown in “sky-blue”. The grey shaded region indicates period with rainfall.123

Figure 5.6: Observed vs. model estimated values for the three adult stages with data collected using CDC light trap both in May 2018 -June 2019. Red lines are the model estimated trajectories with “sky-blue” showing their 95% credible intervals. The blue circles are the observed values from the Light trap catches. Grey areas are the periods with rainfalls episodes.124

Figure 7.1: Expected number of female *Culex* spp. mosquitoes collected with HLC (y-axis), given the number of females collected with alternative traps (x-axis). Continuous line is the prediction of a normal distribution model assuming a linear relationship; dashed lines are 95% credible intervals and black circles are the actual observed values.....152

Figure 7.2: Expected number of female *Anopheles arabiensis* mosquitoes collected with HLC (y-axis), given the number of females collected with alternative traps (x-axis). Continuous line is the prediction of a normal distribution model assuming a linear relationship; dashed lines are 95% credible intervals and black circles are the actual observed values.153

Figure 7.3: Expected number of female *Anopheles funestus* mosquitoes collected with HLC (y-axis), given the number of females collected with alternative traps (x-axis). Continuous line is the prediction of a normal distribution model assuming a linear relationship; dashed lines are 95% credible intervals and black circles are the actual observed values.154

Acknowledgements

This whole PhD turned out to be so much more than expected in the beginning. The flexibility of my supervisors to allow me to spend part of my time in Tanzania for field work and additional time in Glasgow was incredible. Despite the disruption with COVID-19 pandemic in the middle of my PhD (2nd and 3rd year), I have finally managed to complete without delay. This wouldn't have been possible without immense continuous support from my supervisors and colleagues both and at the University of Glasgow and Ifakara Health Institute.

Above all, I want to sincerely thank Heather Ferguson for being a tremendously supportive and wonderful supervisor. My future career will benefit greatly from the many lessons she helped me understand through her advice and constant push to seek improvement. My deepest gratitude also belong to Fredros Okumu for providing me with an opportunity to work with him in his research group for many years until we secured a PhD position at the University of Glasgow. His constant push and great ambition for a future without malaria burden drove the need to start and complete this work. I will forever be grateful for his mentorship which goes beyond the PhD supervisor. My sincerely thanks to Jason Matthiopoulos who shaped my quantitative reasoning and thinking skills to a large extent. He has tirelessly trained me to become a competent quantitative ecologist in the field of malaria and vector control. Thanks for having trust in me from the very beginning and agreeing to be one of my PhD supervisors and the stats mentor. I know there are still lots things to continue working on from where we ended for this project, but I am finishing my PhD with lots of quantitative skills than what I was expecting at the start of PhD. Luca Nelli!! Thank you so very much for all the countless support and for always having an open door for many of my stats problems. You have always set aside a time slot on your very busy schedule just to listen to my coding problems when they happen. I am also very grateful to my two examiners for their constructive feedback during the *viva-voce*, Paul Johnson from University of Glasgow and David Smith from University of Washington.

I would also like to extend by gratitude to the colleagues at Ifakara Health Institute for their support and contributions towards the completion of this PhD, I am thankful to all members of Outdoor Mosquito Control group ("OMC"). All of my PhD research activities have received support both logistically and financially

from this group which is led by Fredros Okumu and myself at Ifakara. I am also thankful to colleagues and friends at the University of Glasgow who has set aside their time just to listen to my problems and provided support. A special credit goes to members of Jason's group who convene for one hour every Tuesday to discuss random stats problems. I have always benefited from this. I am also grateful to all members of the "*vectors and malaria group*" group which is led by Francesco Baldini and Heather Ferguson at University of Glasgow.

I am endlessly gratefully to my parents for seeing the value of education by sending me to school when they have an opportunity to do so. I thank them for their continuous support and encouragement during my PhD period.

To my family, Pilly Azizi and our two little children I owe you all my time. It's always not easy being away from the family especially when you have children who need constant parent attention. Pilly, you have been an unbelievably wonderful partner to me throughout my PhD time, thank you for all the support and caring. Even without knowing the extent of my problem, you have always been there day-in-day out 24/7 with a pure heart full of love and care. Thank you so much!

Finally, I am gratefully to the financial support from the Bill and Melinda Gates Foundation (BGMF) and the Howard Hughes Medical Institute (HHMI). I further would like to acknowledge received Travel Funds from the American Society of Tropical Medicine (ASTMH) to attend one of the Annual international meetings and share my research work.

Author's Declaration

I hereby declare that the work written in this thesis is entirely my own, except where otherwise stated. I honestly recognized the contributions of laboratory and field technicians, volunteers and the co-authorship of my supervisors, Professor Heather Ferguson, Professor Jason Matthiopoulos, Dr. Fredros Okumu and Dr. Luca Nelli. I further declare that, no part of this work has been submitted as part of any other degree.

List of Abbreviations

BGS: Biogents Sentinel Trap
CDC-LT: Centre for Disease Light Trap
DIC: Deviance Information Criterion
EIR: Entomological Inoculation Rate
FANG: Funestus Angola
FUMOZ: Funestus Mozambique
FUTAZ: Funestus Tanzania
GLMM: Generalized Linear Mixed Models
GUI: Graphical User Interface
HBR: Human Biting Rate
HDT: Host Decoy Trap
HLC: Human Landing Catch
IHI: Ifakara Health Institute
IRS: Indoor Residual Spray
ITN: Insecticide Treated Nets
ITT-C: Ifakara Tent Trap-Type C
JAGS: Just Another Gibbs Sampler
LRT: Likelihood Ratio Test
LSM: Larval Source Management
MCMC: Markov Chain Monte Carlo
MET: Mosquito Electrocuting Trap
MMX: Mosquito Magnet Trap
MTR: M-Trap
MTRC: M-Trap with CDC
NMCP: National Malaria Control Program
PCR: Polymerase Chain Reaction
s.l: *Sensu lato*
SNP: School Net Program
s.s: *Sensu stricto*
SSM: State-Space Model
SUN: Suna Trap
TMIS: Tanzania Malaria Indicator Survey
VCRL: Vector Control Research Laboratory
WHO: World Health Organization

1.0 Chapter 1: General Introduction

1.0 Global burden

In 2020, there were estimated to be around 241 million malaria cases and 627,000 deaths worldwide; with the burden spread across 85 countries [1]. The malaria burden is highest in African countries (Sub-Saharan) where 96% of total deaths and 95% of the total global cases occur [1]. Despite a significant decrease in malaria deaths over the last two decades (2000-2020), with annual deaths falling from 896,000 to 627,000, the disease continues to pose a significant public health problem [1]. In Africa, there has been a consistent decline in malaria deaths between 2000 and 2015 [2], but since then progress has flattened with cases even rising in some countries [3]. Several factors have been attributed to this slowing and reversal of progress, including a lack of sufficient resources (i.e. funding), insecticide resistance etc.

In combination, these factors are hindering progress towards elimination and control of malaria [4]. Overcoming this set back will require new funding and new tools to tackle malaria [5,6]. Recently a vaccine against malaria, RTS,S/AS01 (RTS,S), was approved for use by the World Health Organization (WHO) for the first time [7]. This vaccine was approved for use in children in places with moderate-to-high *Plasmodium falciparum* transmission [7]. This RTS,S is designed to target the sporozoites phase of the lifecycle. The vaccine is designed to prevent the parasite from infecting the liver, where it can mature, multiply, re-enter the bloodstream, and infect red blood cells, which can lead to disease symptoms [7]. While the availability of a vaccine marks an important step forward in the fight against malaria, this intervention is only partially protective given the modest efficacy of 30% [7,8] and will thus be insufficient on its own to eliminate malaria. Enhanced and expanded strategies for mosquito vector control, in combination with rapid diagnosis and treatment with effective artemisinin drug delivery, will be essential for further progress [2,9,10]. Current evidence indicates that malaria parasites are developing resistance to the artemisinin drug used for frontline treatment in Africa, which pose a challenge towards malaria control [11]. A range of new tools, including those targeting

mosquitoes and parasites, will be needed to overcome these current barriers and make further progress to elimination.

1.1 Malaria biology and pathology

Malaria is an infectious disease caused by protozoan parasites in the genus *Plasmodium*; of which *Plasmodium malariae*, *P. vivax*, *P. ovale*, *P. knowlesi* and *P. falciparum* cause most of the disease in humans [12]. The parasite which contributes the most morbidity and mortality in Africa is *P. falciparum* [13]. Female *Anopheles* mosquitoes are the vectors of malaria parasites and are widely distributed across the African continent [14,15]. Malaria is transmitted when a female *Anopheles* vector carrying *Plasmodium* parasites bites a person (host) while attempting to obtain a blood meal. Biting is obligatory in female *Anopheles* because they need vertebrate blood to develop eggs [16]. The parasite life cycle comprised of sexual stage that occurs in *Anopheles* mosquito vectors and an asexual stage that occurs inside vertebrates hosts [17]. When an infected female *Anopheles* mosquito bites a human, *Plasmodium* parasites in the form of sporozoites are injected into the blood stream. The parasite life cycle comprised of sexual stage that occurs in *Anopheles* mosquito vectors and an asexual stage that occurs inside vertebrates hosts [REF]. When a female *Anopheles* mosquito bites a human, *Plasmodium* parasites in the form of sporozoites are injected into the human dermis. The parasites then migrate to the liver through blood stream and invade the liver cells, hepatocytes. Sporozoites multiply asexually into merozoites in liver cells over the next 7 to 10 days, with single sporozoites producing more than 40,000 merozoites per cell [REF]. The parasites are later released into the bloodstream as merozoites, where they attack red blood cells and subsequently differentiate through ring-stage into trophozoites and eventually schizonts until the cells burst. Then they invade more blood cells causing fever each time the parasites break free and invade blood cells. Small fractions of these merozoites differentiate into gametocytes, which circulate in the peripheral bloodstream where they can infect mosquitoes during the next blood meal. Gametocytes mate sexually in the mosquito gut after which gametes transform into actively moving ookinetes that burrow through the mosquito's midgut wall to form oocysts on the exterior surface. Inside the oocyst, thousands of active sporozoites develop. The oocyst eventually bursts, releasing sporozoites that travel to the mosquito's salivary

glands. The cycle of human infection begins again when the mosquito bites another person during a subsequent blood meal [8]. Transmission can also occur through exposure to infected blood products and by congenital transmission [18]; however the majority of infections are due to mosquitoes.

After being bitten by an infectious female *Anopheles* mosquito, symptoms of malaria can arise six to ten days later. This duration varies depending on the parasite species (for example, non-*P. falciparum* takes 15-16 days) [18] and other factors such as prophylactic use, host immunity or anti-plasmodial treatment [19] and around 10-11 days in non-immunes. A number of symptoms with ranging severity have been described; with most patients reporting feeling cold and sweating, fever and headache [18,20]. The most severe symptoms that can lead to deaths include respiratory distress, coma, cerebral malaria, acute renal failure and even anaemia. Some other patients will experience nausea, vomiting or stomach discomfort [18,20]. The severity of the disease varies with host age and immune status. The most affected groups by malaria transmission globally are children under the age of 59 months and pregnant women [1].

1.2 Mosquito life cycle

The mosquito life cycle consists of two distinct phases: a juvenile (larval) stage which is aquatic and a terrestrial adult stage. The survival and development of mosquitoes in both stages are highly dependent on environmental conditions. The life cycle begins when eggs are laid into aquatic habitats. These eggs hatch into larvae within 2-4 days depending on environmental conditions [21]. Larvae develop into pupae (pupation) within 8-15 days; with the length of this period varying between Anopheline species and in response to environmental conditions (i.e. Temperature) [22,23]. The insect juvenile hormone regulates the process of entering (pupation) and exiting (emergence) from the pupal stage. Mosquito pupae are highly active and non-feeding during this stage. The pupae stage in Anopheline mosquitos lasts 24-48 hours [24,25], a time interval mostly determined by temperature [26,27]. When the weather is warmer, adult emergence occurs faster than when the weather is cooler [28,29].

After emergence, adult males and females search for energy via sugar sources while female mosquitoes will also require one or two blood meals to trigger egg production after mating [30]. Mating usually occurs in the first 1-2 days after emergence, and usually before females take their first blood meal [31,32]. Many Anopheline mosquitoes mate naturally in aerial swarms [33,34] or, to a smaller extent inside houses [35,36]. Eurygamic species do not exhibit natural mating behaviour such as swarming in confined spaces such as laboratory cages, thus making them difficult to colonize [37-39] while stenogamous species exhibit mating behaviour in confined spaces, this include *Anopheles gambiae sensu stricto*. Several research centres around the world have tried to colonize eurygamic species with limited success. *Anopheles funestus* is one of the eurygamous species. This has resulted in a lack of knowledge about the fundamental biology and ecology of such species and consideration of their quantitative predictions about how they might respond to different vector control interventions.

Adult female vectors usually take their first blood meal between 1-2 days after mating. This meal initiates the gonotrophic cycle, characterised by blood feed, blood meal digestion, egg development and finally oviposition. The length of this gonotrophic cycle varies among mosquito species and always depends on the access to blood hosts and ambient temperature [31,40]. When a host is available, *Anopheles* mosquito gonotrophic cycle length takes between 2-5 days [31,32,41]. Females will repeat this cycle until they die. The median lifespan of an adult mosquito in the wild population being approximately 10 days but with large variation between species and settings [41]. The survival and fecundity of adult mosquitoes are considered to be the most important factors for the stability of their populations (fecundity) and the force of malaria transmission (adult survival) [42-45].

The size and reproductive potential of adult mosquito populations are influenced by a range of environmental and intrinsic factors. Several factors during larval development have a large impact on the fitness of adult Anopheline mosquitoes [25,46]. The speed of larval development and survival through this period is highly dependent on temperature [23,25]. This relationship has a curvilinear nature, where survival will initially start to increase with temperature, then

decline sharply at hotter temperatures [47,48]. The speed of larval development and survival through this period is also affected by the presence of competitors or predators in larval habitats [49,50] as well as pathogens [51,52]. Intraspecific resource competition can also be a major cause of mortality during the larval development [22,45,48,53]. In general, there is a positive relationship between larval and adult abundance in the absence of intense resource competition and predation [54,55]. However, this relationship can be modified by density dependence as occurs when larvae compete for resources in aquatic habitats. This gives rise to negative density dependence, where larvae developing at higher densities often have slower development [26] and lower survival [56,57]. The effects of density during larval development can carry over to the adult stage; with adults developing from high density larval habitats often having reduced body size [58,59], survival [53,60], nutritional reserves and even mating success [61] compared to those from less crowded conditions. Cannibalism can also occur in larval habitats, with older larvae (fourth instar) eating younger larvae (first instar) [62,63]. Both intra-specific competition and predation during larval development influence the densities of adult mosquito populations [63]. In nature, some organisms are most likely to die due to senescence (old age), but it is hypothesized that most malaria vectors will be killed due to predation, diseases and other environmental hazards long before they reach old age [64]. This is the case for many insect species including mosquitoes; whose adult mortality is independent of age [65].

1.3 African malaria vectors

In Africa the major vectors of malaria transmission are the *Anopheles gambiae* complex and *An. funestus* groups [66-68], which are widely distributed across different countries Figure 1.1 [14,66,68]. These two vector groups contribute to almost all the malaria transmission in Africa. Vectors belonging to the *An. gambiae* complex are generally the most abundant, and include 8 morphologically identical species: *An. gambiae sensu stricto*, *An. coluzzi*, *An. arabiensis*, *An. quadriannulatus*, *An. amharicus*, *An. melas*, *An. merus*, and *An. bwambwae* [14,69,70]. *Anopheles gambiae* s.s. is commonly considered to be the most efficient malaria vector in this group, followed by *An. arabiensis* [14,71,72]. The higher efficiency of *An. gambiae* s.s is because it is more

anthropophilic than *An. arabiensis*; making it well suited to a human-specific pathogen. In many places these sister species are sympatric in larval habitats, with *An. gambiae* s.s. being more dominant in wetter settings, and *An. arabiensis* dominating in more arid environments [14,68,73,74]. They prefer breeding in shallow, small, and temporary larval habitats (i.e., puddles, hoof prints, tyre tracks, etc.), which are largely dependent on the rainfall [54]. The ecology of the *An. gambiae* complex has been extensively studied and described [66,67]. Within this group, *An. gambiae* s.s. has been most significantly impacted by Insecticide Treated Nets (ITNs) because of its greater tendency to feed on people indoors and during times they are using nets [75]. Consequently, this vector species has almost disappeared from some African settings where it used to be the dominant vector following sustained high coverage of ITNs [76,77]. *Anopheles arabiensis* has more flexible host choice than *An. gambiae* s.s, and often feeds on both human and livestock hosts [78,79], and can feed and rest outdoors as well as indoors [80]. These behaviours make *An. arabiensis* less susceptible to ITNs by reducing their contact with this intervention [81-83]. Detailed understanding of the ecology and behaviour of these species has enabled identification of more targeted approaches for each species (e.g. Cattle based vector control for *An. arabiensis* and new formulations for indoor insecticides for *An. gambiae* s.s).

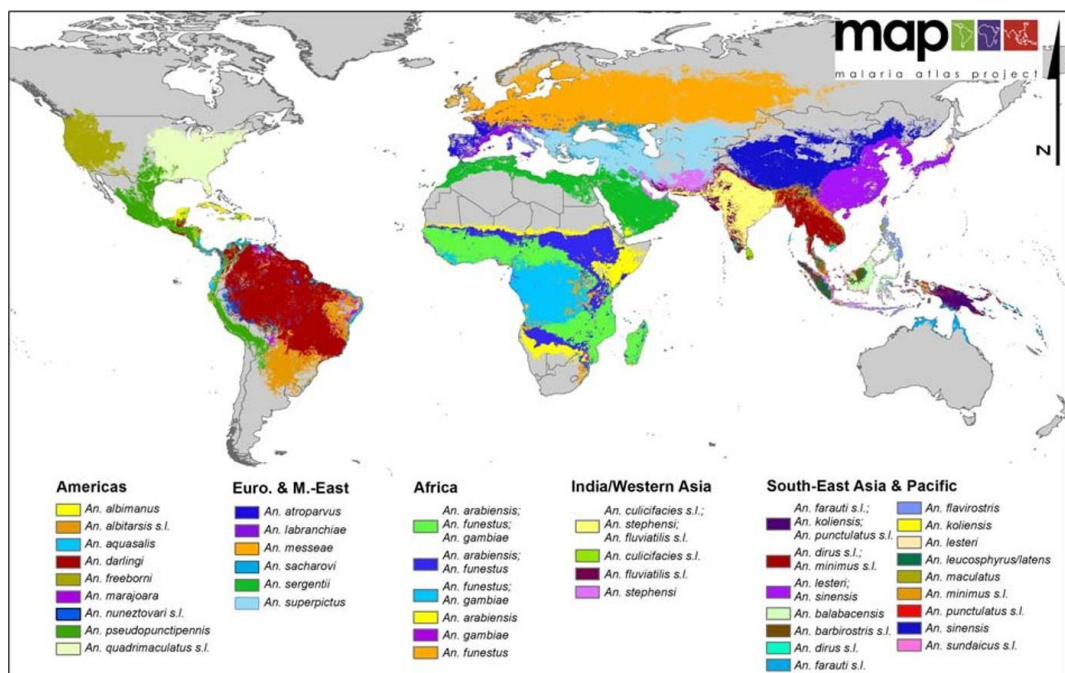


Figure 1.1: A global map of dominant vectors of malaria transmission [68].

In contrast to *An. gambiae* s.l., relatively little is known about the ecology, behaviour and susceptibility of vectors within the *An. funestus* s.l group. *Anopheles funestus* s.l, 1900 is one of the most efficient vectors of malaria transmission world-wide [15]. This group includes at least 13 morphologically identical species: *Anopheles aruni*, *Anopheles brucei*, *Anopheles confusus*, *An. funestus* s.s., *Anopheles funestus*-like, *Anopheles fuscivenosus*, *Anopheles lesoni*, *Anopheles longipalpis* type A, *Anopheles longipalpis* type C, *Anopheles parensis*, *Anopheles rivulorum*, *Anopheles rivulorum*-like, and *Anopheles vaneedeni* [66,84-86]. Only *An. funestus* s.s is considered to have a substantial role in malaria transmission due to its high vectorial capacity [87-89]. This vector has been largely neglected and is often considered a more minor vector of transmission than *An. gambiae* [67,90]. However, in recent years *An. funestus* there is increasing evidence to suggest this species is mediating a significant portion of the transmission in several African settings [89,90,92,93]. In particular, it has been highlighted as a major source of residual malaria transmission [91]. The transmission that remains in areas where high universal coverage with effective ITNs and/or IRS intervention has been achieved is defined as residual [93]. In contrast to the *An. gambiae* complex, *An. funestus* s.s. prefers permanent and semi-permanent larval habitats like swamps and large ponds [94,95]. These habitats are more likely to persist throughout the dry season and thus can sustain *An. funestus* s.s. populations and malaria transmission throughout the year [66,96]. These larval habitats can either be natural water bodies or artificial ones [54,97]. *Anopheles funestus* larvae are most abundant in aquatic habitats containing vegetation; as this feature is crucial for larvae survival [46,95]. This vector is also highly endophilic (feeding indoors) and anthropophilic (feeding on human beings) [98-100]. Although historically described as being an almost exclusive, late-night indoor biter, recent reports of *An. funestus* s.s switching to bite outdoors or in the morning indicate this vector may be changing its behaviour to avoid indoor interventions such as ITNs and IRS or after unsuccessful feeding indoor [101-103]. Another challenge with *An. funestus* s.s. is the inability to rear this species in standard laboratory conditions; meaning that there are very few stable colonies of this species [104]. The lack of stable colonies makes it even harder to study and conduct detailed ecological studies on this mosquito species. This combination

of attributes has allowed *An. funestus* to thrive in areas where other vector species have been more effectively suppressed, and indicates that new and additional control approaches will be required to tackle it. Consequently, identification of optimal vector control strategies is more difficult for *An. funestus s.l.* than *An. gambiae s.l.*; given the considerably larger knowledge gaps on its basic biology and ecology.

1.4 Vector Surveillance

Mosquito vector surveillance is considered a crucial component of malaria control [105]. Several surveillance tools have been designed and used to study different aspects of malaria vector populations ranging from trapping methods that target different life history ages, and molecular methods for identification of vector species and their infection status [71,106,107]. Regular and long-term surveillance is required to understand human exposure to vector populations and the impact of interventions. One of the primary goals of vector surveillance is to estimate the human biting rate (HBR); defined as the number of mosquito bites a person would be expected to receive in specific times and places. The HBR is the most important indicator of human exposure, and often used as a proxy for transmission intensity [108-110]. Since the development of the Ross MacDonal model of malaria transmission, the HBR has been recognized as a crucial predictor of transmission intensity [44,65,111]. This indicator can be directly estimated by sampling the number of mosquitoes attempting to bite a person using a gold standard method (Human Landing Catches-HLC). To perform an HLC, researchers typically expose part of their body (e.g. their legs) and collect any mosquitoes that land on it and try to bite [112,113]. While this method produces the most direct estimates of human exposure [114-116], it has several limitations. First, it puts those doing the collections at risk of infection [112,117]. While in the case of malaria, this risk may be mitigated by provision of prophylaxis [112,117], there remains a risk of exposure to other mosquito borne-diseases (i.e. Dengue, Zika, Rift Valley Fever) that could be circulating in the area [118-120]. Additionally, this approach has logistical challenges of being highly labour intensive and variable; making it ill-suited for mass surveillance. Consequently, there is a long history of exploring alternative trapping methods to provide exposure-free estimates of the HBR. Ideally such trapping methods

should provide consistent estimates with the HLC to be appropriate for quantifying malaria transmission intensity in a given area.

Several exposure-free traps have been developed and evaluated relative to the human landing catch in different African countries [114,121-125]. These studies have used various modelling and statistical approaches to estimate a single value [correction factor] which can be used to convert the catches by a given trap to HLCs [114,124,126]. The most notable and well evaluated trap for vector surveillance is the Centre for Disease and Control light trap (CDC-Light trap) [114,127]. This sampling tool was designed to be effective when sampling mosquitoes which prefer to bite human indoors [116,128,129]. The indoor bias of this trap leaves out mosquitoes which prefer to bite outdoors and on non-human hosts. Increased recognition of the importance of outdoor biting for residual transmission [130] necessitates development and evaluation of different outdoor traps for indirect estimation of HBR.

A limitation of current work is that it has generally focussed on trap validation for *An. gambiae s.l.*, and on indoor settings. It is often assumed that alternative traps will perform similarly well for *An. gambiae s.l.* and *An. funestus*, but this is rarely validated. Additionally, there is increasing evidence of *Anopheles funestus*, biting outdoors in areas of high, widespread usage of indoor interventions [89,101,102]. Given the growing recognition of the importance of outdoor exposure and transmission [77,101,131,132], for *An. funestus* and other vectors, there is a need to explicitly validate and expand range of the range of exposure-free sampling tools for exposure estimation of *An. funestus* HBR in outdoor settings.

1.5 Population dynamics model of malaria vectors

Numerous mathematical models have been developed and used for malaria control decision-making since Ross's original work [43,45,83,133-136]. Mathematical modelling has been used to simulate mosquito population dynamics and examine relationships between larval stages, adult mosquitoes and environmental covariates [133,137-140]. There are several examples of these models being used to explain vector population dynamics and the impact of

intervention at various resolutions [138-142]. These models have served to identify and explain the role of key environmental drivers such as precipitation and temperature on transmission through their impacts of mosquito population dynamics and transmission potential [29,79,143-146]. These meteorological variables are important explanatory variables of mosquito vector borne disease dynamics [140,147,148]. Additionally, annual cycles of rainfall can drive massive seasonal fluctuations in mosquito vector populations [47,149,150], which generally predict transmission dynamics. Rainfall is a key determinant of malaria transmission because it is directly linked to larval habitat availability and regulates the carrying capacity of the vector population [94,150-153]. Temperature also has a large influence on vector population dynamics and demography through its impacts on larval development, survival (adult and larvae) [47,154-156], and the length of gonotrophic cycles [154,157].

Modelling can make a crucial contribution to understanding vector population dynamics through estimating values of demographics and fitness traits, and the impact of environmental variables [150,158,159]. Models of mosquito population dynamics have been used to address a range of fundamental and applied problems with respect to vector ecology and control [133,135,139,160,161], and to predict knock-on impacts for transmission [43,141,162]. While a large body of work has been based on theoretical models under simulated scenarios, increasingly models are developed to address setting-specific issues in Africa, with model frameworks adapted to fit the local ecological context and needs. There is a growing appreciation of the value of incorporating models to support decision making within national malaria control programmes [163-165]. Having a detailed understanding of the dynamics and stability of target vector populations within specific settings is an essential first step to support such localized use of modelling.

Models of vector population dynamics can play a vital role in improving understanding of which additional interventions are likely to generate the most impact in particular ecological and epidemiological contexts. The impacts of a particular intervention approach may vary substantially between settings in relation to local vector ecology and resistance profiles. For example, differences in vector ecology and ambient environmental conditions between locations could alter the stability of vector populations and the effort needed to suppress or

destabilize them. A notable example of this could be differences in vector species. As reviewed above, the major African malaria vectors differ in several aspects of their ecology and behaviour that influence their environmental associations and seasonal dynamics [16,79,81,103,166-168]. Despite these differences, most models of African malaria vector population dynamics are based on parameters from *An. gambiae* s.l. [135,139,141,163,169]. There are few specific models of *An. funestus* dynamics because this species has been very difficult to study in the laboratory and only parts of its life cycle in the wild can be studied [24,170]. Given the unique ecology of *An. funestus*, and growing recognition of its importance in sustaining residual transmission, there is an urgent need to better understand the environmental drivers and determinants of its population stability.

A range of different approaches have been used to model the dynamics of malaria vector populations. These include deterministic models that describe changes in vector populations as a result of pre-defined mechanistic functions and parameters [131,148,150,171-173]. While very useful to outline the general properties of mosquito populations, these dynamic models can be difficult to create when crucial parameter values are unknown. This is often the case with *An. funestus* populations where crucial data on demographic and fitness parameters in the wild are unknown [174]. State-space models (SSM) provide an alternative approach to indirectly estimate these parameters by fitting a population dynamics model to observed time series data [159,175,176]. SSMs have been widely used in different areas of ecology, wildlife management and conservation biology to reconstruct otherwise hidden aspects of population dynamics [159,177-179] and influence management decisions [180]. However, these models have so far had limited application in medical entomology. This modelling approach holds particular promise for investigation of vector species like *An. funestus* whose demography is more challenging to directly monitor. Here, such models could be used to estimate feasible demographic rates that could explain the observed dynamics [159,179]; thus generating information on key parameters that could be used to model response to control.

1.6 Vector control interventions

Several vector control tools have been developed that target African malaria vectors [2,105,137,171,181-184]. These strategies can vary in the life history stages of the mosquito population they target (e.g. larvae versus adult) and their impact on mosquito population dynamics and malaria transmission [141]. The most widely used are Insecticide-Treated Nets (ITNS), Indoor Residual Spraying (IRS) and Larval Source Management (LSM) [2,91,105,137,185]. ITNs and IRS have been approved as core interventions by the WHO while LSM has been approved as complimentary intervention [105]. Vector control (IRS and ITNs) alone accounted for 78% of the total decline in malaria prevalence in African between 2000-2015 [2,3]. Improved vector control and case management, urbanization, improved health care, and higher living conditions, have all contributed to these gains [2,3]. Other vector control interventions include house screening, auto-dissemination of larvicides, space spraying, attractive target sugar baits, and genetically modified mosquitoes [181,186-189]. It is anticipated that vector control will continue to be a major component of malaria control and elimination strategies.

Conventionally, ITNs are delivered through mass campaigns targeting pregnant women during routine visits to health facilities, or through school age children programs (i.e. School Net program SNP) and mass distribution in communities as part of the National Malaria Control Program (NMCP) strategy [105,190-192]. ITNs have the dual advantage of first offering physical protection to users when they are fully intact and without holes, and second by providing a community effect by killing adult mosquitoes that contact insecticides while trying to feed; thus reducing their population [193,194]. The effectiveness of ITNs is determined by their residual efficacy and physical integrity. Consequently the WHO states that mass distribution should occur every three years based on ITN attrition projections. Furthermore, the effectiveness of the intervention is contingent on their consistent use during the transmission season.

Indoor residual spraying (IRS) is spraying of prequalified residual pesticides onto potential mosquito resting surfaces like interior walls, eaves, and ceilings of homes or structures such as domestic animal shelters [105]. The sort of

insecticides deployed and the characteristics of the sprayed wall influences IRS efficacy [105,195]. The WHO recommends that IRS products must have a residual efficacy of at least 6 months on the sprayed surface before being listed as a prequalified product [196]. Unlike ITNs which target host seeking females, IRS impacts resting mosquitoes (both female and males). The effectiveness of IRS depends on the spraying performance, the coverage and susceptibility of the vectors to the insecticide used [105,197]. In most countries, IRS is deployed right before the rainy season in which malaria transmission is concentrated [198,199]. IRS is recommended for application in high transmission areas, and ideally using a rotation of different insecticide classes to mitigate against resistance [105]. Due to the high cost and logistical challenges of implementing IRS, it is not as widely used in many countries as ITNs.

Larval Source Management targets the aquatic stages of the mosquitoes. LSM works by preventing the completion of development of the immature stages (eggs, larvae and pupae), which stops the emergence of adults [200,201]. This can be achieved either through habitat elimination, biological control, and habitat modifications or treating them with a pesticide that kills larvae [202,203]. Deployment of LSM is usually recommended during the driest period of the year when there is no rain or flowing water which might dilute the level of insecticide used in larviciding [105,202,203]. LSM is considered cost-effective and generally recommended in urban settings where the breeding habitats are “fixed, few and findable” [105]. There is evidence that it may also be effective when deployed in the rural setting under specific circumstance [105,201,202]. In African countries, LSM is not widely used in many settings due to its logistical challenges. Despite widespread use and relatively high coverage of ITNs and IRS, malaria vector populations remain widespread and abundant throughout the African continent. Vector abundance and infection rates vary considerably in space and time, leading to high heterogeneity in malaria transmission between regions [109,166,204-206]. The existence of residual transmission presents a number of obstacles for malaria elimination. Tackling residual transmission will require understanding of the mechanism through which vector population persists and additional new interventions to better target them at different life stages.

Key challenges to current vector control approaches include insecticide resistance [204,207-209] and shifts in mosquito behaviour including increased outdoor and early evening/late morning biting in major malaria vectors [77,102,130,169]. Resistance to pyrethroids, the primary insecticide class used in ITNs, has been widely documented in multiple vector species across Africa [104,209-214]. These and other constraints mean that ITNs and IRS alone will not be sufficient to achieve malaria elimination in Africa [215]. More effective strategies are required that can better target the sources of residual transmission; including vector populations with diverse behaviour and resistance profiles. This could include either the implementation of new approaches or a more optimal combination of existing methods (ITNs, IRS, LSM, etc.). Given that both ITNs and IRS target indoor vector populations, they may not be sufficient to disrupt population stability where a considerable portion of target populations feed and rest outdoors. Greater success may be achieved through integration of interventions targeting vectors at different life cycle stages (larvae and adults) and with different behaviours (indoor versus outdoor, etc.). Detailed knowledge of the ecology and behaviour of *An. gambiae s.l.* can facilitate identification of which combination of approaches could most effectively disrupt populations of this vector. However, similar identification of optimal intervention approaches or combinations will be harder for *An. funestus s.l.* without a much better understanding of the key drivers of their population dynamics and stability.

1.7 Research focus

In Tanzania, there has been a significant reduction in the malaria transmission since the scaling-up of ITNs [1,3]. Recent reports from the Tanzania Malaria Indicator Survey (TMIS) show an overall reduction in (national) malaria prevalence from 16.9% in 2007 [216] to 7.3% in 2017 [217]; indicative of an average 55% drop in transmission. Despite progress, more effort is required to tackle residual transmission. In Tanzania, residual transmission has been associated with the increasing in insecticide resistance [88] and changes in biting and resting preferences of the current vectors of malaria transmission [77,79,88,89,91].

In some parts of East Africa including Tanzania, populations of the formerly prolific malaria vector *An. gambiae* s.s., have significantly diminished, or completely vanished following mass ITN distribution leaving *An. arabiensis* and *An. funestus* as the remaining sources of transmission [182,190,218,219]. This scenario occurred in the Kilombero Valley, where the relative abundance of *An. gambiae* (compared to *An. arabiensis*) fell from about 90% to nearly 10% between 1997 and 2009 [77]. *Anopheles arabiensis* is now the most numerically abundant vector in this area [89,103], however, malaria infection rates are considerably higher in the co-occurring, lower density *An. funestus* populations. These *An. funestus* populations account for the bulk of residual transmission (>85% of all infections) [88,89,91]. Studies show that *An. funestus* is not only widely resistant to pyrethroids in Tanzania [88,220,221], but may also have a survival advantage over *An. arabiensis* [100,222,223]. A difficulty with the surveillance of *An. funestus* is that although they are widespread, there is uncertainty about how well trapping methods can detect their relatively low density populations. There is a need to more rigorously validate existing and novel surveillance methods for *An. funestus*, particularly those used to detect “atypical” routes of exposure such as outdoor biting. Given the importance of *An. funestus* in Tanzania, there is a need to better understand how to colonize it, survey it, and assess its population dynamics and stability.

1.8 Objectives and outline

This thesis aims to strengthen knowledge on the ecology and population dynamics of *An. funestus*; the major vector of residual malaria transmission in Tanzania and other parts of Africa. The overall goal is to fill key knowledge gaps on its population dynamics as needed to predict the potential impact of different vector control interventions. The information used in this study was gathered through insectary and field surveys. Although all data collection occurred in the Kilombero Valley of south eastern Tanzania, the methodology developed is meant to provide baseline estimates for demographic parameters of *An. funestus* populations in other parts of Sub-Saharan Africa.

The objectives were:

1. ***To quantify the fitness and behaviour of wild Anopheles funestus from Tanzania and their offspring during repeated colonization attempts under standard laboratory conditions.*** This objective is addressed in Chapter 2 which quantifies different fitness measures (survival, larval development period, mating, and body size) of *An. funestus* under laboratory conditions, with the aim of assessing barriers to successful colonization of this vector. This study also provided data on *An. funestus* demographic processes which provided prior values for the population dynamics models described in later chapters. The study described in this chapter has been peer reviewed and published in Malaria Journal [24].
2. ***To develop and validate a framework for predicting HLC-derived outdoor exposure rates from different exposure-free alternatives traps.*** This objective is addressed in Chapter 3 which describes a field-based evaluation of different methods to predict the HBR of *An. funestus* in outdoor environments. This chapter also describes the development of a calibration tool which can be used to predict the number of *An. funestus* that would be expected in a standard Human Landing Catch (HLC) from the number collected by an alternative trap. This study has already been published in the Parasites & Vectors Journal [224].
3. ***To develop a population dynamics model that can be used to describe the ecology of the wild population of An. funestus.*** This objective is addressed in Chapter 4 which describes the development of a State-Space Model in a Bayesian framework to infer the drivers of wild *An. funestus* populations in Tanzania. This model is used to assess the contribution of environmental variables (temperature and rainfall) and density dependence to *An. funestus* population growth. This framework has already been published in the Malaria Journal [153].
4. ***To assess the generalizability of this population dynamics model and its ability to reconstruct missing data.*** This objective addressed in Chapter 5 which critically re-examines the population dynamics model

developed in the previous chapter (Chapter 4) through investigation of all potential limitations to its generalizability. The investigation provides new insights into the potential existence of hidden demographic processes which may be influencing the overall dynamics of these populations.

Chapter 6 provides a comprehensive discussion of all the previous chapters and their contributions to the overall objective of the PhD; a concise overview of general limitations, challenges, and suggestions for future work.

2.0 Chapter 2: Fitness characteristics of the malaria vector *Anopheles funestus* during an attempted laboratory colonization

Published in Malaria Journal 2021: <https://doi.org/10.1186/s12936-021-03677-3>

Abstract

Background

The malaria vector *Anopheles funestus* is increasingly recognized as a dominant vector of residual transmission in many African settings. Efforts to better understand its biology and control are significantly impeded by the difficulties of colonizing it under laboratory conditions. To identify key bottlenecks in colonization, this study compared the development and fitness characteristics of wild *An. funestus* from Tanzania (FUTAZ) and their F₁ offspring during colonization attempts. The demography and reproductive success of wild FUTAZ offspring were compared to that of individuals from one of the only *An. funestus* strains that has been successfully colonized (FUMAZ, from Mozambique) under similar laboratory conditions.

Methods

Wild *An. funestus* (FUTAZ) were collected from three Tanzanian villages and maintained in an insectary at 70-85% RH, 25-27 °C and 12hr:12hr photoperiod. Eggs from these females were used to establish three replicate F₁ laboratory generations. Larval development, survival, fecundity, mating success, percentage pupation and wing length were measured in the F₁ FUTAZ offspring and compared with wild FUTAZ and FUMAZ mosquitoes.

Results

Wild FUTAZ laid fewer eggs (64.1; 95%CI [63.2, 65.0]) than FUMAZ females (76.1; 95%CI [73.3, 79.1]). Survival of F₁-FUTAZ larvae under laboratory conditions was low, with an egg-to-pupae conversion rate of only 5.9% compared to 27.4% in FUMAZ. The median lifespan of F₁-FUTAZ females (32 days) and males (33 days)

was lower than FUMAZ (52 and 49 for females and males respectively). The proportion of female F₁-FUMAZ inseminated under laboratory conditions (9%) was considerably lower than either FUMAZ (72%) or wild-caught FUMAZ females (92%). This resulted in almost no viable F₂-FUMAZ eggs being produced. Wild FUMAZ body sizes (as estimated from wing size) were larger than that of lab reared F₁-FUMAZ and FUMAZ.

Conclusions

This study indicates that poor larval survival, mating success, low fecundity and shorter survival under laboratory conditions all contribute to difficulties in colonizing of *An. funestus*. Future studies should focus on enhancing these aspects of *An. funestus* fitness in the laboratory, with the biggest barrier likely to be poor mating.

2.0 Background

Malaria transmission in Africa is dominated by species in the *Anopheles gambiae* and *Anopheles funestus* species complexes. Control of these vectors has been the primary driver of malaria reduction since 2000 [2,217], and requires thorough understanding of their ecology, behaviours and transmission potential [45,58,62,103,116,225,226]. Laboratory colonies of *An. gambiae sensu lato (s.l.)* have been an invaluable resource for research by enabling experimental studies under controlled conditions. Such colonies have facilitated the characterization of insecticide resistance [209,227,228], genetics [229,230]), immunity [231,232] and key vector demographic profiles [59,109,233]. Mosquitoes generated from laboratory colonies are also extensively used for semi-field bioassays [58,81,135].

In contrast to *An. gambiae s.l.*, *An. funestus s.l.* has proven extremely difficult to colonize and maintain under laboratory conditions. The *An. funestus* species complex group consists of at least 13 known species: *Anopheles aruni*, *Anopheles brucei*, *Anopheles confusus*, *Anopheles funestus sensu stricto (s.s.)*, *Anopheles funestus-like*, *Anopheles fuscivenosus*, *Anopheles leesoni*, *Anopheles longipalpis* type A, *Anopheles longipalpis* type C, *Anopheles parensis*, *Anopheles rivulorum*, *Anopheles rivulorum-like* and *Anopheles vaneedeni* [66,84-86]. These species vary in vectorial capacity [87], with only *An. funestus s.s.* thought to play a significant role in malaria transmission [88,89]. Others, such as *An. rivulorum*, have been reported as minor vectors in Kenya [234] and Tanzania [235], as has *An. vaneedeni* in South Africa [236].

Colonization of *An. funestus s.s.* has however been problematic. Only two strains have been successfully colonized from wild populations despite several attempts. Both strains were colonized at the Vector Control Reference Laboratory (VCRL) in the National Institute for Communicable Diseases, South Africa, from populations in Angola (FANG) and Mozambique (FUMOZ) [92,104]. The FUMOZ strain is also maintained at other laboratories worldwide, including in Cameroon, the UK [228], and in Tanzania (at the Ifakara Health Institute). Several attempts have been made to colonize new *An. funestus* strains [170] from wild populations, but methods used to establish FUMOZ and FANG have not

been successful elsewhere [237], including when attempted with the same wild populations where FUMAZ was originally derived (Coetzee, *pers. commun.*). This inability to repeatedly colonize and establish *An. funestus* in laboratories is responsible for the more limited understanding of the biology of this species compared to other vector species.

Several factors may account for the difficulty of colonizing *An. funestus*. Chief amongst these is eurygamy the inability to mate in cage/confined space [37,38]. Eurygamic species are difficult to colonize because they do not exhibit natural mating behaviours, such as swarming [238], under insectary conditions [37,239,240]. Many *Anopheles* mosquitoes mate naturally in aerial swarms [33,34,241] or, to a smaller extent, indoors [35]. Whilst *An. gambiae* will mate readily in the laboratory [58], wild and F₁ progeny of *An. funestus* rarely swarm inside cages. Although mating is hypothesized to be the main barrier to *An. funestus* colonization, other factors cannot be ruled out due to incomplete or absence of reporting on other aspects of their life history and fitness during attempted colonization. Therefore, it is crucial to comprehensively evaluate how all aspects of *An. funestus* life history, development and demography respond to standard methodologies for colonization to identify where modifications should be focused.

To address these knowledge gaps, the fitness and behaviour of wild *An. funestus* from Tanzania and their offspring (defined as “FUTAZ”, i.e. *An. funestus* from Tanzania), were quantified during repeated colonization attempts under standard laboratory conditions. The first step to optimize the colonization process is to understand which aspects of *An. funestus* life-history and fitness are most impaired during colonization, and thus target modifications appropriately. To assess this, detailed measurements of the fitness and life-history of wild and F₁ *An. funestus* were conducted during repeated laboratory colonization attempts. Fitness measures of individuals in this nascent colony were compared to those of a stable *An. funestus* colony (FUMAZ) to identify the key barriers that hinder successful colonization of this species. The term “fitness trait” refers to measures of mating success (insemination status), fecundity (number of eggs produced), adult body size and survival (larval and adult).

Insights gained will guide future research to overcome barriers to colonizing *An. funestus*, and also increase knowledge on this important vector and its control.

2.1 Methods

2.1.1 Study area

Wild *An. funestus* adults were collected from three villages (Tulizamoyo, Ikwambi and Sululu) in Kilombero (8.1539°S, 36.6870°E) and Ulanga (8.3124°S, 36.6879°E) districts in Tanzania (Figure 2.1). These villages were selected because of they have high density populations of *An. funestus s.l.*, of which >93% are known to be *An. funestus s.s.* [195]. Wild-caught females were transported to the Ifakara Health Institute and used in experiments at the Vector Biology & Control Laboratory, the “VectorSphere” (Figure 2.1).

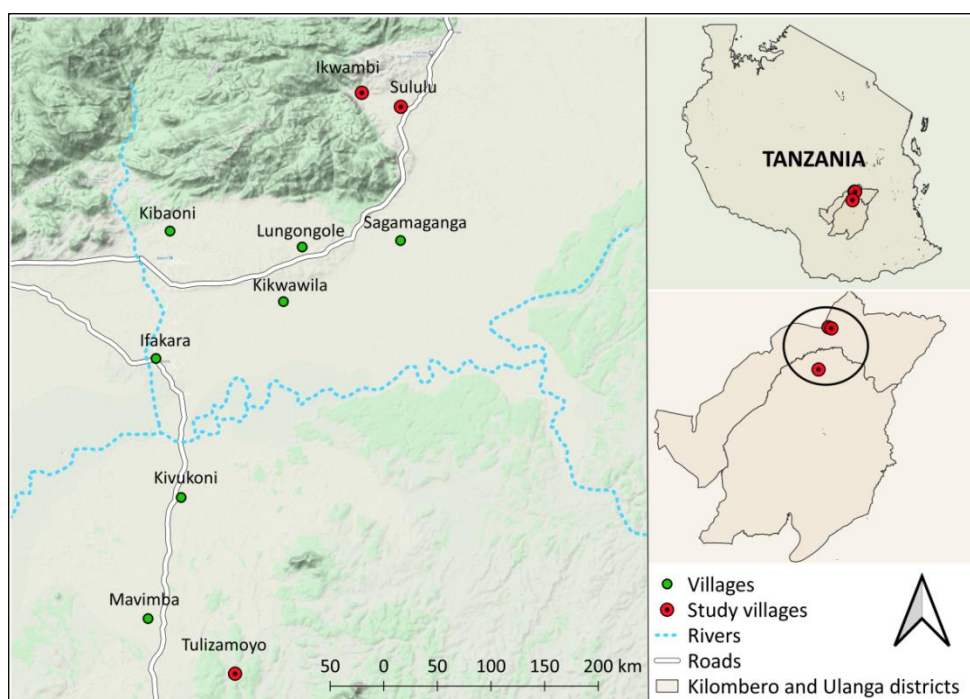


Figure 2.1: A map of study area showing the location of the villages where *Anopheles funestus* females (wild-FUTAZ) were sampled for colonization experiments.

2.1.2 Mosquito sampling

Five houses were selected for mosquito collection in each village. Mosquito collections were conducted for one week in each village in 2019 (Tulizamoyo: 17-23rd June; Ikwambi: 8-16th July and Sululu: 1-10th September). Due to collection logistics and space limitation in the VectorSphere, only one set of experiments (i.e. with mosquitoes from just one village) was done at a time. Trapping was done using CDC light traps [127,242] that were set from 6pm to 6am for five consecutive nights per village (yielding ~200-300 female *An. funestus s.l.* per week). Light traps were fitted with larger catch bags to help keep mosquitoes alive without desiccation until morning. Every morning, live female *An. funestus s.l.* were aspirated from collection bags into netted cages (30 x 30 cm), provided with 10% glucose solution and brought to the VectorSphere for blood-feeding and further rearing. Inside the VectorSphere mosquitoes were kept under standard conditions of 70-85% RH, 25-27°C and a 12hr: 12hr photoperiod.

2.1.3 Laboratory maintenance and fitness measurements for FUTAZ mosquitoes

In the VectorSphere, wild female of *An. funestus s.l.* were given an initial blood meal from a chicken for a maximum of 30 minutes (from 6:30pm) inside cages covered with dark cloth. After this meal, mosquitoes were left in the cage until the next morning when their feeding success was recorded by visual observation. Those with a distended, red abdomen were considered to be fully engorged and transferred into individual oviposition cups for egg laying (Figure 2.2). Cotton pads soaked in 10% glucose solution were placed onto the top netting over the cups for additional nutrition. After three days, a small amount of water (~5ml) was put in each cup to stimulate oviposition. Cups were then inspected daily to record if and when eggs were laid, and dead mosquitoes were removed. Mosquitoes that did not lay eggs after 12 days were killed by freezing for 10 minutes and later dissected to assess insemination. The terminalia and last abdominal segment (segment IX) were cut-open in distilled water to expose the spermathecae. Slide mounts of spermathecae were inspected using a microscope at 400x magnification for presence of sperm (Figure. 2.3a&b).

F₁ eggs from wild-caught *An. funestus s.l.* were identified to species-level based on their morphological characteristics [15]. Eggs were observed under a stereomicroscope, and sub-samples of emergent adults verified by PCR [243]. All eggs morphologically confirmed as belonging to *An. funestus s.s.* were retained for use in subsequent colonization and life history experiments and defined as F₁-FUTAZ (Table 2.1). Here, all F₁-FUTAZ eggs were pooled and redistributed into a series of 5L round plastic basins (30 cm diameter, filled to 3.3 cm with tap water, replaced every two days) at approximate densities of 400-600 eggs per basin and left to hatch. There were a total of 12 replicate basins set up for each of the 3 independent colonization experiments (1 per study village). From here onwards, the term *An. funestus* refers specifically to *An. funestus s.s.*



Figure 2.2: Images of laboratory set-up for the colonization process:

a) Series of wooden cages with oviposition cups, each contains a single fully-engorged *Anopheles funestus* female. Individual cups were used to measure the number of eggs laid by a single mosquito after full blood meal, b) Technician counting the number of eggs and measuring the wing sizes of individual mosquitoes which have laid eggs, c) Technician aspirating mosquitoes from the rearing cage using mouth aspirator and d) bowl contains eggs of *Anopheles funestus*. All experiment was done within the VectorSphere at Ifakara Health Institute.

Larvae were fed daily with a pinch (approx. 0.36 grams) of a mixture of finely crushed dog biscuits and brewer's yeast at a ratio of 3:1 [104]. Basins were checked daily to record egg hatching and larval survival. Pupae that emerged

over three consecutive days were recorded and retained for use in F_1 adult mosquito fitness experiments. The female: male ratio of emerging F_1 adults was recorded by looking at the genital lobe shape (i.e. at the end of the pupae abdominal segments just below the paddles) and also males tend to be smaller than females [188,244]. Pupae were placed in a single cage (30 x 30 cm) and monitored until emergence (1-2 days). A total of three cages were set up for each of the three independent colonization experiments.

F_1 -FUTAZ females were offered their first human blood meal five days post-emergence. Females from the FUMAZ colony whose fitness was compared to F_1 -FUTAZ were also provided a human blood meal on the same day and time (see below). Females of both strains were provided with additional blood meals every five days. The rationale for blood feeding every 5 days was to estimate the survival under conditions where they had access to blood meals at a frequency similar to that expected in the wild. Studies indicate that the gonotrophic cycle length of *An. funestus* ranges between 2-5 days [31,32]; with 5 being selected here due to practical considerations. From the first blood meal onwards, cages were inspected daily to record and remove all dead mosquitoes. A total of three cages were used as replicates in each of the 3 independent colonization experiments. All dead females were dissected to assess insemination status. Random sub-samples of F_1 females were selected after the second blood meal and moved into individual oviposition cups to measure their egg production.

2.1.4 Laboratory maintenance and fitness measurements for FUMAZ mosquitoes

In July 2018, eggs from the FUMAZ *An. funestus* colony were obtained from the VCRL laboratory in South Africa and used to establish a colony within the VectorSphere at Ifakara Health Institute in Tanzania. The founder FUMAZ colony at VCRL has been maintained since 2000 [104]. At IHI, the FUMAZ colony was maintained for four generations before starting these experiments. This colony was kept under the same insectary conditions (70-85% RH, 25-27°C and 12hr: 12hr photoperiod) and same feeding regime as described above for F_1 -FUTAZ. In this study, the following fitness variables were measured in FUMAZ for comparison with FUTAZ: number of eggs laid per mosquito (fecundity),

proportion of eggs hatched, wing lengths, proportion of adult females inseminated, proportion of larvae survived (from 1st instar to pupation), larval development period, the proportion of pupae that emerged as adults, female: male sex ratio at pupae stage and number of days survived by adult both males and females. The definition of all fitness traits measured, and the colonies in which they were made were given in (Table 2.1).

2.1.5 Mosquito wing size measurements

The wing lengths of all female *An. funestus* (Wild FUTAZ, F₁-FUTAZ and FUMOZ) were measured and used as a proxy for their body size. One wing was removed from each mosquito and placed onto a drop of water on a microscope slide. The wing lengths were measured using the micrometre ruler under a microscope (50mm micrometre scale in 0.1mm divisions, 70mm x 20mm x 3mm) [245]. Measurements were taken from the apical notch to the auxiliary margin, excluding the wing fringe (Figure 2.3d).

Table 2.1: Descriptions of terms used and strains compared as used in this study

Variable measured	Strains compared	Definition as used in this paper
Fecundity	Wild-FUTAZ vs. FUMAZ	Number of eggs laid by a single female mosquito
Wing size	Wild-FUTAZ vs. F ₁ -FUTAZ vs. FUMAZ	Length (mm) of a wing from apical notch to the auxiliary margin
% eggs hatched	F ₁ -FUTAZ vs. FUMAZ	Number of eggs hatched as a percentage of the total number of eggs laid
% Larvae survival	F ₁ -FUTAZ vs. FUMAZ	Number of larvae pupating, as a percentage of all eggs produced per individual female
Larval development period	F ₁ -FUTAZ vs. FUMAZ	Number of days from 1 st instar larvae to pupation
Sex ratio	F ₁ -FUTAZ vs. FUMAZ	Ration of the number of females to number of males as identified at the pupal stage
% Adult emerging	F ₁ -FUTAZ vs. FUMAZ	Number of adult emerged as a percentage of pupae stage
% Female inseminated	Wild-FUTAZ vs. F ₁ -FUTAZ vs. FUMAZ	Number of females found to be inseminated as a percentage of total dissected
Adult survival rate	F ₁ -FUTAZ vs. FUMAZ	Number of days survived by an adult mosquito in the laboratory

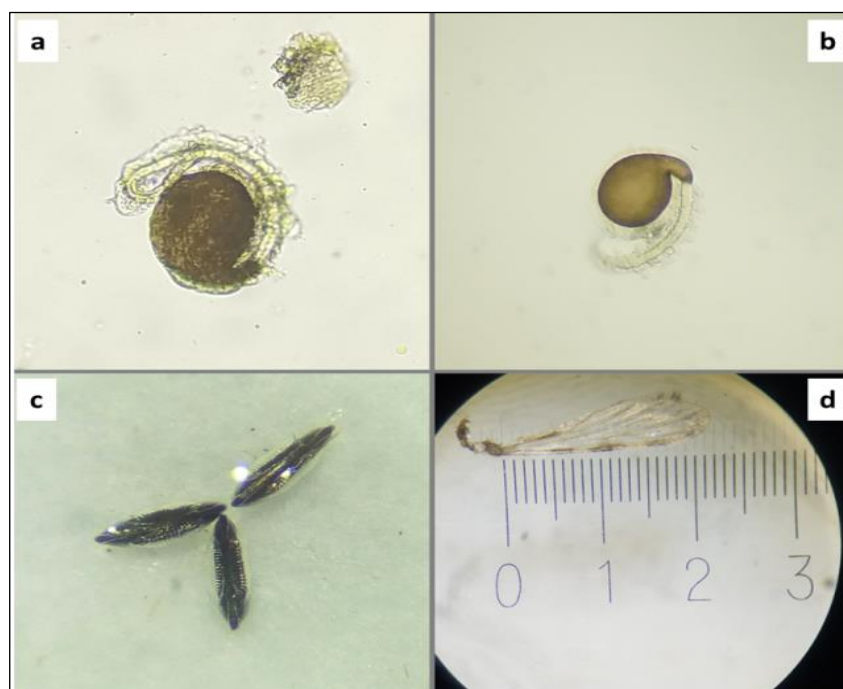


Figure 2.3: Microscopic images of different parts of *Anopheles funestus*: showing the a) presence of the spermatozoa as the confirmation for insemination and b) absence of spermatozoa suggesting non-inseminated, c) Egg structure of the female *Anopheles funestus* s.s. as seen under microscope, a quick and cheap method of species distinction within *Anopheles funestus* group during colonization instead of standard Polymerase Chain Reaction (PCR) and d) the wing measurement under microscope showing the apical notch and the auxiliary margin.

2.1.6 Statistical analysis

Data analyses were conducted using the R statistical software version 3.5.0 [246]. Mean values of these fitness traits were measured and compared between FUTAZ and FUMAZ (Table 2.1). Where possible, fitness traits (i.e. wing length and proportion inseminated) were also compared among the wild FUTAZ, F₁-FUTAZ and FUMAZ. Additional analysis was conducted to assess the relationship between female body size and fecundity (number of eggs produced) in wild FUTAZ and FUMAZ. It is known for other species that, the larger the body size the higher the number of eggs laid per female mosquitoes [247,248].

Generalized linear mixed models (GLMM) implemented in *lme4* package [249] were used to estimate mean values of fitness traits in wild, F₁-FUTAZ and FUMAZ strains. Fecundity (the number of eggs laid per mosquito) was modelled as following a Poisson distribution with wing length included in the model as a fixed

effect. Proportion data (here, emergence, insemination, larval survival and sex ratio) were modelled as binomial variates with strain used as fixed effects. Wing length and strain were also fit as fixed effects when assessing insemination rates. Wing length was modelled as a Gamma variate with an inverse link function, incorporating strain as fixed effect. In all the model fitting process, experimental replicates and villages were included as random effects. Tukey's post-hoc tests were used to assess the means differences for different fitness measurements.

Analysis of adult survival was conducted using a Cox proportional hazard model using the *survival* package [250] to assess the odds of mortality in males and females and of different strains (F₁-FUTAZ vs. FUMOZ). Here, the response variable was the death occurring on each day of observation, while strain and sex were included as fixed explanatory variables. In the analysis of F₁-FUTAZ, site of collection (village) was included as a random effect by fitting a frailty function [251,252] using a Gamma distribution. Separate analyses were performed for each strain except when the differences between strains were investigated. Log likelihood ratio tests (LRT) were used to test the significance of each variable of interest in all models. All figures were produced using *ggplot2* [253] and *survminer* [254] R packages.

2.2 Results

A total of 1,130 adult females of the wild-FUTAZ strain were collected from the three different villages of Tulizamoyo (n=332); Ikwambi (n=425); Sululu (n=373). More than two-thirds (n=804) of these successfully fed when offered a chicken blood-meal in the insectary, of which 39% (n=316) laid eggs in the insectary.

2.2.1 Mosquito wing lengths, mating status, fecundity and pupation

Anopheles funestus wing lengths varied significantly between groups ($\chi^2=14.97$, $p<0.001$, Figure 2.4a). A Tukey's *post-hoc* test showed that wild-collected FUTAZ were larger than lab reared F₁-FUTAZ ($z=3.23$, $p<0.01$, Figure 2.4a) and FUMOZ ($z=2.52$, $p<0.05$, Figure 2.4a). There was no difference in wing lengths between

the two laboratory-reared strains, FUMOZ and F₁-FUTAZ ($z=1.43$, $p=0.303$, Figure 2.4a).

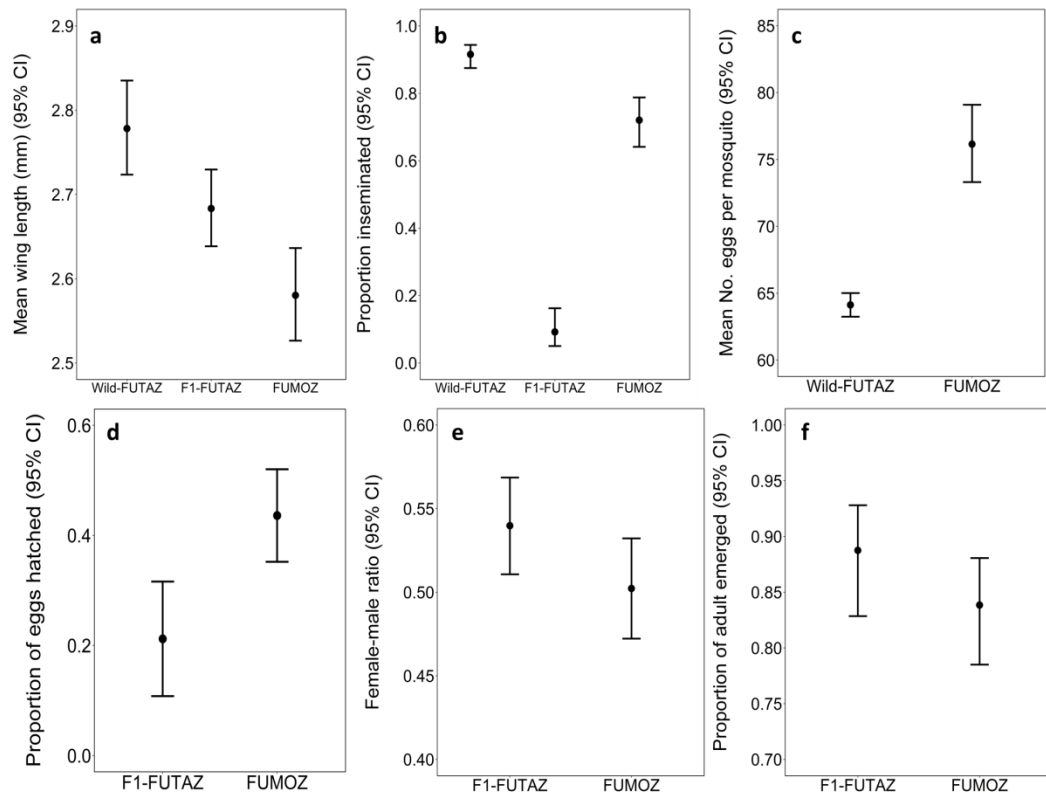


Figure 2.4: Showing *Anopheles funestus* a) wing sizes; b) female inseminated, c) fecundity, d) eggs hatched, e) sex ratio, f) adult emerged for Wild-FUTAZ, F₁-FUTAZ and FUMOZ strain. Error bars are 95%CI predicted from the GLMM.

The wing lengths of F₁-FUTAZ ($\chi^2=10.4$, $p<0.01$) but not FUMOZ ($\chi^2=0.123$, $p=0.688$) were positively associated with insemination status. Furthermore, the proportion inseminated varied significantly between strains ($\chi^2=177.2$, $p<0.001$, Figure 2.4b, Table 2.2), and the two generations of FUTAZ ($\chi^2=172.3$, $p<0.001$, Figure 2.4b, Table 2.2). Insemination was considerably lower in F₁-FUTAZ (9%) compared to wild caught FUTAZ females (92%) and FUMOZ (72%; Figure 2.4b, Table 2.2).

Table 2.2: Relative odds (OR) and means of insemination, sex ratio, pupation and adult emergence for different strains of *Anopheles funestus*, number in brackets are 95% confidence intervals with their respective p-values.

Variable	Strain	Mean \pm 2SE	OR [95% CI]	P-value
% Insemination	Wild-FUTAZ	91.5 \pm 1.30	1	
	F ₁ -FUTAZ	9.2 \pm 4.99	0.009 [0.004, 0.020]	<0.001
	FUMOZ	72.0 \pm 5.16	0.24 [0.13, 0.42]	<0.001
% Sex ratio (F/M)	F ₁ -FUTAZ	53 \pm 4.0	1	=0.049
	FUMOZ	50 \pm 2.9	0.86 [0.74, 0.99]	
% Larval survival	F ₁ -FUTAZ	5.3 \pm 3.5	1	<0.001
	FUMOZ	27.4 \pm 12.5	12.05 [4.27, 34.03]	
% Adult emergence	F ₁ -FUTAZ	88.8 \pm 7.35	1	=0.174
	FUMOZ	81.6 \pm 8.90	0.66 [0.36, 1.20]	

Fecundity varied between strains ($\chi^2=66.54$, $p<0.001$) with FUMOZ females producing significantly more eggs than wild-FUTAZ (Figure 2.4c, Table 2.3). FUMOZ clutch size ranged from 41-137 eggs while wild-FUTAZ clutch sizes ranged from 3-236 eggs. The proportion of eggs hatched into 1st instar larvae was 21% [95% CI; 10.8, 31.6] in F₁-FUTAZ and 44% [35.2, 52.0] in FUMOZ (Figure 2.4d). No eggs were produced by F1-FUTAZ. The impact of wing length on fecundity varied between strains ($\chi^2=62.57$, $p<0.001$, Figure 2.5a).

Table 2.3: Relative rate (RR) and means of fecundity for different strains of *Anopheles funestus*, number in brackets are 95% confidence intervals.

Variable	Strain	Mean \pm 2SE	RR [95% CI]	P-value
Fecundity	Wild-FUTAZ	64.1 \pm 5.26	1	
	FUMOZ	76.1 \pm 7.61	0.84 [0.81, 0.88]	<0.001

The median larval development period from 1st instar larvae to pupation was 22, IQR: 21-23 days in FUMOZ, and only 13, IQR: 11-14 days in F₁-FUTAZ (Figure 2.5b). Overall, the proportion of eggs surviving to pupation was 5.87% in F₁-FUTAZ and 27.4% in FUMOZ, reflecting significant variation between strains ($\chi^2=11.28$, $p<0.001$). The sex ratio (females: males) in pupae varied marginally between strains ($\chi^2=3.89$, $p=0.049$, Table 2.2 & Figure 2.4e), with a slightly

higher proportion of females in F₁-FUTAZ compared to FUMOZ (Table 2.3). The proportion of adults that emerged from pupae was similar in F₁-FUTAZ and FUMOZ ($\chi^2=1.91$, $p=0.167$, Figure 2.4f), with most adults emerging on the second day of pupation (Figure 2.5c).

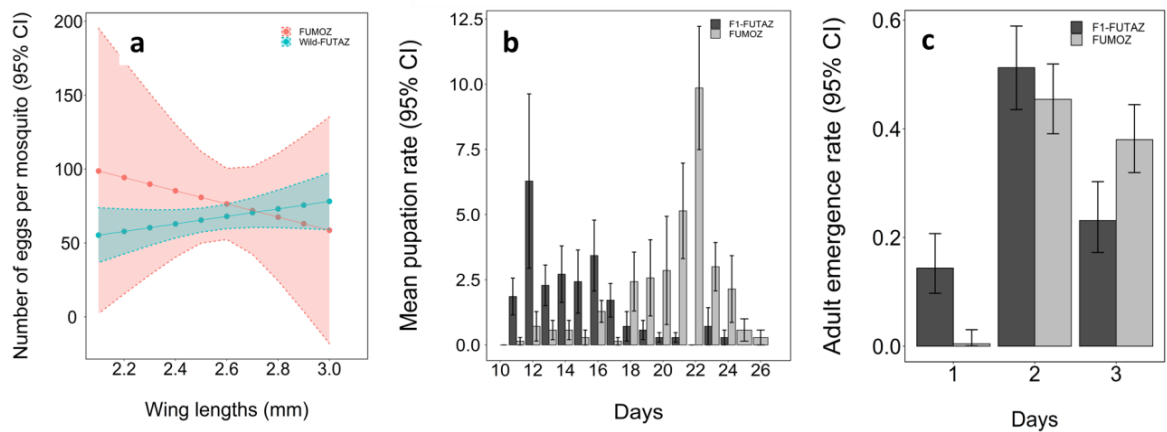


Figure 2.5: *Anopheles funestus* a) relationship between mosquito body sizes and number of eggs produced per *Anopheles funestus* mosquito, b) larvae period and c) adult emergence rate from pupae

2.2.2 Adult survival

The median survival of adult female F₁-FUTAZ was 32 (IQR: 26, 40) and 33 days (IQR: 27, 41) for males (Figure 2.7a, Table 2.4). In FUMOZ, the median survival for females was 52 days (IQR: 39, 56) and 49 days (IQR: 42, 56) for males (Figure 2.7b). There was no difference in the survival of males and females within either strain, F₁-FUTAZ ($p=0.468$, Table 2.4) and FUMOZ ($p=0.752$, Table 2.4). However, restricting analysis to adult females, survival was significantly lower in F₁-FUTAZ than FUMOZ ($p<0.001$, Table 2.3, Figure 2.7c). Likewise, adult male survival was significantly lower in F₁-FUTAZ than FUMOZ ($p<0.01$, Table 2.4).

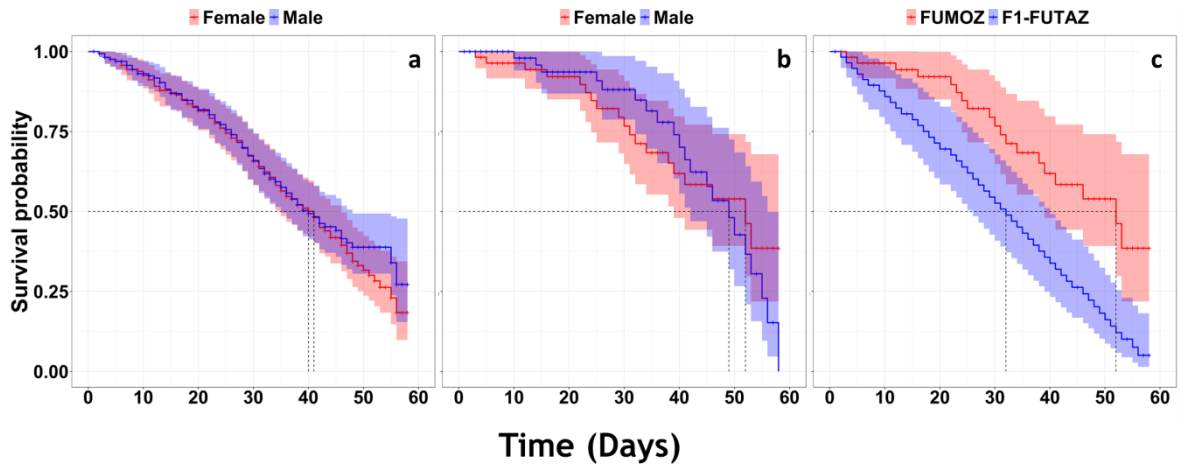


Figure 2.6: Survival curve for *Anopheles funestus* males and females: a) *Anopheles funestus* (F1-FUTAZ) and b) *Anopheles funestus* (FUMOZ) when fed after every five days, c) females of both F1-FUTAZ and FUMOZ. Lines represent the survival function as estimated from fitting the Cox proportion hazard model and shaded area express 95% CI. Dotted grey horizontal and vertical lines show the median survival days.

Table 2.4: Hazard Ratio and median values of the adult survival between males and females of the F₁-FUTAZ and FUMOZ, associated p-values indicate the significance difference of sex and species on the number of days survived by F₁-FUTAZ and FUMOZ strains.

Strain	Sex	Median [IQR]	HR [95% CI]	P-value
F ₁ -FUTAZ	Female	32 [26, 40]	1	=0.468
	Male	33 [27, 41]	0.89 [0.65, 1.24]	
FUMOZ	Female	52 [39, 56]	1	=0.752
	Male	49 [42, 56]	1.11 [0.59, 2.06]	
Female	FUMOZ	52 [39, 56]	1	<0.001
	F ₁ -FUTAZ	32 [26, 40]	2.63 [1.55, 4.46],	
Male	FUMOZ	49 [42, 56]	1	<0.01
	F ₁ -FUTAZ	33 [27, 41]	2.05 [1.22, 3.45]	

2.3 Discussion

Limited understanding of mosquito biology and ecology poses a challenge for the development of effective vector control approaches. Laboratory colonization of target species provides an opportunity to address these knowledge gaps by facilitating detailed investigation of vector biology under controlled conditions where experimental manipulation is possible. Here the fitness traits of *An. funestus* during colonization attempts from a wild population in Tanzania were characterized to identify the bottlenecks that make this species so difficult to colonize. This is the first documentation of fitness constraints during attempted colonization of this species and the first report of attempted colonization of *An. funestus* from Tanzania.

Consistent with most previous attempts, colonization of this wild *An. funestus* population proved unsuccessful with no offspring being produced from the F₁ generation. Several life history processes and demographic traits were identified as being impaired when FUTAZ were brought into the laboratory. First, the number of eggs laid by wild FUTAZ when brought in the insectary was lower than in the well-established FUMAZ line, as were hatching rates, larval survival, mating success and adult female/male survival. F₁-FUTAZ body sizes were slightly smaller compared to their maternal generation in the wild, but did not differ with the FUMAZ strain indicating this trait is unlikely to predict colonization success. Of all these fitness traits, the primary hurdles to colonization are likely to be the extremely low mating success and larval survival of F₁ *An. funestus* in the laboratory. Until these fitness traits can be improved under laboratory conditions, the colonization of *An. funestus* is unlikely to be successful and repeatable.

Eggs laid by wild-FUTAZ *An. funestus* had a low proportion of hatching compared to those of FUMAZ. In both strains, insemination rates were lower than 50%, indicating many were unviable eggs laid by non-inseminated females. Previous studies investigating the impact of different water sources used for larval rearing in an *An. funestus* colony (FUMAZ) indicated that their egg hatching rate can exceed 70% [222,255]; confirming hatch rates in this study were uncharacteristically low. It is known that females of other *Anopheles* species can

produce unviable eggs without successful mating, or after mating with spermless males [256]. Therefore, poor hatching observed in the nascent strain (FUTAZ) here is likely due to the low mating success of *An. funestus* in captivity as has been previously documented in other *Anopheles* species [237], and low hatch rates. Low hatch rates could have been due to suboptimal temperatures in the laboratory relative to conditions in the field; which FUMOZ strain might have been well adapted to it but not FUTAZ [257].

The larval development period of F₁-FUTAZ (11-14 days) was similar to that reported for *An. funestus* in other laboratory settings [222,255,258], but faster than FUMOZ development period (21-23 days) observed in this study. The duration of larval development in *An. funestus* (FUTAZ and FUMOZ) observed here were considerably longer than described for *An. gambiae* complex in the laboratory [259]. For example, life table analyses of *An. gambiae* indicate a larval development period from eclosion to adult emergence of about 11 days at 27°C [32,48,52,259,260]. This extended larval development period for F₁-FUTAZ results in a long estimated generation time of 30 - 33 days from eggs to first oviposition; which is higher than estimated for other African *Anopheles* species [255,261,262]. Other life table analyses performed on *An. funestus* colonies estimated a generation time of approximately 33 days in insecticide-resistant (FUMOZ) and susceptible strains (FANG) [222]. As a consequence of this extended period of larval development, egg to pupa survival was very low; approximately 6% for F₁-FUTAZ and 27% for FUMOZ. Due to this long larval development and associated high larval mortality, very large numbers of eggs would be required generate modest numbers of adults in the laboratory. Therefore, the fitness and reproductive success of these resulting adults would have to be very high to yield a further generation.

Analysis of wild FUTAZ adults and their F₁ offspring indicate their fitness is reduced compared to that of a stable *An. funestus* colony (FUMOZ). Wild-FUTAZ *An. funestus* brought into the laboratory laid 16% fewer eggs than the FUMOZ colony, and the F₁ generation of FUTAZ produced no viable eggs at all. A previous study measuring the fecundity of F₁ *An. funestus* using Madagascan population reported that this species can lay an average of 56 to 108 eggs per mosquito in captivity [237], which corroborates with 65 and 76 eggs from wild-

FUTAZ and FUMUZ, respectively, from the current study. The number of eggs here is consistent to that reported in resistant and susceptible *An. funestus* strains in the laboratory, [222].

Mosquito body size is often interpreted as a proxy of their fitness [61,263,264]. Here, wild FUTAZ were somewhat larger in body size than F₁-FUTAZ and FUMUZ. Consistent with the hypothesis of body size being an indicator of fitness, wing length was positively correlated with fecundity in the wild population of *An. funestus* (FUTAZ). However, the opposite was seen in the stable FUMUZ strain where wing size was negatively associated with fecundity. Thus, at least in this one stable laboratory colony, large body size in *An. funestus* was not a good indicator of reproductive success. Caution is required in extrapolating fitness differences based on *An. funestus* body size, particularly between field and laboratory strains. Although body size was higher in wild-FUTAZ than F₁-FUTAZ, the latter strain was still bigger than the FUMUZ which had the highest fecundity.

The mating success of *An. funestus* from these populations was extremely low in the laboratory, supporting hypothesis that mating is the key bottleneck for the colonization of this species. Compared to wild-FUTAZ, insemination rates in F₁-FUTAZ were extremely low (9.2% vs. 72%) and insufficient to establish a further F₂-FUTAZ generation. This poor mating success is likely due eurygamy, the inability of some *Anopheles* species including *An. funestus* to initiate natural swarming behaviour in flight [265,266]. These findings match those of other studies documenting mating as the major obstacle for successful colonization of *An. funestus* [170,237,267]. To overcome this problem, techniques such as forced mating and exposing mosquitoes during sunset to induce swarming have been applied [268,269]. Other studies have experimented with the use of large cages to stimulate natural mating for *Anopheles*, and simulate sunset which may be crucial cue for mating [270,271]. However so far these methods have had little or no success over multiple attempts [104,170]. In the current study, no F₂-FUTAZ offspring were generated because none of the F₁-FUTAZ laid viable eggs. Further research on how to induce mating behaviour in *An. funestus*, particularly using more realistic semi-field systems, would be of great value. Such studies

must focus on both females and males, to determine if males are unwilling to initiate swarming behaviour or not fit enough to do so.

Analysis of adult mosquito survival indicated that the nascent Tanzania colony (F₁-FUTAZ) had a reduced lifespan compared to stable *An. funestus* colony (FUMOZ). However adult survival in both cases was relatively high (32 median days for FUTAZ and 52 days for FUMOZ); with both strains living well beyond the minimum period required to produce eggs and transmit malaria. Another laboratory study conducted on FUMOZ where adult life span ranged from 39 to 64 days [222]; again much higher than F₁-FUTAZ here. The shorter life span of FUTAZ relative to FUMOZ may be a result of the stress from the change of environment, or lack of adaption to laboratory conditions. Nevertheless, this F₁-FUTAZ survived much longer compared to another competent vectors of malaria transmission, *Anopheles arabiensis* and *An. gambiae* s.s. in laboratory conditions [81]. Previous experiments on parity shows that the median survival of *An. funestus* in the wild is much shorter, ranging from 7-10 days [41]. Thus, poor adult survival relative to the wild cannot explain the failure of colonization here.

A potential limitation of my study is that the unfed *An. funestus* females were used to seed laboratory colonies, requiring me to blood feed them artificially (on chicken blood) in the laboratory to acquire eggs for the next generation. Thus, the mating status and age of the wild females used for colonization were uncertain and likely variable. An alternative would have been to collect only visibly blood fed females during field collections (these individuals would likely had fed on humans if caught inside houses), and used their eggs to generate the F1 generation. This was considered, but given the much lower abundance of blood fed *An. funestus* inside houses compared to the numbers of unfed females that can be obtained in CDC light traps; the latter approach was chosen to ensure sufficiently large samples were obtained for colonization experiments. These wild mosquitoes could not be provided with a human blood meal given their malaria infection status was unknown and they were not adapted to membrane feeding, thus chicken blood was provided. This variation in host blood source could have generated some differences in fitness between strains. However, this is unlikely given that previous studies indicate that human and

chicken blood meals generate similar egg production in other African malaria vector species under laboratory conditions (*An. arabiensis* and *An. gambiae* [78,81]). The F₁ population, upon which the main fitness indicators were assessed, was fed on human blood. Further investigation is required to confirm whether *An. funestus* fitness is impacted by the type of host blood meals provided and whether there is an optimal diet for laboratory maintenance.

2.4 Conclusions

Laboratory colonies remain fundamental for research on the biology and control of mosquito vectors by providing a stable and standardized source of mosquitoes for experimental studies. This study provides additional evidence of the intractability of *An. funestus* to colonization. By quantifying a comprehensive range of fitness traits during unsuccessful attempts, this study generates insights into the most important barriers to colonization. Of the range of traits investigated, the primary barrier to colonization was identified as low mating success, compounded further by the slow development and poor survival of the small numbers of larvae produced. Additionally, both the fecundity and adult survival of *An. funestus* offspring from wild parents were reduced under laboratory conditions, but these impacts may have been relatively minor compared to the consequences of poor mating success and poor larval survival. This combination of fitness deficits presents a major challenge for successful colonization and mass rearing of *An. funestus*. To overcome this, future research should focus on enhancing the efficiency these life-cycle processes under insectary conditions. Additionally, the demographic rates estimated from wild and F₁ FUTAZ will provide useful baseline information for understanding and modelling *An. funestus* population dynamics in general, and guiding further attempts to its colonization.

3.0 Chapter 3: A statistical calibration tool for methods used to sample outdoor-biting mosquitoes

Published in Parasite & Vectors Journal 2022: <https://doi.org/10.1186/s13071-022-05403-7>

Abstract

Background

Methods for sampling outdoor-biting mosquitoes are urgently needed to improve surveillance of vector-borne diseases. Such tools could potentially replace the human landing catch (HLC), which, despite being the most direct option for measuring human exposure, raises significant ethical and logistical concerns. Several alternatives are under development but detailed evaluation still requires common frameworks for calibration relative to the HLC. The aim of this study was therefore to develop and validate a framework for predicting HLC-derived outdoor exposure rates from different exposure-free alternatives for African malaria (*An. arabiensis* and *An. funestus*) and filariasis (*Culex* spp.) vectors.

Methods

I obtained mosquito abundance data (*Anopheles arabiensis*, *Anopheles funestus* and *Culex* sp.) from a year-long Tanzanian study comparing six outdoor traps and the HLC. The outdoor traps were: Suna Trap (SUN), BG Sentinel (BGS), M-Trap (MTR), M-Trap + CDC (MTR-C), Ifakara Tent Trap-C (ITT-C) and Mosquito Magnet Trap (MMX). Four generalised linear models were developed within a Bayesian framework to investigate associations between traps and the HLC; considering intra- and inter-specific density dependence. The best model was used to create a calibration tool for predicting HLC-equivalents of each trap for each vector group.

Results

For *An. arabiensis*, SUN catches had the strongest correlation with HLC ($R^2=19.4$), followed by BGS ($R^2=17.2$), MTRC ($R^2=13.1$). The least correlated was MMX ($R^2=2.5$). For *An. funestus*, BGS had the strongest correlation with the HLC ($R^2=53.4$), followed by MTRC ($R^2=37.4$), MTR ($R^2=37.4$). The least favoured was SUN ($R^2=14.5$). For *Culex* mosquitoes, the traps most highly correlated with the HLC were MTR ($R^2=45.4$) and MTRC ($R^2=44.2$). In general, the association between the HLC and alternative trapping methods was the best described through a simple linear relationship. Only BGS in all the three species exhibit a non-linear relationship which is modified by intra and interspecies mosquito density. An interactive *Shiny App* calibration tool was developed for this and similar applications.

Conclusion

I successfully developed a calibration tool to assess the performance of outdoor-traps relative to this HLC to provide a framework for assessing human exposure. The performance of candidate traps relative to the HLC varied between mosquito taxa, thus there was no single optimal method. Though all the traps underestimated HLC catches (proxy for human-biting rates), it was possible to mathematically define their representativeness against HLC. Further studies should focus identifying traps that have the greatest consistency and representativeness relative to the HLC, as opposed to simply finding traps that catch the most mosquitoes.

3.0 Background

Malaria control primarily relies on the use of Insecticide Treated Nets (ITNs) and Indoor Residual Spraying (IRS) [123,182,183,272]. LLINs and IRS provide protection by targeting mosquitoes that are host seeking or resting indoors. Wide-scale use of these tools has yielded significant progress but there are still challenges such as insecticide resistance [176,212,214,273] and outdoor-biting [77,89,90]. Drivers of outdoor-biting may include human behaviours [274-276], plasticity in mosquito behaviours (e.g. shifting from feeding indoors to outdoors) [16,79,103,212] and the effects of some indoor interventions [181,277]. Sampling mosquito populations is a core component of malaria surveillance activities [278], and it's aims include determining when and where people are most at risk. For best results, this surveillance should consistently capture the key drivers of biting risk indoors and outdoors. Unfortunately, representative sampling of mosquito vectors remains a challenge; particularly in outdoor settings.

The main entomological indicators assessed during vector surveillance include the Human Biting Rate (HBR) [103,279], sporozoite infection prevalence in mosquitoes [280,281], the Entomological Inoculation Rate (EIR) [88,279], time of exposure and proportion of exposure prevented by ITNs [108,109,124,282]. The HBR is a fundamental variable for estimating the transmission of malaria and other mosquito-borne diseases [65]. As defined in the Ross MacDonald model, the HBR is required for estimation of the reproductive rate (R_0) of malaria. Both the HBR and sporozoite prevalence are required for estimation of EIR [65]; calculated as the number of infectious bites a person would be expected to receive in a given location over a given time period. The HBR and EIR are frequently used to estimate the impact of vector control interventions by highlighting how much they reduce exposure [76,93,182,279].

The Human Landing Catch (HLC) has been the gold standard for direct measurement of human exposure and other key entomological variables. However, this method has several limitations and ethical constraints [118,119,283-285] due to its requirement that human volunteers expose parts of their body (usually lower legs) to mosquitoes [129,282,286]. Due to this combination of ethical concerns and practical limitations, it is widely

recognized that alternative exposure-free methods for measuring the HBR are needed [121,122,282,286,287]. Alternatives such as CDC light traps are already widely used for sampling host-seeking mosquitoes indoors [114], but are unsuitable in outdoor settings. The urgency to identify suitable methods for measuring exposure outdoors is therefore greater [123,125,282,288], especially due to the growing recognition of the importance of outdoor exposure to residual transmission [77,93,274].

To date, a number of alternative exposure-free methods have been independently developed and tested in different settings in Africa (e.g. [122-124,282,286,288-291]). Some methods provide a good representation of vector species composition and their biting activities, but underestimate density (e.g. [123,287,288]). Others catch more mosquitoes than the HLC and thus overestimate typical human exposure (e.g. [122,292]). Finally there are some traps that are easy to implement, but which provide biased estimates of outdoor exposure by disproportionately sampling endophilic rather than exophilic species (e.g. [293]). These strengths and weaknesses suggest that different traps are optimal for different surveillance applications. Unfortunately, there are no standardized calibration methods to allow estimation of HLC-equivalent exposure from different outdoor sampling methods. Development of a standardized and validated calibration framework for such prediction would enable comparison of results from different studies and methods. Such a calibration tool would need to reflect the potential non-linear relationship between trap counts and HLC values; meaning that no single conversion 'value' between methods may apply across the full range of mosquito densities or species.

Several studies have indicated that trap performance relative to the HLC is density dependent [114,294]. However, density dependence is often considered in terms of "intraspecific" density (e.g. the baseline density of the target vector species [282,294]) but not the density of all mosquitoes, target vectors or not, that are attracted to the trap. However, the mechanisms that could give rise to intra-specific density dependence in trap performance could also generate dependence with the overall densities of all mosquitoes attracted to the trap; including other species not of interest. While such interspecific dependence on the wider mosquito community is plausible, this has not been

formally evaluated in trap evaluation studies.

The overall aim of this study was to provide an extensive comparison of six exposure-free traps for 3 vectors (*An. arabiensis*, *An. funestus* and *Culex* sp. which is the common mosquito group and a vector of filariasis in Tanzania). Specifically, I aimed to 1) identify valid and safe alternatives to the HLC for outdoor mosquito' sampling that are exposure-free and do not rely on human participants, 2) assess of contribution of intra and interspecific mosquito density dependence to trap performance, and 3) develop an interactive calibration tool (in the form of a Shiny App) through which the number of a given species caught in an HLC can be predicted from catches made by alternative traps.

3.1 Methods

3.1.1 Study area and vector species

Prior to the start of my PhD., a team from the Ifakara Health Institute carried out a mosquito trapping study in six adjacent villages in the Ulanga and Kilombero districts of south-eastern Tanzania, namely: Kivukoni (8.2135°S, 36.6879°E), Minepa (8.2710°S, 36.6771°E), Mavimba (8.3124°S, 36.6771°E), Milola (8.3306°S, 36.6727°E), Igumbiro (8.3511°S, 36.6725°E) and Lupiro (8.385°S, 36.670°E). Data were collected over 12 months between 2015 and 2016. The valley has relatively high mosquito abundance which peaks at the end of the rainy season. The common vectors of malaria transmission are *Anopheles arabiensis* and *Anopheles funestus* [88,103,295]. Mosquitoes in the *Culex* genera are also highly abundant, with some species being potential vectors for arboviruses found in the study area [120,296].

3.1.2 Data collection

I was not involved in the design of this study or the field data collection, but the data were made available to me for analysis in my PhD. Mosquito sampling was carried out in both the wet and dry seasons, using six different traps for sampling outdoor-biting mosquitoes around human dwellings. The traps were: Mosquito Magnet trap (MMX) [297], BG-Sentinel trap (BGS) [298], Suna trap (SUN)

[123], Ifakara Tent Trap-C (ITT-C) [291], M-Trap (MTR) [299], M-Trap fitted with CDC Light trap (MTRC) (this study) and the Human Landing Catches (HLC) [123]. Most of these traps have been extensively described elsewhere except for the MRT fitted with a CDC light trap (MTR), which was adapted from the original exposure-free M-trap designed by Mwangungulu *et al* [299]. In this current study, the original MRT was divided into two compartments made of UV-resistant shade netting: one in which a human volunteer sat to attract mosquitoes and the other section in which mosquito are entered [299]. A CDC light trap was suspended inside the other section of the trap to attract more mosquitos to the light source.

The traps were located at least 100m apart. Initial trap allocation was random, but their positions were switched over successive sampling nights in a Latin square design. This way each trap was used in each position once over a seven night cycle. After completion of each cycle, the study team moved to the next village so that one round of sampling in all six villages was completed over 42 trap-nights. Six rounds of data collection were completed spanning the wettest and the driest periods of the year (252 trap nights between April 2015 and April 2016). Mosquito sampling was done overnight from 6pm to 6am. The collected mosquitoes were morphologically sorted by taxa. A subsample of *An. gambiae* s.l. (n=1,405, 26% of total) were analysed by PCR [71] to assess sibling species composition within the complex.

3.1.3 Model fitting

The main goal of analyses was to create a calibration tool to evaluate outdoor mosquito traps and to validate the tool by comparing the performance of candidate trapping methods relative to HLC, the “gold standard”. In particular, I wanted to test the shape of the association curve linking the numbers of mosquitoes collected by each trap type with those collected by the HLC. First, I pooled all the hourly collections into a single collection cup per trap per night. Then, for each of the focus mosquito groups (*Culex* genera, *An. arabiensis* and *An. funestus* s.l), I modelled nightly HLC catches as a function of the catching rate of each alternative trap.

Four linear models were developed within a Bayesian model fitting framework to allow me to test for linear and non-linear associations through increasing the levels of complexity. The Bayesian approach allowed specific constraints on parameters based on biological plausibility, in the form of priors and uncertainty when converting the counts from alternative traps into HLC equivalent values in the form of full posteriors.

For any given trap and mosquito group, I defined the response variable (N_i) as the number of female mosquitoes on every i^{th} sampling night. Preliminary investigation of data using Poisson likelihood showed over-dispersion for all the three mosquito groups. Final models did not account for other environmental covariates at specific trap locations (e.g. temperature, humidity). Initial analysis suggests that, environmental covariates did not improve model fitting. I accounted for the over-dispersion by using a negative binomial likelihood model formulated as a Gamma-Poisson mixture distribution [300]:

$$N_i \sim \text{Poisson}(\theta_i \lambda_i)$$

with

$$\theta_i \sim \text{Gamma}(\tau, \tau)$$

Where the Poisson rate λ_i is defined by the shape of the relationship between N_i and the number of mosquitoes collected with the alternative trap (n_i , Table 3.1) and theta θ_i was drawn from a gamma distribution with parameter tau τ as rate and shape of 1.

Since the algebraic form of this relationship is not known, I made three assumptions with specified mathematical definitions, as follows: 1) that the relationship must start at the origin (i.e. when HLC catches zero mosquitoes, the other traps will, on average also collect zero mosquitoes), 2) that the relationship is positive (i.e., no negative relationships between trap catches), and 3) that any given trap could potentially suffer from a density effect (i.e., the slope of the relationship is not constant and it can change according to the abundance of mosquitoes, either just of the same mosquito group or of all mosquitoes).

To define λ_i , I therefore formulated four possible scenarios to describe the relationship between HLCs and other trapping methods as summarized in Table 3.1 and Figure 3.1. In Model 1, I considered a simple linear relationship between N_i and n_i (Table 3.1, Figure 3.1A)¹. In Model 2 I tested if the efficiency of the alternative trap was dependent on the density of the focal mosquito (e.g. “intra-specific” density dependence) by adding a quadratic term n_i^2 (Table 3.1, Figure 3.1B). In Model 3 I tested if the captures of a given group by a given trap were dependent on the abundance of the other taxonomic groups (e.g. “inter-specific” density dependence) by adding, an interaction term between n_i and the number of all the females from other mosquito groups collected with the same trap (m_i) (Table 3.1, Figure 3.1C). Model 4 was similar to Model 3, but I considered all the other K_i taxonomic groups separately. Therefore it included all the pair wise interaction terms between n_i and the number of females of each k^{th} mosquito group (s_{k_i}) (Table 3.1, Figure 3.1D). My analysis mainly focused on three mosquito groups, but I collected a higher number of species hence $K > 3$ (Table 3.2).

Table 3.1: Description of models used to investigate the relationships between female mosquito catches by human landing catch and the alternative traps.

Model	Structure
Model 1	$\log(\lambda_i) = \beta_1 n_i$
Model 2	$\log(\lambda_i) = \beta_1 n_i + \beta_2 n_i^2$
Model 3	$\log(\lambda_i) = \beta_1 n_i + \beta_2 n_i m_i$
Model 4	$\log(\lambda_i) = \beta_1 n_i + \sum_{k=1}^K \beta_k n_i s_{k_i}$

The analysis was performed in the statistical environment R version 4.0 [246], with Bayesian model fitting to the data done using the program JAGS [301] interfaced within R via the package *rjags* [302]. For parameters β_1 , β_2 and β_k I used a gamma prior (shape = 0.1, rate = 0.1). The prior for β_1 was chosen to ensure a positive relationship between n_i and N_i and a positive effect of the

¹ Note that this relationship is not linear. See Chapter 7 (Addendum to chapter 3) for a corrected version of this analysis including model formulas as described in Table 3.1.

quadratic and the interaction terms for β_2 and β_k . To achieve convergence, the models were run for up to 3×10^4 iterations. Means of posterior distributions with corresponding credible intervals were obtained for each model coefficient β . I compared different models by their Deviance Information Criteria (DIC) and the goodness of fit of each model using pseudo R^2 values. Models with the lowest DIC were selected as best.

3.1.4 Interactive calibration tool

I designed a lookup table (Table 3.3) containing means of posterior predictions for different combinations of mosquito taxa, trap types and models. This allowed me to predict the expected number of a given mosquito taxa from an HLC (with credible intervals) based on the number caught in the alternative traps. I also developed an interactive online tool, in the form of an *R Shiny* App [303] to facilitate these evaluations. This tool provides users with an interactive graphical user interface (GUI) to select the number of captured mosquitoes for a group of interest by trap type, and to explore the predicted number of mosquitoes caught in an HLC by method.

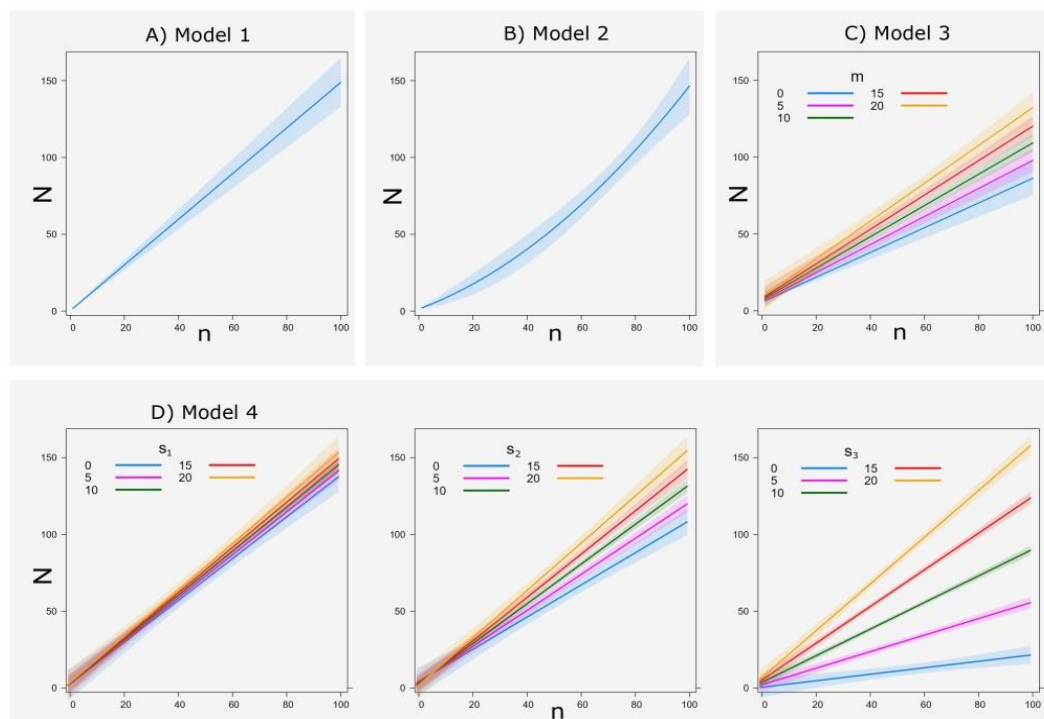


Figure 3.1: Illustration of models used to investigate the relationship between number of female mosquitoes collected with human landing catch and six alternative traps.

N : Number of female mosquitoes collected with human landing catch; n : number of female mosquitoes collected with a given alternative trap; m : pooled female

mosquitoes of all the other species collected with the same alternative trap of n ; s_1 , s_2 and s_3 : number of female mosquitoes of each of the other K species, where K refers to all the species collected I developed the focus one (here $K = 3$). Model 1 considers a simple linear relationship with n (A). Model 2 considers a quadratic term n^2 (B). Model 3 includes an interaction term between n and the number of all the females of the other species collected with the same trap (m) (C). Model 4 considers all the pairwise interaction between n and s_1 , s_2 and s_3 (D).

3.2 Results

The statistical correlations between HLCs and other trapping methods for each of the three mosquito groups are summarized in Table 3.2. The fit of models varied between trap types and mosquito group, with correlations with the HLC (R^2 values) ranging from 0.8% - 53.4% (Table 3.2). The strength and nature of associations (Models 1-4) varied considerably between mosquito groups and traps; thus no one single model was best in all cases. I provide an example of a prediction table (Table 3.3) which describes how mosquito abundance in a HLC can be estimated from catches made by the alternative traps (using model 1, with intervals grouped by 10). Other models (model 2-4) outputs/predictions can be easily retrieved from the *Shiny* App tool. Environmental covariates (temperature and humidity) were dropped during the initial model fitting process as they were not improving the goodness of fit of the model (Model 1-4).

Table 3.2: Summary of all other mosquitoes collected for each trap type including the Human Landing Catches (HLC)

Species	HLC	SUN	BGS	ITT-C	MMX	MTRC	MTR
<i>Anopheles arabiensis</i>	5282	1187	531	615	370	2125	1454
<i>Anopheles funestus</i>	226	66	40	76	37	115	115
<i>Anopheles coustani</i>	670	1216	207	3	444	564	314
<i>Anopheles pharoensis</i>	101	906	82	0	69	103	76
<i>Anopheles squamosus</i>	56	196	49	1	99	145	127
<i>Anopheles wellcomi</i>	16	3	3	0	9	72	25
<i>Anopheles ziemani</i>	204	1368	183	0	269	340	156
<i>Culex sp.</i>	7191	3666	3709	4970	1018	7710	6645
<i>Mansonia sp.</i>	2101	4527	1001	111	1961	2314	1273
<i>Aedes aegypti</i>	20	2	5	2	30	7	5
<i>Coquellitidia</i>	240	84	117	14	56	127	229

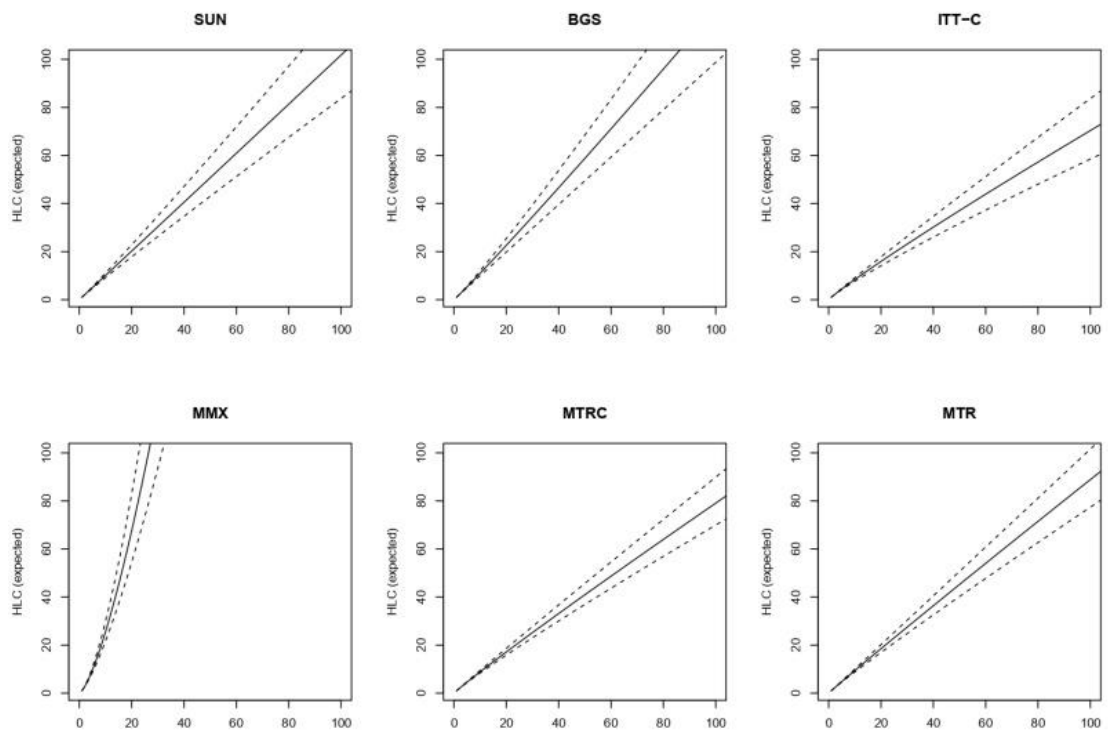


Figure 3.2: Expected number of female *Culex spp.* mosquitoes collected with HLC (y-axis), given the number of females collected with alternative traps (x-axis). Continuous line is the prediction of a Gamma-Poisson model assuming a linear relationship; dashed lines are 95% credible intervals.

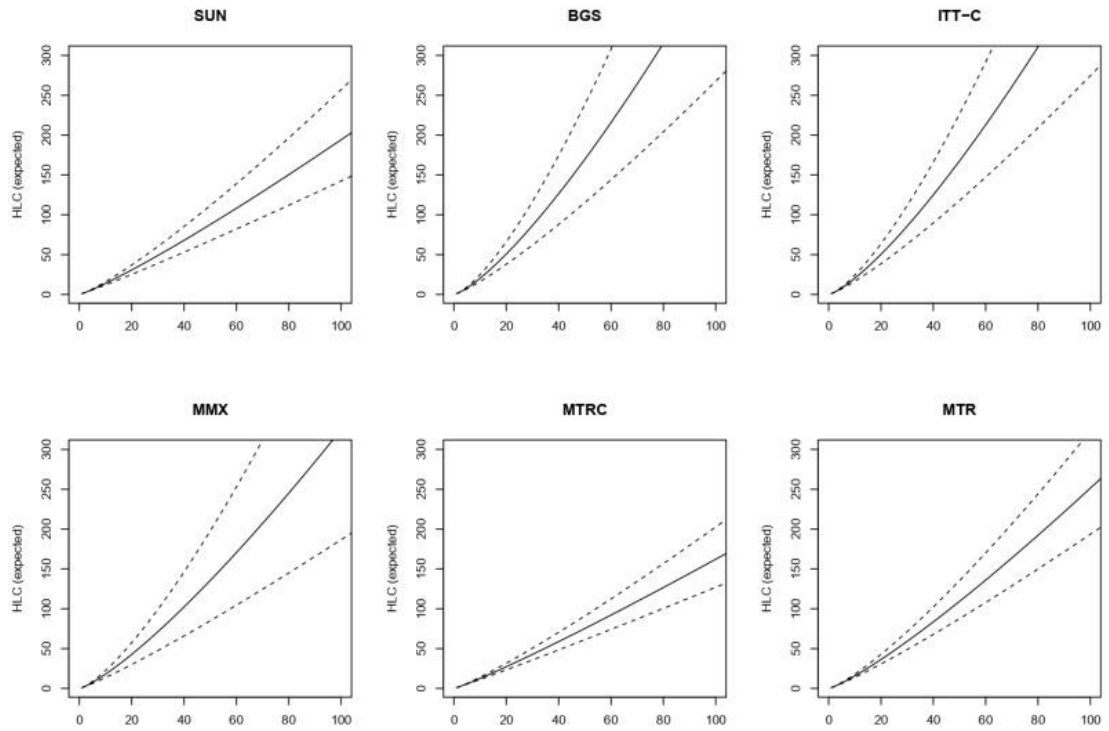


Figure 3.3: Expected number of female *Anopheles arabiensis* mosquitoes collected with HLC (y-axis), given the number of females collected with alternative traps (x-axis). Continuous line is the prediction of a Gamma-Poisson model assuming a linear relationship; dashed lines are 95% credible intervals.

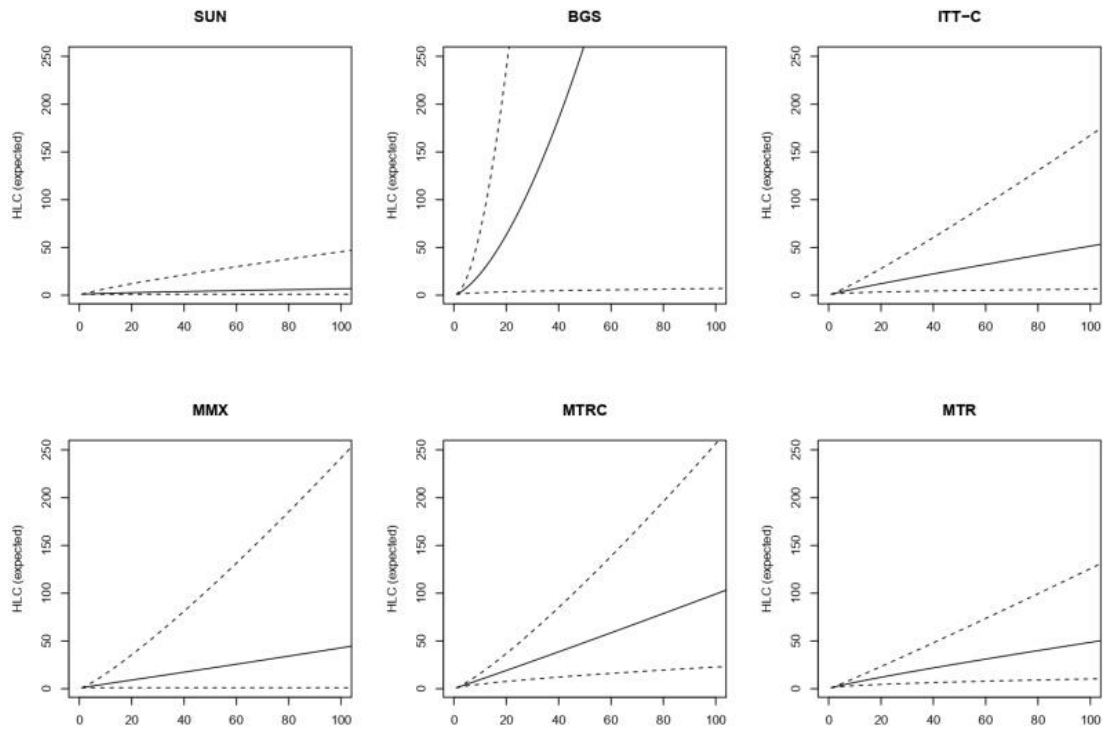


Figure 3.4: Expected number of female *Anopheles funestus* mosquitoes collected with HLC (y-axis), given the number of females collected with alternative traps (x-axis). Continuous line is the prediction of a Gamma-Poisson model assuming a linear relationship; dashed lines are 95% credible intervals.

3.2.1 *Anopheles arabiensis*

In most of the models, trap catches of *An. arabiensis* were only weakly correlated with HLC counts (Table 3.2b). SUN was the only alternative trap where the correlation with the HLC was consistently 17% or more ($R^2 > 17$). For this trap, the relationship with HLC catches was best described by Model 4 ($R^2 = 19.4$, Table 3.2b), which incorporates both intra- and interspecific density dependence. The DIC values however did not vary much between models of differing complexity ($\Delta DIC = 1.32$, Table 3.2b). Overall, SUN consistently underestimated HLC catches (for example 100 mosquitoes collected with SUN corresponded to 194 [CIs: 142-257]; Table 3.3b, Figure 3.3).

Table 3.3: Summary (R^2 and DIC values) of models used to investigate the relationship between the numbers of female mosquitoes collected with human landing catch (HLC) and the six alternative outdoor traps. See Table 1 for description of models.

Species and Model	SUN R^2	SUN DIC	SUN Δ DIC	BGS R^2	BGS DIC	BGS Δ DIC	ITT-C R^2	ITT-C DIC	ITT-C Δ DIC	MMX R^2	MMX DIC	MMX Δ DIC	MTRC R^2	MTRC DIC	MTRC Δ DIC	MTR R^2	MTR DIC	MTR Δ DIC
a) <i>Culex</i>																		
Model 1	27.3	1026.6	2.36	25.1	1038.3	0.00	19.0	769.3	5.07	12.4	841.0	12.50	44.7	1236.5	7.95	44.2	1174.7	6.00
Model 2	27.1	1025.3	1.05	25.1	1045.2	6.88	19.2	770.2	5.88	12.8	838.7	10.27	44.8	1236.1	7.62	44.2	1177.1	8.42
Model 3	27.2	1027.5	3.25	24.9	1040.6	2.32	19.4	769.1	4.78	12.8	828.5	0.00	44.7	1228.5	0.00	44.2	1168.7	0.00
Model 4	28.1	1024.3	0.00	25.5	1044.5	6.23	21.9	764.3	0.00	15.9	835.5	7.03	45.4	1235.8	7.29	43.8	1172.5	3.77
b) <i>An. arabiensis</i>																		
Model 1	17.4	780.3	0.00	10.8	549.6	0.61	9.3	534.7	6.37	0.8	383.9	3.51	13.1	991.6	4.43	11.3	1077.6	12.95
Model 2	17.5	780.3	0.03	10.8	549.0	0.00	9.4	528.3	0.00	0.4	382.8	2.46	10.0	1000.8	13.68	11.3	1073.0	8.37
Model 3	17.4	782.5	2.21	10.7	550.9	1.89	10.4	534.5	6.17	1.4	385.8	5.42	13.1	987.1	0.00	11.3	1070.5	5.84
Model 4	19.4	781.6	1.32	17.2	551.2	2.19	11.8	530.6	2.30	2.5	380.3	0.00	12.7	990.5	3.39	11.1	1064.6	0.00
c) <i>An. funestus</i>																		
Model 1	14.6	76.5	2.79	46.6	52.9	0.00	33.9	111.5	0.00	31.8	40.9	0.62	32.6	151.1	1.43	36.8	120.0	0.00
Model 2	14.5	77.0	3.30	50.2	53.7	0.78	33.6	112.5	0.97	30.6	40.3	0.00	32.4	149.6	0.00	36.6	120.6	0.56
Model 3	14.5	76.0	2.29	52.6	53.4	0.50	34.3	112.4	0.87	30.6	40.7	0.35	33.4	151.2	1.53	36.3	122.5	2.45
Model 4	16.2	73.7	0.00	53.4	53.8	0.87	34.3	112.2	0.69	30.0	40.4	0.09	37.4	152.8	3.13	37.4	120.7	0.65

SUN: Suna trap, BGS: BG-Sentinel trap, ITT-C: Ifakara Tent Trap version C, MMX: Mosquito Magnet trap, MTRC: M-trap combined with CDC Light, MTR: M-trap;

BGS was the only trap where R^2 values substantially increased with model complexity. Here, the most complex model (Model 4), which incorporated intra- and interspecific density dependence had an R^2 value of 17.2% (Table 3.2b). For all other trap types, correlations with the HLC were best explained by the simplest linear relationship (Model 1). Collections from BGS also underestimated the number of mosquitoes caught by HLC, and to a larger extent than the SUN (e.g. 100 mosquitoes caught by BGS is equivalent to 423 [CIs: 268-629] by HLC; Table 3.3b, Figure 3.3).

The MMX trap had the poorest correlation and was least representative of the HLC (R^2 values: 0.8 - 2.5%); particularly at low densities where it often failed to capture any individuals. This trap therefore also significantly underestimated the catches relative to HLC (for example 100 catches of MMX is equivalent to 325 [CIs: 187-504]; Table 3.3b, Figure 3.3).

3.2.2 *Anopheles funestus*

There were no major differences between the alternative models when describing associations between HLC and the other traps for collecting *An. funestus*. Thus on the basis of parsimony, I concluded that the simple linear model (Model 1) was sufficient to describe these relationships. BGS was the most highly correlated with the HLC (R^2 ranged from 46.6% to 53.4%) in *An. funestus*. The highest R^2 value was from the most complex model (Model 4). However, similar to *An. arabiensis*, the BGS underestimated the number of *An. funestus* caught by HLC (Table 3.3c). On the other hand, MTR, MTRC, ITT-C and MMX traps were only moderately correlated with HLC (R^2 values ranging from 30.0 to 37.4%), and SUN was the worst performing trap for this species (Table 3.2c).

In general, predictions obtained with all *An. funestus* trap models (Models 1-4, for all trap types) were characterized by very large credible intervals (Figure 3.4), meaning that there was insufficient precision to define a useful calibration factor. This large uncertainty amount HLC equivalent of trap catches was particularly pronounced at higher *An. funestus* densities.

Table 3.4: Predicted values for estimating the expected mosquito catches by human landing catch and alternative traps, according to the linear model (Model 1). Numbers in the first column refer to the mosquitoes collected with a given trap. To obtain the estimate of the equivalent number that one would collect with HLC, refer to the column corresponding to the trap itself. Numbers in brackets are (95% credible intervals).

	Collected	Expected HLC					
		SUN	BGS	ITT-C	MMX	MTRC	MTR
a) <i>Culex spp.</i>	10	10 (9-11)	11 (10-12)	8 (8-9)	25 (22-30)	9 (8-9)	9 (9-10)
	20	20 (18-23)	23 (20-25)	16 (14-18)	68 (54-83)	17 (16-19)	19 (17-20)
	30	30 (26-35)	35 (30-39)	23 (20-26)	120 (94-150)	25 (23-28)	27 (25-30)
	40	41 (35-47)	47 (40-54)	30 (26-35)	179 (137-230)	33 (30-37)	36 (33-40)
	50	51 (43-59)	59 (49-68)	37 (32-43)	246 (185-320)	41 (37-46)	45 (40-51)
	60	61 (51-72)	71 (59-83)	44 (37-51)	318 (236-418)	49 (44-55)	54 (48-61)
	70	71 (59-84)	83 (69-98)	51 (43-59)	395 (290-525)	56 (50-63)	63 (55-71)
	80	81 (68-97)	96 (79-114)	57 (48-68)	476 (347-639)	64 (57-72)	72 (63-81)
	90	92 (76-110)	108 (89-129)	64 (53-76)	562 (406-760)	72 (63-81)	80 (70-91)
	100	102 (84-123)	121 (99-145)	70 (59-84)	652 (467-888)	79 (70-90)	89 (77-102)
b) <i>An. arabiensis</i>	10	14 (12-16)	20 (16-25)	20 (17-24)	18 (14-22)	13 (11-14)	16 (14-18)
	20	31 (25-37)	51 (38-66)	50 (39-64)	43 (30-57)	27 (23-32)	36 (31-43)
	30	49 (39-60)	87 (62-117)	86 (63-112)	71 (48-99)	43 (36-51)	59 (49-71)
	40	68 (53-85)	126 (88-175)	125 (90-166)	102 (66-146)	59 (48-70)	84 (68-102)
	50	88 (67-111)	170 (115-239)	168 (118-227)	135 (85-198)	75 (61-91)	109 (88-135)

	Collected	Expected HLC					
		SUN	BGS	ITT-C	MMX	MTRC	MTR
b) <i>An. arabiensis</i>	60	108 (82-139)	216 (144-308)	213 (147-292)	170 (105-253)	92 (74-112)	136 (108-170)
	70	129 (97-167)	264 (174-382)	261 (178-361)	207 (125-311)	109 (87-134)	164 (129-207)
	80	150 (112-196)	315 (204-460)	311 (209-435)	245 (145-373)	127 (100-157)	192 (150-244)
	90	172 (127-226)	368 (235-543)	363 (241-512)	284 (166-437)	144 (114-179)	222 (172-283)
	100	194 (142-257)	423 (268-629)	417 (275-592)	325 (187-504)	162 (127-203)	251 (194-323)
c) <i>An. funestus</i>	10	2 (1-7)	22 (3-67)	7 (3-13)	5 (1-16)	10 (5-16)	7 (3-11)
	20	3 (1-12)	63 (4-237)	12 (3-28)	9 (1-35)	19 (8-37)	12 (5-23)
	30	3 (1-17)	118 (4-497)	17 (4-44)	13 (1-58)	29 (10-60)	17 (6-36)
	40	4 (1-21)	185 (5-840)	22 (4-60)	17 (1-81)	39 (12-85)	22 (6-48)
	50	4 (1-26)	263 (5-1262)	27 (5-77)	21 (1-106)	49 (14-111)	26 (7-61)
	60	5 (1-30)	352 (6-1760)	32 (5-95)	26 (1-131)	59 (16-139)	31 (8-74)
	70	5 (1-34)	452 (6-2332)	37 (6-113)	30 (1-158)	69 (18-167)	35 (9-86)
	80	6 (1-38)	561 (6-2975)	42 (6-131)	34 (1-185)	79 (20-196)	40 (9-99)
	90	6 (1-42)	679 (7-3689)	47 (6-149)	38 (1-213)	89 (21-226)	44 (10-113)
	100	7 (1-46)	807 (7-4471)	51 (6-167)	43 (1-242)	99 (23-256)	49 (10-126)

In that sense, the trap that resulted in (relatively) narrower prediction was the MTR, where for 100 mosquitoes collected, the model would estimate 49 HLC-equivalent, with CIs ranging between 10 and 126 (Table 3.3c).

3.2.3 *Culex* species

Overall, there were moderately higher correlations between the alternative traps and HLC for *Culex* catches than for the *Anopheles* groups (Table 3.2). There was however no major differences between the tested models (based on Δ DIC estimates), thus the simplest linear model was adopted based simply on being the thriftiest. Full details of all models are presented in Table 3.2a. Catches from MTRC and MTR traps had the highest correlations with HLCs (R^2 values ranging between 44.2% and 45.4%). On the other hand, MMX and ITT-C were the worst performing traps, and significantly underestimated the HLC catches (Table 3.2a, Figure 3.2).

3.2.4 Interactive calibration tool

To support detailed assessment and comparison of these and any future trap types for outdoor-sampling, I developed an interactive calibration tool incorporating the key parameters as identified in the analysis above. This tool is designed with simple user interfaces to simplify model inputs and outputs. For example, reporting full conversion tables for the Model 3 and 4, which include density dependence, would be challenging since the associated interaction terms would require every possible combination of mosquito group, trap types and catch range. To get estimates according to these models, readers can use the interactive online tool, which is available as an [R Shiny App](#). The coefficients of these models will be updated regularly as additional data are gathered. This tool may be expanded to cover additional geographic regions and mosquito species not currently captures. The tool is hosted by an online server of the “Boyd Orr Centre for Population and Ecosystem Health” (University of Glasgow), and it is freely available at <https://boydorr.gla.ac.uk/lucanelli/trapcalibration/>.

3.3 Discussion

Despite the growing importance of outdoor-biting mosquitoes and their role in malaria transmission in different settings, there are limited methods for sampling outdoors. Human Landing Catches remain common and are sometimes considered as the gold standard, but there are multiple ethical, cost and logistical concerns limiting their application [112,117]. Multiple alternative tools have therefore been tested as potential HLC replacements in different settings (e.g. [114,115,121,124,287,291,293]). While most efforts have focused on finding an alternative that catches as many mosquitoes as HLC, it is now recognized that what matters more is how representative the catches from any specific trap are relative to HLC catches. It means therefore that efforts to improve surveillance methods should include not just new traps, but also a statistical tool for assessing their representativeness.

In this study, I therefore developed and validated a statistical framework for predicting credible intervals of HLC-derived exposure rates based on catches from multiple exposure-free alternatives. I have provided extensive comparison and correction factors for the different trapping methods, as well as evidence for the most representative alternative to the HLC. Furthermore, I have translated the results of my modelling approach into an easy-to-use interactive calibration tool, which generates the expected means and credible intervals of nightly human biting rates (using HLC as a proxy) based on inputs of other trap catches.

Of several trapping methods that have been proposed for outdoor mosquito sampling of malaria vectors; only a few have been calibrated relative to the HLC (e.g. [114]); and even fewer in outdoor setting (e.g. [282,288]). These traps provide disparate levels of efficacy relative to HLC, but rely primarily on two mutually inclusive principles; i) substituting human subjects by human odours and a carbon dioxide source (e.g. [182,289]); or ii) designing traps that protect human volunteers from bites with physical barriers (e.g. [124,287,288,299]). Many studies have assessed the correlations between mosquito abundance as estimated from the HLC and an alternative (e.g. [122,123,242,286-288,291,294,304]), but only a few provide the relevant quantitative estimates of “accuracy” (i.e. how close the estimates are to HLC) and precision (i.e. how

variable the estimates are) [122,286-288,291]. Furthermore, to my knowledge none have provided an explicit calibration tool to facilitate rapid predictions of mosquito counts from an alternative trap into an HLC-equivalent. Such a calibration tool would need to reflect the potential non-linear relationship between trap counts and HLC values; meaning that no single conversion “value” between methods may apply across the full range of mosquito densities. This hypothesis is backed-up by a multi-country study which evaluated the limitations of CDC light traps for estimating exposure to African malaria vectors indoors after observing non-linearity in its association with HLC [114].

In general, the overall measure for goodness of fit (R^2) for models predicting HLC counts was highest in *An. funestus*, followed by *Culex* species and *An. arabiensis*. Despite the higher value of R^2 in *An. funestus*, the wider credible intervals were probably due to the much small sample sizes of this species (total mosquito caught with HLC: *An. funestus* = 226, *An. arabiensis* = 5282, *Culex* = 7191); although there could also have been affected by other ecological features that were not directly captured with this study (e.g. other environmental conditions apart from humidity and temperature). During the model fitting exercise, temperature and humidity were excluded. The proportion of *An. funestus* in the study area compared to other species such as *An. arabiensis* and *Culex* has been historically low [88,89,103] though this species carries a significant amount of infection compared to other commonly known malaria vectors [88]. Study shows that they do bite outdoors in appreciable numbers but hard to relate trap counts from other methods to HLC equivalents for this species because of very high variability in data.

The performance of some alternative traps in comparison to the HLC has been shown to be density dependent in several investigations (e.g. [114,294]). However, such density dependent impacts are usually only considered in terms of “intra-specific” dependencies, such as the baseline density of the target vector species [282,294], overlooking the larger mosquito community. However, the same mechanisms that cause intra-specific density dependence in trap performance may also cause dependence on the overall densities of all mosquito species lured to the trap, including species that aren't of public health importance. While such reliance on the wider mosquito community is plausible, it has yet to be tested in trap evaluation studies. This study and the calibration

tool that I developed therefore also included a robust assessment of how density dependence may play a role. Model 3 and 4 included these variables and will allow users to incorporate these as covariates when predicting outdoor-biting rates in their settings of interest.

Overall, this study found little evidence that the relative performance of the trapping methods investigated here is modified by the density of the target mosquito taxa or other members of the mosquito community. Models that incorporated intra or inter specific density dependence in trap performance did not yield any substantial improvements over those assuming simple linear relationship between mosquito counts in the HLC and alternative method. This indicates that neither intra nor interspecific density dependence has a large impact on the relative efficiency of the alternative traps tested here. This was generally the case with exception of BGS and SUN trap which shows signs of both intra and interspecific density dependencies. Given the wide range of trap catches, the calibration tool I developed here allows users to incorporate such density dependence effects (both within and between species) and to examine if these are applicable in their settings. Previously, (intraspecific) density dependence has been detected in the performance of some trapping methods [288,291,292]. However, evidence of density dependence in trap performance can be variable even for the same trapping method. For example, studies investigating the performance of the Mosquito Electrocuting Trap relative to the HLC have detected density dependence in some cases [114,124], but not others [288].

One limitation of this study is that while the HLC is broadly considered the gold standard for collecting host seeking mosquitoes both indoors and outdoors, I only focused on traps for outdoor sampling. Although I compared a large number of trap types commonly used in Africa settings, other traps may perform differently and potentially better than some of the candidates investigated here [124,287,288]. Additional studies including other alternative traps for indoor and outdoor use would be of further value; with the calibration tool developed here providing a useful framework for their evaluation and comparison. Based on the results presented here, I recommend that for whatever trap used, the users should generate credible estimates of what the human biting rates (as estimated from HLC) could be. Due to the potential variation in trap performance between

different ecological settings and mosquito species, I do not yet recommend any one specific trap as the best replacement for the HLC. Instead, I recommend that users consider and define the statistical relationships between a prospective trap and the HLC when planning surveillance and interpreting results. The interactive conversion tool I have developed here can be used for that purpose and is now [available online](#) as a *Shiny App* interface.

3.4 Conclusion

Methods for sampling outdoor-biting mosquitoes are urgently needed to improve surveillance of vector-borne diseases. Even if an alternative trap does not catch as many mosquitoes as the HLC, it is desirable to define the statistical relationship between them so that credible ranges of actual biting risk can be predicted in units of HLC equivalents. In this study, I successfully evaluated six different outdoor traps and developed a calibration tool to assess their performance relative to the HLC. This tool was validated using data from year-round field collections and enabled a framework for predicting HLC-derived exposure rates representative of individual human biting risk. The tool incorporates multiple models, including two that allow assessment of effects of both inter and intra-specific density dependence of the performance of candidate traps. In the specific field trials from which data was obtained here, density-dependence between and within mosquito species influenced the performance of only one trap, BGS, but not any others. An interactive *Shiny App* calibration tool was developed for this and similar applications. I conclude that this calibration approach provides a valuable framework for assessing human exposure from different outdoor trapping methods. As the performance of candidate traps relative to the HLC varied between mosquito taxa, there was no single optimum. While all the candidate traps underestimated HLC catches, and thus human-biting rates. Further studies of trapping methods and associated evaluation criteria should focus on consistency and representativeness as opposed to simply finding traps that catches as many mosquitoes as HLC.

4.0 Chapter 4: Using Bayesian state-space models to understand the population dynamics of the dominant malaria vector, *Anopheles funestus* in rural Tanzania

Published in Malaria Journal 2022: <https://doi.org/10.1186/s12936-022-04189-4>

Abstract

Background

It is often assumed that the population dynamics of the malaria vector *Anopheles funestus*, its role in malaria transmission and the way it responds to interventions are similar to the more extensively characterized *Anopheles gambiae*. However, *An. funestus* has several unique ecological features that could generate distinct transmission dynamics and responsiveness to interventions. The objectives of this work were to develop a model which will: 1) reconstruct the population dynamics, survival, and fecundity of wild *An. funestus* populations in southern Tanzania, 2) quantify impacts of density dependence on the dynamics, and 3) assess seasonal fluctuations in *An. funestus* demography. Through quantifying the population dynamics of *An. funestus*, this model will enable analysis of how their stability and response to interventions may differ from that of *An. gambiae sensu lato*.

Methods

A Bayesian State Space Model (SSM) based on mosquito life history was fitted to time series data on the abundance of female *An. funestus sensu stricto* collected over 2 years in southern Tanzania. Prior values of fitness and demography were incorporated from empirical data on larval development, adult survival and fecundity from laboratory-reared first generation progeny of wild caught *An. funestus*. The model was structured to allow larval and adult fitness traits to vary seasonally in response to environmental covariates (i.e. temperature and rainfall), and for density dependency in larvae. The effects of density dependence and seasonality were measured through counterfactual examination of model fit with or without these covariates.

Results

The model accurately reconstructed the seasonal population dynamics of *An. funestus* and generated biologically-plausible values of their survival, larval development and fecundity in the wild. This model suggests that daily *An. funestus* survival and fecundity values annual were highly variable across the year, but did not show consistent seasonal trends in association with rainfall or temperature. While the model fit was somewhat improved by inclusion of density dependence, this was a relatively minor effect and suggests that this process is not as important for *An. funestus* as it is for *An. gambiae* populations.

Conclusion

The model's ability to accurately reconstruct the dynamics and demography of *An. funestus* could potentially be useful in simulating the response of these populations to vector control techniques deployed separately or in combination. The observed and simulated dynamics also suggests that *An. funestus* could be playing a role in year-round malaria transmission.

4.1 Background

Anopheles funestus is one of the major malaria vectors in Africa and is widely distributed across the continent [66,68]. With the exception of *Anopheles gambiae sensu stricto* (s.s.), the species appears to have higher vectorial capacity than other members of the *Anopheles gambiae* complex [77,88,89,104,305,306]. *Anopheles funestus* makes a higher contribution to transmission than *An. gambiae sensu lato* (s.l.) in numerous parts in sub-Saharan Africa [88,109,204,207,307]; particularly in settings where *An. gambiae* abundance has plummeted due to either effective indoor-based vector control interventions [76,185] or environmental change. It is hypothesized that *An. funestus* persistence despite the recent scale-up of insecticide-treated nets may have been facilitated by their earlier development of strong physiological resistance [91].

Anopheles funestus is typically grouped with *An. gambiae s.l.* when modelling transmission and formulating policies for malaria vector control [9,198,308]. The lack of explicit consideration of *An. funestus* ecology and transmission potential may be partially due to this species having been relatively neglected compared to *An. gambiae*. Comparatively the ecology of *An. funestus s.l.* is less well understood, and it is much more difficult to maintain under insectary or semi-field conditions ([24], Chapter 2). However, this species has several unique ecological features, such as its different larval habitat and dry season persistence [95], that could give rise to distinct population dynamics and differentiate its response to core and supplementary interventions. For example, *An. funestus* prefers larger aquatic habitats that are semi-permanent or permanent throughout the year, and contain clear water with some emergent vegetation [95]. This differs from *An. gambiae s.s.* which generally prefer small temporary habitats, such as puddles, ditches or animal hoof prints [54,95], or *An. arabiensis*, which can breed extensively in rice fields and other sunlit open pools [66]. The use of more permanent larval habitats means that *An. funestus* has greater persistence through the driest periods of the year compared to *An. gambiae* [103], whose habitats evaporate quickly in the absence of rainfall [54,309]. This ecological feature means that the seasonal phenology of *An. funestus* and its response to aquatic microclimate differs from *An. gambiae*

[54,96,103]; and could thus generate differential response to seasonally-targeted interventions, such as Indoor Residual Spraying (IRS) and larviciding.

Differential use of aquatic habitats may also impact the relative importance of key intrinsic drivers of mosquito population dynamics such as density dependence. Density dependence in malaria vectors occurs during larval development as a product of competition for space and nutritional resources [59,310]. In space-limited habitats, high larval densities can influence larval development rates and survival, but also subsequent adult fitness traits such as body size, survival, fecundity and mating success [53,57,61,311]. While there is evidence that density dependence is an important driver of *An. gambiae* population dynamics [59], the relative importance of this process for *An. funestus* is unknown. Given that larval crowding and competition are less likely within the larger habitats preferred by *An. funestus*, density dependence is hypothesised to be less pronounced for this vector species. Quantifying the strength of density dependence is important to inform the ease with which vector populations can be suppressed and how quickly they can recover [57,310,312].

Models of vector population dynamics and their response to interventions must be parameterised by reliable estimates of their demography and fitness. For vectors in the *An. gambiae* complex, such estimates are often acquired from insectary and semi-field studies (e.g. [78,81,135,176,225,313]) as well as field studies. Similar data has been difficult to obtain for *An. funestus* because of its poorly understood ecology and the difficulties of creating laboratory colonies; which so far has been achieved on only two occasions [24,207,222]. State-space models (SSM) provide an alternative approach to indirectly estimate these parameters by fitting a population dynamics model to observed time series data [159,175]. These models are widely used in other fields of ecology and conservation biology to investigate the population dynamics of other animals [159,180] and guide management decisions [180]. However, these models have so far had limited uptake in medical entomology. Given data on population fluctuations are available, these models can infer and estimate plausible demographic rates that could generate the observed dynamics [179].

SSMs are time-series models that distinguish between two stochastic components, namely, the process (i.e. biological) which captures sequential dependencies between population components (e.g. eggs, larvae, pupae), and an observation component which captures and corrects for biases and imprecisions in the data-collection process. Prior knowledge of model parameters is used to bolster the information content of the time series data with existing expert or laboratory data and uncertainty in estimates. Population projections are then quantified on the basis of posterior probability distributions for parameters and population states. SSMs have recently been used to elucidate the dynamics and impacts of interventions on malaria vectors in laboratory and semi field populations [135,176], but have not yet been applied to estimate *An. funestus* vector demographics in the wild. Here, an innovative SSM application was developed to describe the dynamics of wild *An. funestus* populations in Tanzania, and use it to assess extrinsic (environmental) and intrinsic (density dependent) drivers of their fitness and demography for the first time. Empirical data from laboratory experiments on *An. funestus* colonization (Chapter 2, [24]) were incorporated together with published literature and the wild population data to develop an SSM. Time series field data collected in 2015 [88] and 2018 in southern Tanzania, and corresponding environmental information were used to validate the model. Specific aims were: 1) to accurately reconstruct the population dynamics, survival and fecundity of wild *An. funestus* populations in southern Tanzania, 2) assess the impact of density dependence on the dynamics, and 3) to identify and quantify seasonal variations in *An. funestus* abundance and demography.

4.2 Methods

4.2.1 Time series data on wild *An. funestus* populations

Indoor densities of female *An. funestus s.l.* adults were recorded over 12 months of entomological surveys conducted in three villages (Tulizamoyo, Ikwambi and Sululu) in Kilombero (8.1539°S, 36.6870°E) and Ulanga (8.3124°S, 36.6879°E) districts, south-eastern Tanzania from June 2018 to May 2019 (Figure 4.1). The villages were selected because of the high abundance of *An. funestus s.l.* within which *An. funestus s.s.* is the dominant sibling species (93%) [1]. Annual rainfall

was 1200mm-1800mm, and temperature, 20 °C-32 °C. CDC Light traps [129] were used to sample host-seeking mosquitoes from 6pm to 6am for 5 days per week, 4 weeks a month for 12 months in 10-15 houses per village (repeated collection from the same households). The houses were randomly selected and consent obtained from household heads. The mosquitoes were sorted by taxa and sex, and females further classified as unfed, blood-fed or gravid. Daily climatic data (rainfall and temperature) were obtained from a weather station, approximately ~20km from the farthest village.

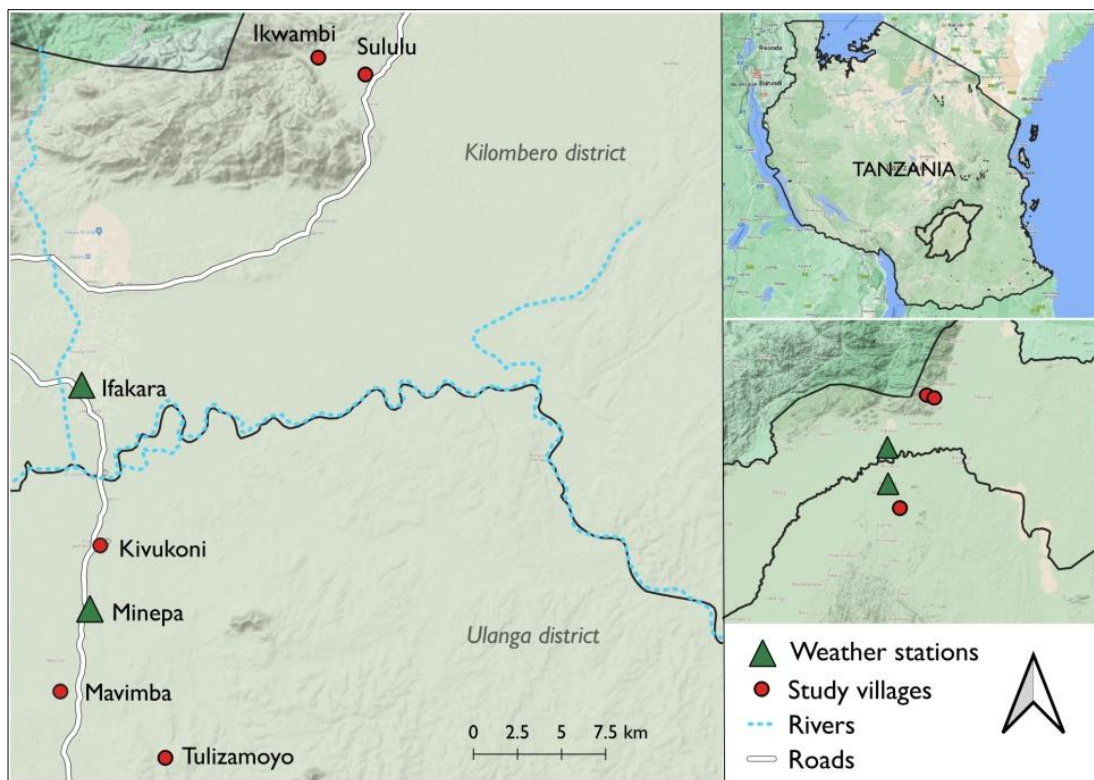


Figure 4.1: A map depicting the locations of various study villages where mosquito sampling was carried out in 2015-2016 and 2018-2019.

To complement this, additional data on *An. funestus* were extracted from a 2015 dataset from three other villages in Ulanga district (Mavimba, Minepa and Kivukoni) (Figure 4.1) [88]. These data were collected five days per week for a period of 12 months. This data allowed me to fit the model simultaneously to multiple time series so that it could learn hierarchically from *An. funestus* trajectories unfolding in different years and locations. This additional data has previously been described elsewhere and used to demonstrate the epidemiological dominance of *An. funestus*, which now contributes >85% of all

malaria infections in the region [88]. Here, time series data collected in 2015 was aggregated and considered as “*population 1*” and collection in 2018/2019 was considered as “*population 2*”

4.2.2 Prior information on life-history and gonotrophic cycle stages

Female *An. funestus* adults collected from the same three villages in 2018 were maintained in insectary conditions for one generation to estimate baseline fitness traits as already described in Chapter 2 and Ngowo *et al.* [24]. Data collected from this 1st-generation laboratory progeny included: a) proportion of eggs that hatched into larvae, larvae that transitioned to pupae, and of pupae that emerged into adults, b) the length of the transition periods (days) between life stages : (i) eggs to 1st instar larvae, (ii) 1st instar larvae to pupae, and (iii) pupae to unfed adult female (one day post emergence), c) transition period of adult females between three different stages of their gonotrophic cycle, i.e. unfed, blood-fed and gravid.

The gonotrophic cycle starts with ‘unfed’ females who transition to ‘blood-fed’ after obtaining a blood meal. In the wild, the first gonotrophic cycle usually starts after unfed females have mated [31]; which is assumed to happen soon after emergence. In insectary experiments, females had access to males immediately on emergence. As the blood meal is digested, blood-fed females transition into the ‘gravid’ state during which eggs develop. Gravid females then oviposit their eggs into aquatic habitats and return to the ‘unfed’ stage with the cycle begins again (Figure 4.2). In the wild, the rate of transition between these gonotrophic stages is governed by both intrinsic and extrinsic environmental conditions including the availability of blood-meals and oviposition sites [157]. In the insectary, the first blood-meal (arm-feeding) was offered 5 days post emergence to ensure individuals had sufficient time for mating.

Per capita fecundity was defined as the number of eggs laid per fully bloodfed adult female. The rate of surviving between life-history stages or gonotrophic stages were calculated as the inverse of the number of days required to transit from one stage to the next:

$$s_m = (j_m)^{1/r} \quad (1)$$

Here, m is the life cycle stage, j is proportion survived as the percentage of the total from preceding life stage, r is the average number of days it took to transit from one life stage to another, and s is the daily rate of survival within the stage (Table 4.1).

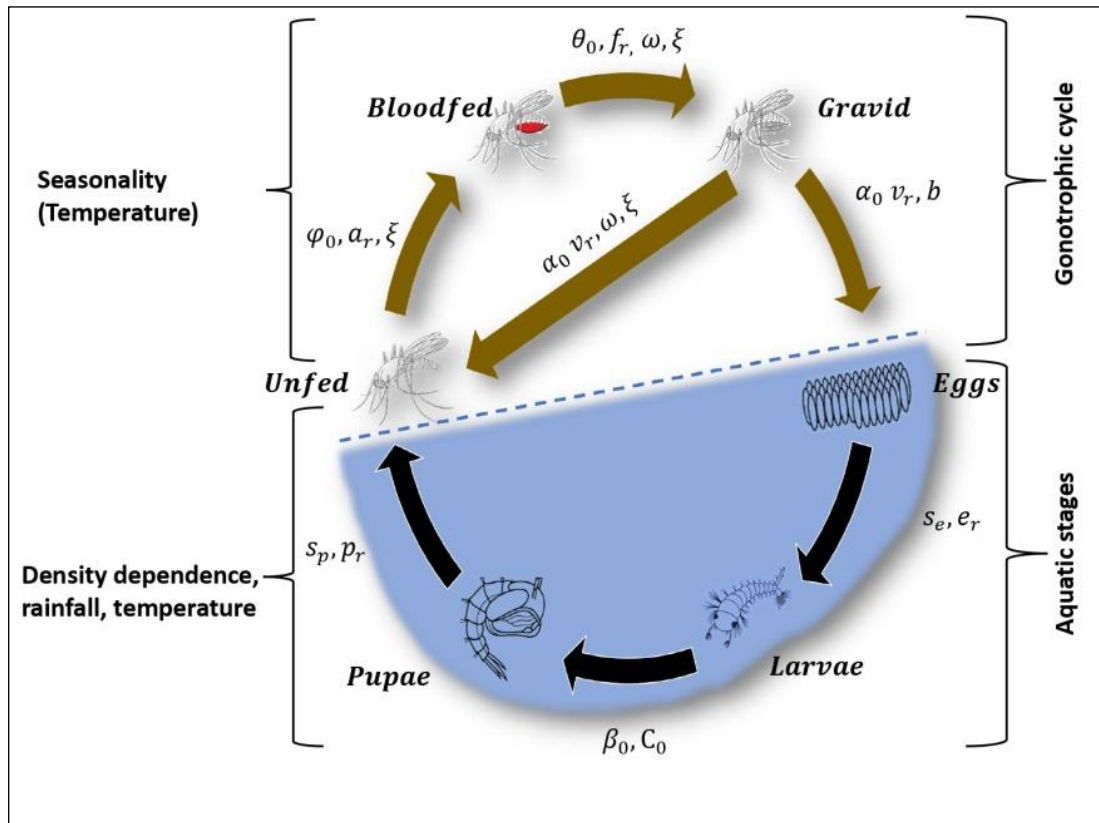


Figure 4.2: Schematic representation of the state-space population model showing different life stages compartment (circles) and flows (arrows) of *Anopheles funestus*. Abundance data were only available for unfed, blood-fed and gravid stages. The model assumes that once a gravid mosquito has laid eggs, they return to the unfed stage. The annotations are described in Table 4.1. The model incorporates six life stages (eggs, larvae, pupae, unfed, bloodfed and gravid) of *An. funestus*.

4.2.3 Biological process components of the Bayesian SSMs

Daily survival: The daily survival of larval stages was assumed to be the same for all instar stages. Adult survival was assumed to be the same for unfed, blood-fed and gravid females. Survival probabilities (s_l, s_a, s_f, s_v) were linked to their covariates through a *logit* transformation of linear predictors (here, subscripts l, a, f, v refer to larvae, unfed, blood-fed and gravid, respectively). Pupal (s_p) and egg (s_e) survival probabilities were considered to be independent of any

climatic and density-dependent covariates, and were treated as a binomial distribution, with baseline rates assigned priors as described in eq. 16-17.

A range of covariates hypothesized to be associated with the demography of *An. funestus* were incorporated to allow baseline larval and adult survival to vary with environmental conditions. Rainfall (current and 1 week-lagged) and temperature were incorporated into the larval survival model. Rainfall regulates the availability and permanence of aquatic habitats, thus influencing both survival and carrying capacity of larval habitats [62]. Density dependence was incorporated into the model of larval survival [59] to assess whether this could improve the fit of the adult population dynamics model. Additionally, the speed of larval development was modelled as a function of temperature based on its known importance [25,26]. The daily survival of larvae was thus defined as a function of daily rainfall (current and lagged), daily temperature and density dependence. The daily survival rates (lowercase $s_l(t)$) of larvae were estimated through a logit transformation of linear predictors (uppercase $S_l(t)$).

$$s_l(t) = \frac{\exp(S_l(t))}{1 + \exp(S_l(t))} \quad (2)$$

Specifically, $S_l(t)$ is written as a function of both intrinsic and extrinsic drivers:

$$S_l(t) = \beta_0 - \beta_1 R_{(t-1)} - \beta_2 D_{(t-1)} \left(1 - \frac{\beta_3 Q_{(t-1)}}{\max(Q)}\right) + \beta_4 T_{(t-1)} - \beta_5 T_{(t-1)}^2 + \varepsilon_{l,t} \quad (3)$$

$$\varepsilon_l \sim \text{Normal}(0, \sigma_{l,t}) \quad (4)$$

Here, β_0 is the baseline daily larval survival on the linear scale. A survival probability prior was assigned under zero rainfall and average temperature (i.e. 27°C) and then calculated the intercept of β_0 to reflect this prior information. When there is no effect of any environmental covariates prior takes values between 0.80-1, Table 4.1. The coefficient β_1 quantifies the effect of current rainfall (R); with the envisioned scenario being that higher R (i.e. flooding) tends to wash away larvae hence reducing the baseline survival [314]. This β_1 was defined by an informative gamma prior with shape = 5.382 and rate of 46.4

(Table 4.2) which permits anything from no rain effects to 100% mortality. The coefficient β_2 quantifies the effect of larval density at time t on larval survival. A monotonic negative relationship was assumed based on the biologically-plausible hypothesis that larval survival is reduced at high larval density because of resource competition and intraspecific cannibalism [53,63]. This coefficient β_2 was defined by an informative gamma prior with shape of 0.5 and rate of 1 (Table 4.2), which allows the impact of density to range from no effect to complete annihilation.

The term inside brackets in Eq. (3) represents the fact that density dependence needs to be modulated by the availability of larval habitat. The availability of suitable aquatic habitats for oviposition will increase with rainfall; thus potentially reducing the crowding of larvae into the remaining habitats that persist during the dry season. This hypothesis has been supported for *An. gambiae s.l.*, where their seasonal population dynamics can be explained by models incorporating a rainfall-dependent carrying capacity [59]. Here, the coefficient β_3 was a proportion that captures the potential interaction between larval habitat availability (defined as the cumulative rainfall (Q) over the past week) and larval density (D). When rain in the recent week has been the maximum observed (i.e. $Q = \max(Q)$), then $(1 - \frac{\beta_3 Q_{(t-1)}}{\max(Q)})$ would be the smallest amount of density dependency experienced by *An. funestus*. The prior distribution for β_3 was defined by an upward-biased beta prior with mean 0.9 and variance of 0.01 allowing β_3 to have positive impact on larvae survival.

Additional covariates were incorporated to assess the role of temperature on larval survival (via the coefficients β_4, β_5). The parameter β_4 captures the potentially positive effects of temperature on daily larval survival, which were defined by an uninformative gamma prior with mean of 1 and variance of 0.1 considering 27°C as the optimal temperature (ρ) for maximum survival [315]. This prior allows temperature to vary from having no impact, to high positive impact on larval survival. Alternatively, the relationship between larval survival and temperature may be characterized by survival being reduced at low or very high temperature, and peaking in the middle [47]. The coefficient β_5 was incorporated to capture this potential curvilinear relationship but was

dependent on β_4 , to ensure that the optimum temperature was fixed at 27°C, ($\beta_5 = \frac{\beta_4}{2\rho}$). The prior of β_4 allowed extreme temperatures values away from the optimum to range from having no effect to generating 100% mortality. The parameter ε_l is capturing the unexplained stochasticity associated with larval survival. This error term was defined by a normal prior with mean of 0 and a precision σ_l from a gamma distribution with both shape and rate of 10.

The linear predictors for survival of unfed, blood-fed, gravid (uppercase $S_a(t), S_f(t), S_v(t)$) and daily probabilities of survival (lowercase $s_a(t), s_f(t), s_v(t)$) were structured similarly to eq 3. The daily survival probabilities of adult stages were thus defined as the functions of daily temperature; such that an increase in temperature would result in an increase in the survival of all three adults stages and reduction in survival when temperature become lethal [103,316]. The biological relationship between adult survival and temperature was assumed to be curvilinear [103,316,317].

$$S_a(t) = \varphi_0 + \varphi_1 T_{(t-1)} - \varphi_2 T_{(t-1)}^2 + \varepsilon_{a,t} \quad (5)$$

$$S_f(t) = \theta_0 + \theta_1 T_{(t-1)} - \theta_2 T_{(t-1)}^2 + \varepsilon_{f,t} \quad (6)$$

$$S_v(t) = \alpha_0 + \alpha_1 T_{(t-1)} - \alpha_2 T_{(t-1)}^2 + \varepsilon_{v,t} \quad (7)$$

$$\varepsilon_{t*} \sim Normal(0, \sigma_{t*}) \quad (8)$$

Here, φ_0 , θ_0 , and α_0 refer to the baseline survival of unfed, blood-fed and gravid females respectively on a linear scale, under fixed temperature conditions of $27 \pm 2^\circ\text{C}$ (insectary standard under which *An. funestus* have maximum survival [47,317]), and assumes no blood meal limitation. The positive impact of temperature on all three life stages was represented by the coefficients φ_1 , θ_1 and α_1 with an uninformative gamma prior with mean 12.5 and variance of 6.25. The coefficients φ_2 , θ_2 and α_2 correspond to the curvilinear effect of temperature on the survival of all three adult stages with their priors derived from the ratio between the linear coefficient and twice

optimum temperature. This formulation ensured that the optimum temperature is fixed at (27°C). The stochastic terms ε_a , ε_f , ε_v capture unexplained variation associated with survival during the distinct gonotrophic stages. These error terms (ε_*) were defined by normal priors with mean of 0 and a precision σ^* from a gamma distribution with both shape and rate of 10 for unfed, blood-fed and gravid females.

Development between stages: The daily development probability from one life stage to the next was defined as the reciprocal of the development time (days) between the stages (assuming that all development times take longer than a day). An increase in temperature was assumed to reduce the development period of larvae [26,316,318,319].

$$l(t) = \frac{\exp(L(t))}{1 + \exp(L(t))} \quad (9)$$

Specifically, $L(t)$ is written as the function of temperature covariates:

$$L(t) = C_0 + C_1 T_{(t-1)} \quad (10)$$

Here C_0 is the baseline daily development period on a linear scale defined by an informative beta prior with range defined in eq 16-17 (Table 4.1). The coefficient C_1 explains the positive effect of temperature on larval development period, with its prior values derived from an uninformative gamma prior with mean 0.001 and standard deviation 0.001.

The development time for other life history stages (eggs and pupae) and the time between gonotrophic stages were assumed to be independent of temperature and other environmental covariates. The numbers of individuals (\mathcal{K}_m) graduating from one stage to the next each day were modelled as a binomial process Eq 11.

$$\mathcal{K}_m(t) \sim \text{Binomial}(r_m, \mathcal{W}_{m-1}(t)) \quad (11)$$

Here r_m is a development rate as defined in eq 11 for m stage, with assigned informative prior values as described through a generic prior in eq 16-17. Parameter $\mathcal{W}_{m-1}(t)$ refers to the number surviving the preceding life stage.

Fecundity: The number of eggs laid at each time step was drawn from a Poisson distribution whose rate was the product of per-capita fecundity (number of eggs laid by blood-fed *An. funestus* under insectary conditions (b_0), a penalized rate for the egg survival (s_e), the number of gravid mosquitoes ($V_{(t-1)}$) and ratio of females-males (assumed to be 0.5) as assessed at the pupae stage [24].

$$b_t = \exp(b_0 + \varepsilon_{b,t}) \quad (12)$$

$$B(t) \sim \text{Poisson}(0.5b_t s_e V_{(t-1)}) \quad (13)$$

The error term ε_b was defined as a normal process with mean of 0 and a precision from a vague gamma prior with both shape and rate of 10.

4.2.4 Observation-derived components of the Bayesian SSMs

Observations of the abundance of adults (unfed, bloodfed, gravid) A at time t were modelled as a normal distribution with varying daily means \bar{a} determined by the biological model and a precision τ representing observation error. A fixed coefficient of variation (ξ) for the daily observation process was assumed and assigned an uninformative prior with values between 0.1-0.9 (Table 4.1). The CDC light trap typically samples mosquitoes from populations of unknown size, for which the daily catch rates are difficult to quantify independently. A parameter ϑ was therefore incorporated both into the precision τ and daily varying means to account for an observed weekly periodicity in adult abundance, which was otherwise hard to interpret. The weekly periodicity observed here was a consistent reduction in the catches between the first day of weekly collection and the last day. This parameter was allowed to vary both by day of the week j and between the two populations k (2015 and 2018-19 datasets). The ϑ values were derived from a logit function $\exp(\rho)/(1 + \exp(\rho))$, with ρ defined from the uninformative normal prior with mean and standard deviation of 0 and

10 respectively. Therefore precision τ can be written as $\frac{1}{(\xi_t \bar{a}_t \vartheta_{jk})^2}$ for all the adult stages. Thereafter, the observation abundance was estimated as follows:

$$A(t) \sim Normal\left(\bar{a}_t \vartheta_{jk}, \frac{1}{(\xi_t \bar{a}_t \vartheta_{jk})^2}\right) \quad (14)$$

Trap bias: The trapping method (CDC Light traps) primarily targets unfed host-seeking mosquitoes [129]. Blood fed and gravid mosquitoes are assumed to no longer host-seek, and represent a small proportion (~0.5-3%) of the females caught in CDC traps [88,103]). To account for these biases in sampling, a new parameter of “trap-biasness” ω was added in the observation model for both precision τ and varying daily means \bar{a}_η . The prior values for ω were estimated from independent studies from the same locations [88,195], and ranged from 0.05-0.15 (Table 4.1), with variations between the two life stages η . Therefore, the observation model for blood-fed and gravid (A_η) was rewritten by modifying eq 14 as follows

$$A_\eta(t) \sim Normal\left(\bar{a}_\eta \vartheta_{jk} \omega_\eta, \frac{1}{(\xi_t \bar{a}_\eta \vartheta_{jk} \omega_\eta)^2}\right) \quad (15)$$

Prior distributions: Since this model contains a large number of parameters, use of un-bounded informative priors restricted model convergence and mixing. I therefore opted for bounded and rescaled beta distributions of the informative priors [320]:

$$Y \sim Beta(5, 5) \quad (16)$$

$$X = X_{min} + Y(X_{max} - X_{min}) \quad (17)$$

Here Y is a dummy variable that takes values in the interval $[0, 1]$ with mean of 0.5 and standard deviation of 0.15, selected to provide low likelihood at the extremes of its range, 0 and 1. The values of X_{min} and X_{max} define the range of the parameter of interest as dictated by the prior information. Since the information on priors was provided in form of mean (μ) and standard deviation

(σ), these rescaling values were defined as $X_{min}, X_{max} = \mu \pm 2\sigma$. Survival, development period, trap-biasness, variability in daily catches and fecundity parameters were all assigned priors according to Eq. 17.

4.2.5 Model selection, model fitting and outputs

Model fitting was done using the R statistical software version 4.0.5 [246]. Population models were fitted using a Markov Chain and Monte Carlo sampling (MCMC) algorithm via the JAGS software [301] interfaced to R via the *runjags* package [302] (code provided in Appendix 4). To achieve convergence, the model with 6 chains was run in parallel for 10^5 samples with a burn-in of 10^5 , keeping every 10^{th} iteration for memory-saving reasons. Convergence was assessed by visual investigation of the trace plots, prior-posterior distribution using the *coda* package [321], effective sample sizes and the Gelman Rubin diagnostic [322]. Model comparisons were done using the deviance information criterion (DIC) [323], and the ones with the lowest DIC selected as the most preferred. The predicted and observed densities of *An. funestus* adult females were plotted to evaluate consistent prediction biases visually. Posterior means and 95% credible intervals for the key survival parameters, development period, density dependence, environmental covariates (temperature and rainfall) and fecundity were also reported to reveal different dynamical aspects of the system.

4.3 Results

4.3.1 Population trajectories and seasonal trends

A Bayesian state-space model was used to describe the dynamics of wild populations of *An. funestus*. The full results, including summaries of posterior means for all the fitness and demographic parameters are reported in Table 4.1. The most parsimonious model (model-7, Table 4.3) included density dependence, and temperature and rainfall (current and lagged) impacts on larval survival, and the effect of temperature on the larval development period. The only covariate that was not retained in the “model-7” was temperature impacts on adult survival. This model satisfactorily reconstructed the population

dynamics of *An. funestus* in the study villages, with all environmental covariate relaxation applied based on DIC selection. Population trajectories were estimated for all six *An. funestus* life history and gonotrophic stages after accounting for potential impacts of environmental covariates and density dependence (Figure 4.3).

These trajectories reflect the annual trend in abundance spanning in periods from low or no rainfall to high rainfall. All trajectories show a relatively high abundance of *An. funestus* right after the rainy season (May-June), followed by reduced but sustained abundance during the dry period (August-October) for all the life stages. After accounting for observation biases during sampling, the observed abundance of unfed, gravid and blood-fed groups largely falls within the credible intervals of the predicted values (Figure 4.4).

4.3.2 Survival and fecundity

Estimated *An. funestus* larval survival trajectories demonstrate substantial mean variability during the two seasons, with no clear pattern of seasonality (Figures 4.5a and 4.5b, Table 4.1) due large credible intervals. Similarly, the survival trajectories of the adult stages (all gonotrophic states) were variable throughout the year, with daily survival rate ranging from 0.2 to 1.0 and not consistently differing between wet and dry seasons (Figures 4.5c to 4.5h, Table 4.1). Per capita fecundity was estimated to be between 75 and 81 eggs per female *An. funestus* (Table 4.1). While the abundance of this species fluctuated seasonally, per capita fecundity remained consistent throughout the year (Figures 4.5k and 4.5l).

Temperature was an important predictor of larval survival with a curvilinear relationship (Δ DIC = 138, Table 4.3, Figure 4.6b). Temperature also had a positive monotonic relationship on the larval development rate (Δ DIC = 336, Table 4.3, Figure 4.6a); with the larval development period estimated to last about 16 days on average.

Table 4.1: Priors as used in the state-space population models of *Anopheles funestus* and the estimated posteriors mean and 95% credible intervals. Day (d^{-1}) was considered as a unit of time in this modelling development.

Parameter		Prior distribution				Posterior distribution	
Notation	Description	Type	Source	Mean	95-percentiles	Mean	95-percentiles
s_e	Eggs daily survival rate	Beta	This study	0.794	[0.619, 1]	0.789	[0.776, 0.804]
λ	Eggs development rate (d^{-1})	Beta	This study	0.5	[0.4, 0.6]	0.499	[0.485, 0.514]
β_0	Baseline larval daily survival	Beta	This study	0.923	[0.801, 1]	0.950	[0.943, 0.956]
C_0	Baseline larval development rate (d^{-1})	Beta	This study	0.063	[0.055, 0.071]	0.063	[0.062, 0.064]
s_p	Pupae daily survival rate	Beta	This study	0.941	[0.874, 1]	0.944	[0.930, 0.950]
p_r	Pupae development rate (d^{-1})	Beta	This study	0.522	[0.253, 0.792]	0.525	[0.506, 0.546]
φ_0	Baseline unfed daily survival	Beta	This study	0.935	[0.877, 0.992]	0.937	[0.933, 0.941]
a_r	Unfed development rate (d^{-1})	Beta	This study	0.20	[0.19, 0.21]	0.200	[0.198, 0.201]
θ_0	Baseline blood-fed daily survival	Beta	This study	0.807	[0.654, 0.961]	0.810	[0.799, 0.820]
f_r	Blood-fed development rate (d^{-1})	Beta	This study	0.25	[0.05, 0.45]	0.269	[0.256, 0.280]
α_0	Baseline gravid daily survival	Beta	This study	0.904	[0.848, 0.961]	0.903	[0.899, 0.907]
v_r	Gravid development rate (d^{-1})	Beta	This study	0.333	[0.133, 0.533]	0.311	[0.297, 0.324]
b_0	No. eggs/female (Per capita fecundity)	Beta	This study	80	[60, 100]	78	[75, 81]
ξ	Coefficient of variability	Beta	Uninformative prior	0.5	[0.1, 0.9]	0.79	[0.810, 0.825]

Parameter		Prior distribution				Posterior distribution	
Notation	Description	Type	Source	Mean	95-percentiles	Mean	95-percentiles
$\omega_{\eta=f}$	Coefficient of “Trap biasness” for the blood-fed	Beta	Msugupakyula et al. [195] and	0.1	[0.05, 0.15]	0.122	[0.117, 0.127]
$\omega_{\eta=v}$	Coefficient of “Trap biasness” for the gravid		Kaindoa et al. [88]	$0.505^* \omega_f$	[0.025, 0.076]	0.062	[0.059, 0.064]

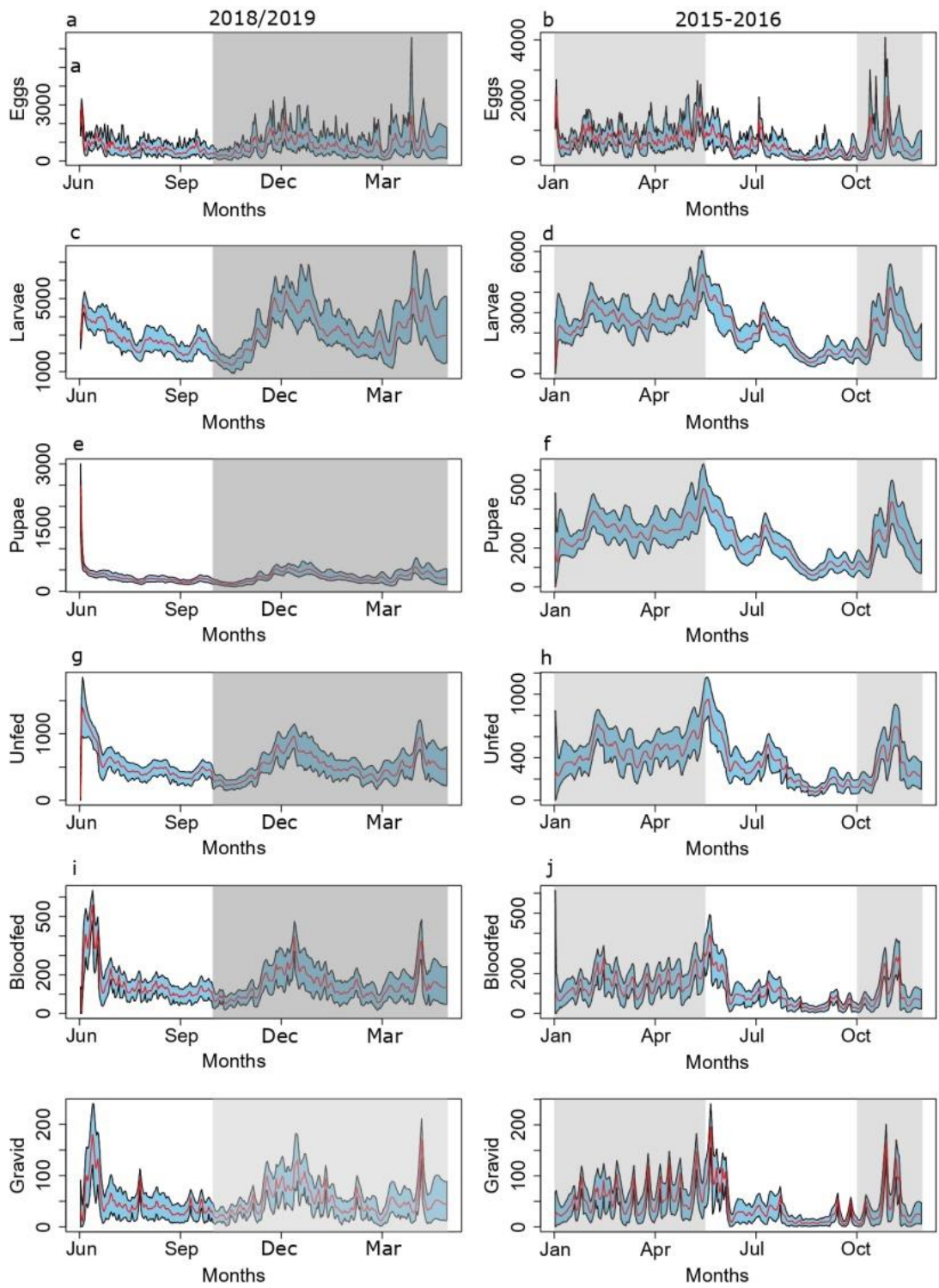


Figure 4.3: Reconstruction of the abundance trajectories for all the six life-stages. The red line indicates the mean posterior values and the respective 95% confidence intervals are shown in “sky-blue”. Left column (a,c,e,g,i,k) is data collected from June 2018 to May 2019 and right column (b,d,f,h,j,l) is data collected from Jan-Dec 2015. The grey area indicates the period with rainfall.

Additionally, daily rainfall (flooding) was estimated to be an important driver for of dynamics of *An. funestus* by reducing larval survival ($\Delta\text{DIC} = 5605$, Table 4.3, Figure 4.6c) with a negative monotonic relationship.

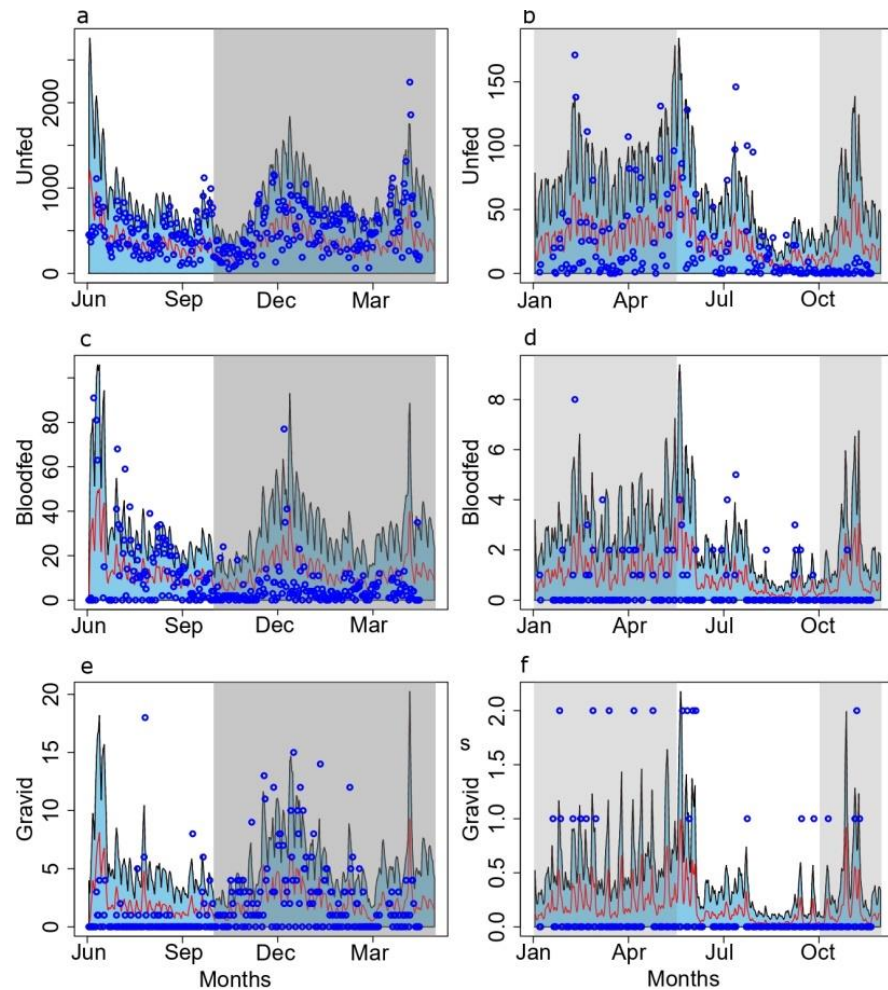


Figure 4.4: Observed vs. model estimated values for the three adult stages with data collected using CDC light trap both in June 2018 -May 2019 (left column- a,c,d) and Jan-Dec 2015 (right column- b,d,e). Red lines are the model estimated trajectories with “sky-blue” showing their 95% credible intervals. The blue circles are the observed values from the Light trap catches. Grey areas are the periods with rainfalls episodes.

4.3.3 Effects of density dependence

Density dependence was the only intrinsic feature incorporated in this dynamic model of *An. funestus*. The model was able to converge efficiently without crashing when density dependency was removed, suggesting this process plays a detectable but relatively minor role population regulation when compared with extrinsic factors ($\Delta\text{DIC} = 222$, Table 4.3, Figure 4.6e). To verify this, a simulation

was run and discovered that the estimated density dependence was actually quite low (this was detailed described in the next Chapter 5). The model fitting process also suggested an interaction parameter (β_3) between larvae density (D) and one week cumulative rainfall before sampling day (Q) contributes to *An. funestus* dynamics by positively increasing larval survival ($\Delta\text{DIC} = 38$, Table 4.3, Figure 4.6d).

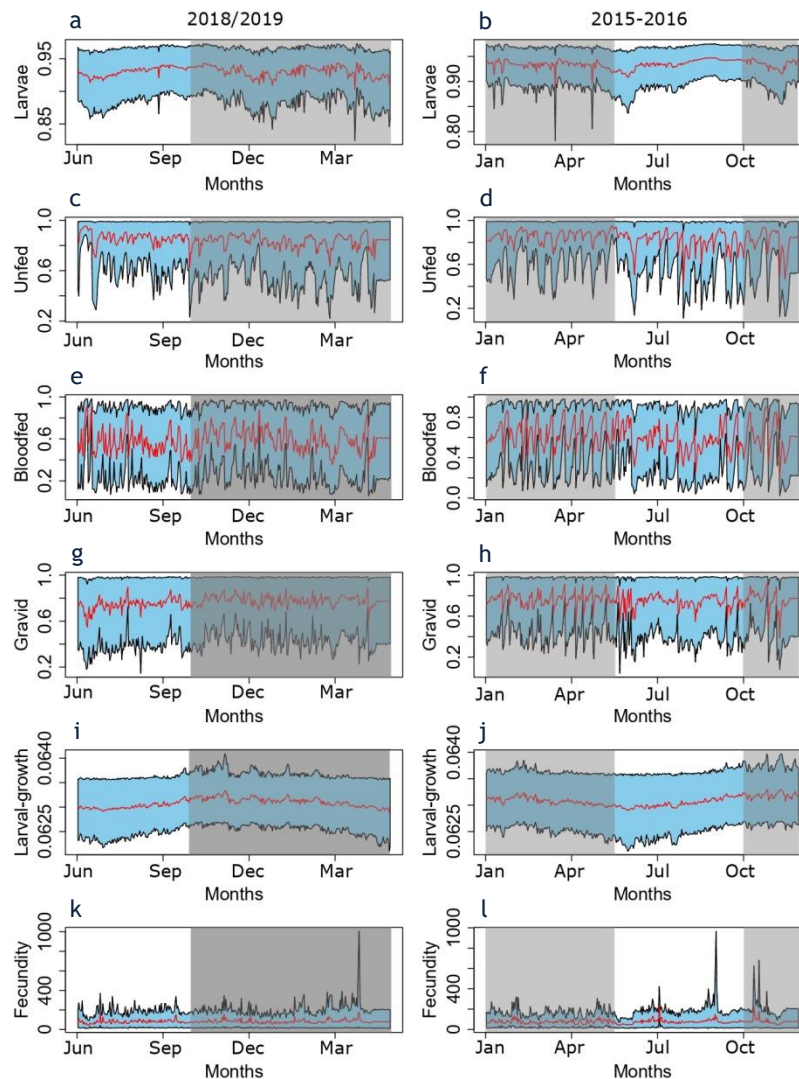


Figure 4.5: Reconstruction of the survival trajectories for all the four stages (larvae, unfed, bloodfed, and gravid) which were affected by the environmental covariates. The two bottom rows show the larval development period and fecundity trends. Left column (a,c,e,g,i,k) is trajectories from June 2018 to May 2019 and right column (b,d,f,h,j,l) is from Jan-Dec 2015. Grey area is the period with rainfall. Y-axis shows the survival rates of different life stages and the bottom row (k&l) shows per-capita fecundity

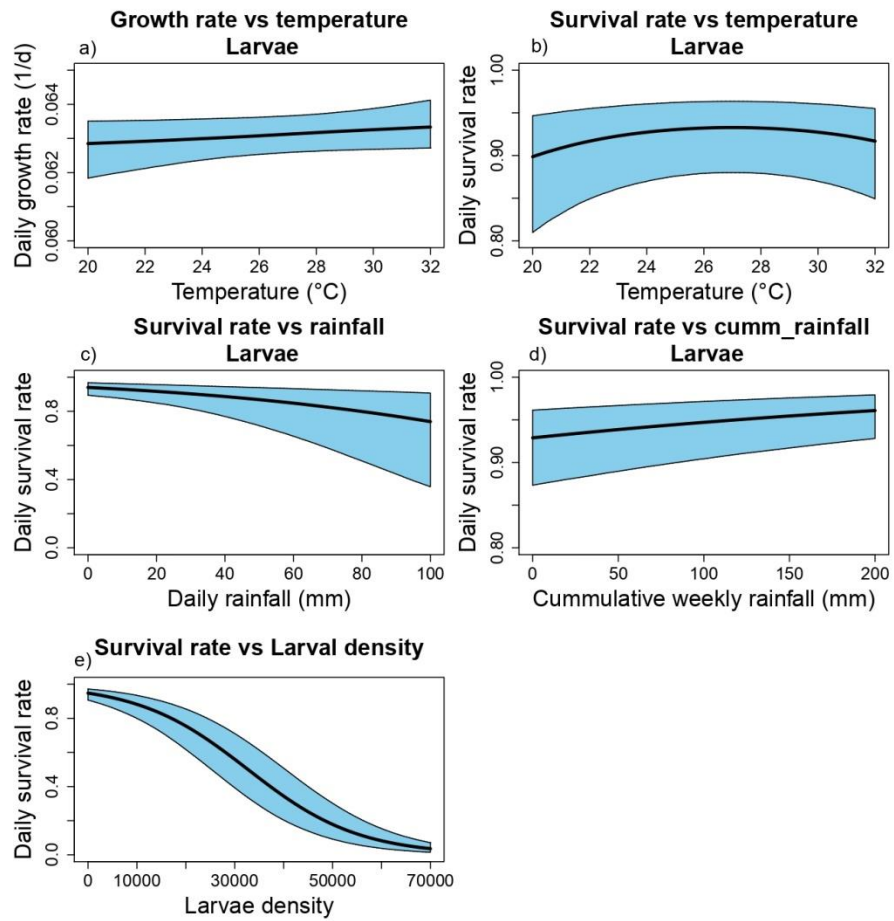


Figure 4.6: Relationship between environmental covariates and fitness parameters as estimated from the SSMs of population dynamic of *Anopheles funestus*. The predictions were produced from a posterior value.

Table 4.2: Priors for the intrinsic and extrinsic drivers of the population dynamic as used in the state-space model of *Anopheles funestus* and the estimated posteriors mean and 95% credible intervals.

Parameter		Prior distribution				Posterior distribution	
Notation	Description	Type	Source	Mean	sd	Mean	95-percentiles
β_1	Linear coefficient for rainfall on larvae survival rate	Gamma	Uninformative prior	0.1	0.05	0.01681	[0.00604, 0.0308]
β_2	Density dependent coefficient for larvae on larvae survival rate	Gamma	Uninformative prior	0.5	0.7	1.0283e-4	[1.0e-4, 1.1205e-4]
β_3	Coefficient of interaction between larvae and rainfall on larvae survival	Beta	Upward-Biased prior	0.9	0.1	0.9601	[0.80810, 0.99999]
β_4	Linear coefficient for temperature on larvae survival rate	Gamma	Uninformative prior	1	0.316	0.487	[0.203, 0.806]
β_5	Quadratic coefficient for temperature on larvae survival rate		a function of β_4	$\beta_5 = \frac{\beta_4}{2 * \rho}$		-0.00902	[-0.01492, -0.00376]
C_1	Linear coefficient for temperature on larvae development rate	Gamma	Uninformative prior	0.001	0.001	5.362e-4	[2.51e-8, 2.311e-3]
φ_1	Linear coefficient for temperature on unfed, survival rate	Gamma	Uninformative prior	1	0.316	0.074	[0.068, 0.081]
φ_2	Quadratic coefficient for temperature on unfed survival rate	Gamma	a function of φ_1	$\varphi_2 = \frac{\varphi_1}{2 * \rho}$		-1.378e-3	[-1.50e-3, -1.26e-3]

Parameter		Prior distribution				Posterior distribution	
Notation	Description	Type	Source	Mean	sd	Mean	95-percentiles
θ_1	Linear coefficient for temperature on bloodfed survival rate	Gamma	Uninformative prior	1	0.316	0.074	[0.068, 0.081]
θ_2	Quadratic coefficient for temperature on bloodfed survival rate	Gamma	a function of θ_1	$\theta_2 = \frac{\theta_1}{2 * \rho}$		-1.378e-3	[-1.50e-3, -1.26e-3]
α_1	Linear coefficient for temperature on gravid survival rate	Gamma	Uninformative prior	1	0.316	0.074	[0.068, 0.081]
α_2	Quadratic coefficient for temperature on gravid survival rate	Gamma	a function of α_1	$\alpha_2 = \frac{\alpha_1}{2 * \rho}$		-1.378e-3	[-1.50e-3, -1.26e-3]

Table 4.3: Model selection: Description of all models fitted with and without environmental covariates and their corresponding delta-Deviance Information Criterion Δ DIC

Model	Removed covariate(s)	Fitness measure	Penalized Deviance (pD)/DIC	Δ pD/DIC
Model 1-Full	None		35500	25339
Model 2	Temperature	Larval survival	10555	394
Model 3	Rainfall	Larval survival	10277	116
Model 4	One week cummulative rainfall*density dependency	Larval survival	11886	1725
Model 5	Density dependency	Larval survival	11011	850
Model 6	Temperature	Larval development period	10873	712
Model 7 [^]	Temperature	Adult survival	10161	0
Model 8	Model 7 - Temperature	Larval survival	10299	138
Model 9	Model 7 - Rainfall	Larval survival	15766	5605
Model 10	Model 7 - 1 week rainfall:density dependency	Larval survival	10199	38
Model 11	Model 7 - Density dependency	Larval survival	10383	222
Model 12	Model 7 - Temperature	Larval development	10497	336

[^] The best model (lowest DIC/Penalized Deviance) value-model-7 followed by model-10. **Model 8-12** consists of model-7 minus one more environmental covariate. **Model 4** involved the removal of the interaction term.

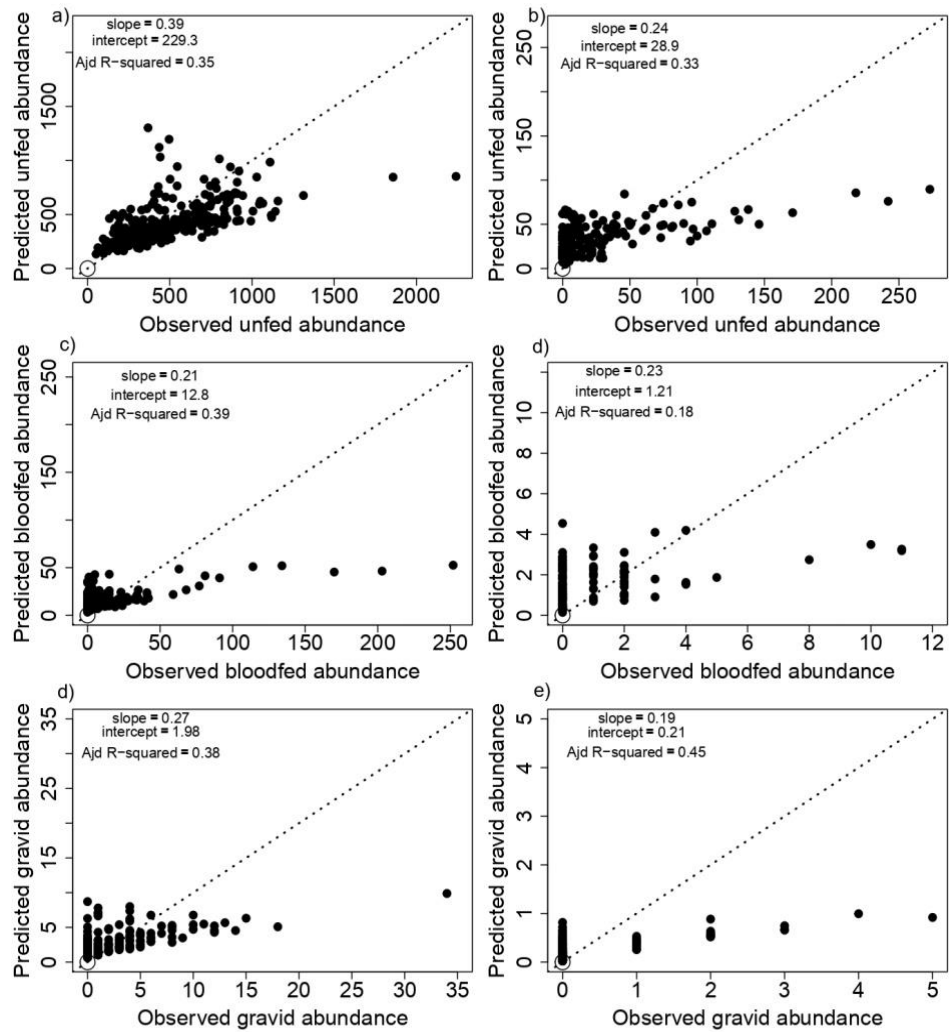


Figure 4.7: Goodness of fit: Observed versus predicted unfed, bloodfed and gravid densities across all populations. Adjusted R-squared, intercept and slope values are from a linear model of the predicted against observed values. Dotted lines correspond to 1:1 line. Left column (a,c,d) is data collected from June 2018 to May 2019 and right column (b,d,e) is data from Jan-Dec 2015.

4.4 Discussion

A state-space model (SSM) was developed and fit to field and laboratory data to accurately reconstruct the population dynamics of wild population of *An. funestus* from Tanzania. The SSM inferred the trajectories of multiple life-cycle and gonotrophic stages of wild *An. funestus* females. This allowed the reconstruction of the observed trajectories of larvae and adult females for wild *An. funestus* in Tanzania for the first time. This analysis indicated that the dynamics of *An. funestus* were best explained in a model that included density dependency, temperature (curvilinear relationship), daily rainfall (negative monotonic relationship), an interaction between larvae density and one week cumulative rainfall before sampling on larval survival. Temperature effect on the larval development rate (positive monotonic relationship) was also used to describe the model. In contrast, model fit was not improved by incorporating temperature dependency into adult survival (all gonotrophic stages). *Anopheles funestus* abundance vary seasonally between wet (highest abundance) and dry periods (lowest abundance); but demographics rates (i.e. survivals, fecundity and development period) did not show a clear seasonal pattern after accounting for the impact of environmental covariates and density dependence. These results are very useful for generating hypotheses about the nature and relative magnitude of drivers of *An. funestus* population dynamics in the wild. This model can be extended to include a component on malaria dynamics in humans; or to compare the efficacy and effectiveness of different interventions in combination or singly. This would allow more sophisticated evaluation of the suitability of *An. funestus*-specific interventions; including prediction of the potential combined effect of strategies that act at different life-cycle stages and/or target different demographic processes (e.g. survival versus fecundity).

Extrinsic covariates such as rainfall and temperature were all hypothesised to be the main drivers for the dynamics of this vector species. This study supports the hypothesis that rainfall is a significant driver of the population dynamics of wild *An. funestus*. Overall, the abundance of all life stages was relatively higher in rainy compared to dry periods of the year as previously documented [79,103,223,324]. Rainfall covariates were directly included in the larval survival model since it is the only stage on which rainfall was hypothesized to have a

significant impact. Daily larval survival as estimated by the SSM showed high variability both within seasons and across the year. There was support for a monotonic association between rainfall and larval survival; characterized as reduction in larval survival during periods of heavy rainfall. In previous studies, *Anopheles funestus* abundance has been shown to be positively associated with the cumulative lagged rainfall [103]. Here one week cumulative rainfall was included in the model to account for its effect on larval survival. In this work, an interaction between one week cumulative lagged rainfall and larval density shows an increase in the larval survival. Similar to other vectors of malaria transmission such as *An. gambiae*, rainfall has always been considered as the main factor regulating the dynamics [27,62,103,325]. In contrast to *An. gambiae* abundance which peaks much earlier in the rainy season, *An. funestus* on the other hand peaks at the very end of the rainy season.

The SSM also provided support for the hypothesis that temperature is an important driver of *An. funestus* dynamics; although the nature of temperature effects was complex and variable between life history stages. For example, temperature was associated with both larval survival and development, but not adult survival or fecundity. Furthermore the estimated impacts of temperature on larval ecology were complex; with the SSM suggesting a curvilinear relationship with survival but a positive monotonic impact with the larval development rate. These findings validate the prior studies that demonstrated that temperature had a curvilinear influence on *Anopheles* larval survival, with a rise in temperature above/below the optimum lowering survival [26,48,60]. The larval development period of *An. gambiae* is temperature dependent [48,318]; thus this model incorporated a positive monotonic effect such that development period is shorter when temperature is high and just below maximum threshold for larval development [23,48]. In this work, indeed temperature has been shown to speed up the development rate of the larvae to pupation. In the final model the effect of temperature on the survival of adult females (all gonotrophic stages) was not found to be an important across the range of values observed, and was thus removed during the model selection process.

Little is known about the effect of density dependence on *An. funestus* due to its ecology and reliance on the large semi-permanent and permanent breeding

habitats [54,95]. However, density dependence is already well-known to be an important driver for dynamic of other malaria vectors like *An. gambiae* [53,57,59,61,312,324,326] and other non-malaria vectors like *Aedes aegypti* [327,328]. Here the SSM fit better when density dependence of larval survival was included, however the relative magnitude of this process was quite small and thus likely to have minor impact on the overall dynamics of *An. funestus* populations. These findings suggest that *An. funestus* populations are likely to be regulated more by extrinsic than intrinsic processes; and corroborate the original hypothesis that density dependence may have a weaker regulatory role in this species than on those that use smaller, less permanent habitats (e.g. *An. gambiae s.s.*). The larger and more permanent habitat used by *An. funestus* (e.g. [95,329]) can likely sustain higher resources and thus reduce competition. This is among of the first report documenting the role of density dependence on the dynamics of the wild populations of *An. funestus*. A recent laboratory study on the effect of larval density on the life history traits of *An. funestus* shows that increasing larval density lengthens the larval development period [330]. Now that colonies are becoming more feasible, more thorough investigation on the role of density dependence in the dynamic of *An. funestus* is prerequisite.

In addition to highlighting potential drivers of *An. funestus* populations, the SSM here generated plausible estimates of key demographic and life-history processes in the wild. This model estimated that *An. funestus* larvae takes an average of 15.6-16.1 days to grow from first instar larvae to pupae; which is relatively long compared to the other major vectors in the *An. gambiae* complex (9-11 days [60,318]). This apparently longer development period of *An. funestus* may be a product of their adaptation to more permanent, year-round breeding habitats that are unlikely to dry up; thus reducing selection for rapid development. The SSM estimated that the daily survival rate of wild *An. funestus* larvae could be as high as 0.95, compared to the 0.83 [0.80, 0.86] mean daily survival rate of other African malaria vectors like *An. gambiae* [60,174]. This also matches observations from insectary experiments conducted by myself (Chapter 2 [24]) and others [100,222] in which *An. funestus* larvae have higher survival than *An. gambiae*. Given the apparently higher larval survival in *An. funestus* than in *An. gambiae*, these findings suggest that more lethal

intervention may be required to control *An. funestus* both at larvae and adult stages.

The impact of any vector control largely depends on the ecology of the specific vector species. Differences in ecology between *An. gambiae* and *An. funestus* are likely to affect the relative impact of interventions. For instance, *An. gambiae* prefer breeding in small and temporary habitats which dry up quickly when there is no rainfall; in contrast to the larger and more permanent aquatic habitats of *An. funestus*. This makes *An. funestus* habitats more likely to be "few, fixed, and findable" and thus suitable for targeting for larviciding [95]; particularly during the dry season. However treating large habitats such as rivers or bigger ponds could also pose logistical challenges. The persistence of *An. funestus* throughout the year even during the driest periods suggest this vector is less seasonal compared to *An. gambiae s.l.*, which experiences much more dramatic "boom and bust" dynamics in relation to seasonal rains [88,103,223]. This model suggests that *An. funestus* is likely responsible for year-round malaria transmission, while other vector species that rely on temporary aquatic habitats only be a substantial source of transmission during the rainy season.

Models of vector population dynamics can provide a useful guide for the selection of optimal vector control strategies; particular through enabling more focal investigation of the benefits of seasonal or spatial targeting and use of combined versus single interventions. Despite its complexity, this population dynamics model provides a useful framework for investigation of the stability of *An. funestus* populations. With additional data, this model can be further refined to include additional modifications related to vector ecology and behaviour that may impact intervention (e.g. host choice and its impacts on fitness, predation during larval or adult phase and spatial components). Such further elucidation may increase the predictive accuracy of this SSM (Figure 4.7) in specific contexts, but even the more general framework developed here has flexibility to introduce stage-specific mortality effects expected from different types of vector control [135,176,308]. For example, this framework could be used to model the impact of combined interventions including those that target adult females (insecticide-treated nets (ITNs), IRS) and larviciding; and assessment of how mortality varies with different coverage [135,308]. It can also

be used to investigate the possible response of vector population to climate change anticipated in Tanzania and other African countries. An important limitation of this study is lack of knowledge on what percentage of the *An. funestus* mosquito population is sampled by the trap, which is important for understanding the relative magnitude of demographic stochasticity in modelled dynamics. This highlights the need to explicitly incorporate this source of uncertainty into vector and transmission dynamics; including the need for further calibration and standardization of the efficiency and biases associated with particular mosquito trapping methods (e.g. Chapter 3).

4.5 Conclusions

This study used Bayesian State Space Models (SSM) parameterized with empirical data to quantify key demographic and fitness processes underpinning the population dynamics of *An. funestus* in Tanzania. This is the first use of SSM to understand the population dynamic of the wild vector of residual malaria transmission, *An. funestus* in Tanzania. The model identified that both environmental covariates (i.e. rainfall and temperature) and density dependence influence *An. funestus* and can contribute to observed patterns of seasonality; although the magnitude of density dependent effects was much smaller than that of environmental factors. The ability of this model to accurately reconstruct the seasonal dynamics and demography of *An. funestus* indicates its value for simulating the response of these populations to vectors control measures applied either individually or in combination. Finally, this model also highlights the clear importance of accounting for regional and daily observation biases when modelling mosquito population dynamics.

5.0 Chapter 5: Density dependence and demography alone cannot explain explosive dynamics in *Anopheles funestus*

Abstract

Background: Population dynamics models are regularly used to understand the ecology of vectors of malaria transmission and how these vectors respond to varying environmental conditions. Recently, I developed the first State-Space Model to describe the population dynamics of the *Anopheles funestus* malaria vector in southern Tanzania (Chapter 4). While this model was able to adequately reconstruct the observed dynamics of these populations and detect associations with climatic variables, there was uncertainty about its generalizability and ability to predict missing data. This was mainly driven by the following shortcomings 1) the detection of weak relationship between demographic parameters and environmental covariates, 2) the difficulty with fitting the model simultaneously to two different populations (Chapter 4) and 3) the model had not been tested under conditions of prediction (i.e. by removing data and validating). Here, I addressed three issues through model fitting and simulation exercises. First, I examined whether inferences about the relative importance of intrinsic and extrinsic population drivers derived from the hierarchical model were representative of individual populations. Second, by investigating the ability of the model to capture key features of population rises and declines, I assessed the potential existence of additional, unexplained drivers of dynamics. Third, I examined the ability of the model to predict *An. funestus* population dynamics outside of the seasons on which it was parameterized. By quantifying the prediction shortfalls of this model, it is possible to derive insights into *An. funestus* population dynamics and the potential existence of regulatory forces beyond known demographic and density dependent processes.

Methods: A Bayesian State Space Model (SSM) based on *An. funestus* life history was refitted to time series data from one of the two female populations on which the original hierarchical SSM model was developed (Chapter 4). To address these shortcomings I tried to see how much of the data could be accounted for

as signals and not noise by i) creating a focused model fit to one of the two populations, ii) increasing the flexibility of the density dependence formulation in the model, and iii) testing the predictive performance of the model under data removal condition. Here, the ability of the model to predict dynamics over different seasons was evaluated by removing a segment (i.e., 25%, 50%) of the time series data used in fitting and observing the impact on reconstructed trajectories.

Results: In general, the dynamics of the local *An. funestus* population were much better described by the single population SSM model than the hierarchical model generated from two populations. The ability of flexible forms of density dependence to account for observed dynamics remains minimal, suggesting the presence of additional factors regulating the dynamics. Model fitting to a single population revealed a stronger association between demographic processes and environmental drivers. The model was able to reconstruct missing time series data as long as some data from both wet and dry seasons was included in initial fitting.

Conclusion: This single population model's ability to explain the response of demographic processes to environmental covariates indicates its value in simulating the response of *An. funestus* populations to vector control. However, need to specify the model to single-village level before strong environmental links were revealed indicates that these relationships may be spatially non-stationary. The difficulty of capturing sustained troughs and explosive peaks purely via flexible density dependent modules indicates the need for additional currently missing biological processes (i.e., aestivation or diapause) in the life-history of the mosquitoes. The overarching importance of seasonality in capturing environmental and intrinsic population regulation was underlined by data-removal experiments which showed dramatic loss of predictive power when the model did not have access to information from both the wet and dry seasons.

5.1 Background

Models have been widely used to understand the dynamics of populations and how they interact with their surroundings [331,332]. In the context of infectious diseases, mathematical models have served as powerful, explanatory and predictive tools for identifying the intrinsic and extrinsic determinants of mosquito vector populations [43,44] and forecasting the knock-on effects for transmission in the face of global climate change [9,43,333-338]. The size of the mosquito population, which is highly dependent on the availability of aquatic larval habitats, is one of the predictors of malaria transmission [339]. Consequently, extensive effort has been devoted to developing models that can predict the abundance and seasonal dynamics of mosquito vector populations [161,166,324], and other life-history and demographic rates of direct relevance to transmission (e.g. adult survival [24,40,133,161]).

Vector-borne diseases are known to be highly sensitive to environmental conditions [47,62,103,340]. A range of biotic and abiotic variables are strongly associated with the distribution and transmission intensity of vector-borne diseases [150,167,206,339], and drive the abundance, seasonal dynamics and demography of mosquito population [166,341-343]. Most models of mosquito dynamics are parameterized using mean values of demographic rates or environmental conditions from a limited number of well characterized laboratory or wild populations [150,279,344]. Use of such mean values likely dampen out heterogeneities under diverse environmental conditions, and thus may give rise to predictions that are poorly representative of specific scenarios or ecological settings of interest. While models using mean or non-random parameter values still hold great value for analysis of general population trends and responses, they may not be appropriate for providing more targeted, setting-specific information. While limitations with model generalizability are generally recognized [345]; the magnitude of these problems are rarely quantified. Formal assessment of the generalizability of model predictions on drivers of population dynamics in other areas or time periods from which model parameters were derived is a useful first step to assess their applicability.

A desired requirement of mosquito population models is the ability to predict dynamics across a full range of seasonal variation. In the case of malaria in Africa, mosquito vector populations undergo substantial seasonal variation in response to changes to micro-climatic factors such as temperature and rainfall [79,153,346]. Seasonal changes in the environmental conditions that impact vector populations have a significant impact on malaria transmission; with incidence peaking during wet warm months when mosquito densities may be more than 100-fold higher than dry periods [88,99,166,347]. Another desirable feature of a mosquito population model is ability to predict the relative contribution of extrinsic and intrinsic factors to dynamics, such that inferences can be extrapolated to different populations beyond which the model was parameterized on. For example, density dependence is often an important intrinsic driver of population growth [22,59,61,326], and has been implicated in the population dynamics of the African malaria vector *An. gambiae* s.l. [326,348]. Here, density dependence arises through resource competition during larval development which impacts larval and adult survival, and hence overall abundance [46-49]. However, little is known about whether the relative importance of this process varies between populations; and how that influences the generalizability of inferences arising from models of one mosquito population to another.

Recently, Ngowo *et al* developed the first hierarchical state-space population dynamics model of *An. funestus*; a major vector of residual malaria transmission in the southern Tanzania (Chapter 4 [153]). This detailed biological model encapsulated the full life cycle of mosquitoes and was fit to data from two time-series data (referred here and in Chapter 4 as two populations) in southern Tanzania. Data from different populations were used to ensure that spurious features of the data from one population would be eliminated. This hierarchical model was used to assess the relative importance of extrinsic (temperature and rainfall) and intrinsic (density dependence) to population dynamics (Chapter 4). In this hierarchical model I have specified known facets of *An. funestus* life-history into a detailed population model incorporating the based on laboratory and published literature into parameter priors. I also allowed a mixture between process stochasticity and observation error and fitted the model to multiple time series of integrated population data while recognising latent variables. Given

these steps, any residual disagreement of the model with the data is informative about what aspect of the model is specific to each population (for example, the strength of seasonal patterns and the absolute abundances sampled) and what aspect of the model is insufficient (for example the density dependence).

The rationale for re-fitting the hierarchical model to a single population was to explore the limitations of the observation model. In doing so, emphasis was on whether there was only a weak relationship detected between demography and population regulation, which would indicate that the observation model was assigning much of the fluctuations to noise and not signals. I also assessed how hard it was to fit the model simultaneously to two different populations, in terms of whether the observation models required for that exercise required many differences between the subpopulations. Finally the model was tested under conditions of prediction by removing portions of the time series dataset during fitting and validating.

These model fitting and simulating analysis exercises allowed me to address the following aims: First, I examined whether inferences about the relative importance of intrinsic and extrinsic population drivers derived from the hierarchical model were representative of an individual population. Second, by investigating the ability of the model to capture key features of population rises and declines, I assessed the potential existence of additional, unexplained drivers of dynamics. Third, I examined the ability of the model to predict *An. funestus* population dynamics outside of the seasons on which it was parameterized. In combination, this will enhance understanding of *An. funestus* population dynamics through investigation of the strengths and limitations to current model generalizability. This can facilitate development of a more robust population dynamics model that could be used to guide selection of optimal packages of vector control interventions for *An. funestus* in specific settings.

5.2 Methods

5.2.1 Population dynamic model

A hierarchical State-Space population model (SSM) of *An. funestus* dynamics was developed by Ngowo et al (Chapter 4, [153]) to investigate extrinsic and intrinsic

drivers of populations in southern Tanzania, and to assess observational uncertainty. This model was developed in the JAGS [301] platform using a State-Space approach in a Bayesian framework. In brief, the model used daily time series data on the abundance of adult *An. funestus* females collected in 2015 [88] and 2018/19 from two populations respectively for model fitting and validation. Prior information on maximum survival (adult and larval) and larval development rates were derived from a mixture of laboratory experiment performed on F_1 *An. funestus* in an insectary [24] and other published literature [88,195]. This model was structured to consider four mosquito life history stages (eggs, larvae, pupae, adult female), with the adult stage being further subdivided into the physiological stages of unfed, blood-fed and gravid.

This population model also incorporated microclimatic data on temperature and rainfall on a daily average scale. Rainfall and temperature were prioritized as the primary environmental covariates in the model given their strong, known impacts on mosquito populations. Further explanation and justification of the choice of these covariates is given in Chapter 4 (methods section).

In the current work, I re-fitted the model with the same prior information to one of the two time series data (i.e. 2018/2019 time series data). To address the first aim, the joint posterior parameter values generated from this single population model were used to plot the responses of demographic values across the full range of observed environmental covariates to assess and investigate, a) the relationship estimated between rainfall and larval survival rate, and b) the relationship between temperature and larval and adult survival. Here, I examined whether the associations estimated from the single population response were consistent with those inferred by the hierarchical model (Chapter 4). To address the second aim, I increased the flexibility of the density dependence formulation in the model. This process allowed observation of volatility in the system and any factors which can be causing population decline/increase beyond density dependence and demographic parameters. To address the third aim, I tested the model predictive performance under data removal conditions. Specifically, I refitted the current single population model under two scenarios: the first being using 75% of the time series data to predict the remaining 25%. This 75% cut across both the wet and dry seasons, such that the model could learn from observed dynamics during both periods of the

year. In the second scenario, 50% of the data the time series data were used to predict the remaining 50%. The latter did not allow the model to learn from both seasons, as a large part of the wet season dataset was removed.

5.2.2 Model fitting and diagnosis

The state-space model with all environmental covariates was fit using a Markov Chain-Monte Carlo (MCMC) algorithm via the JAGS software [301] interfaced to R via the *runjags* package [302]. A model with 3 chains was run in parallel for 10^5 samples and a burn-in of 10^5 , thinning every 10^{th} iteration. Two single population dynamic models were refitted with missing time series data (i.e. 25% and 50%) and their prediction capability was assessed visually by looking at the proportion of curve within the credible intervals. Convergence was assessed by visual inspection of the trace plots and prior-posterior distribution using the *coda* package [321], effective sample size and the Gelman Rubin diagnostics [322]. Posterior means and 95% credible intervals for the environmental covariates and density dependence were reported. The differences between posterior means were estimated using a Bayesian t-test [349] implemented using *BayesFactor* Package [350]

5.3 Results

5.3.1 Generalizability of inferences from a single population and hierarchical model

By re-fitting the hierarchical model of *An. funestus* dynamics (Chapter 4) to a single population, I assessed generalizability of inferences about the role of environmental covariates and density dependence. The full summaries of the posterior means for all the environmental covariates evaluated in the single population model are reported in Table 5.1. The model reconstructed the dynamics of the single *An. funestus* population very well (Figure 5.1). Population trajectories (abundances, survivals) were reconstructed for each of the six life stages together with fecundity (Figure 5.1) after consideration of the impact of environmental covariates. Temporal values for larval development periods were reconstructed, and showed no clear variation between the dry and wet season

(Figure 5.2). There was no noticeable contrast between the seasonal trend in *An. funestus* abundance as estimated in the hierarchical model and single population model (Figure 5.1 and Figure 4.3). The population trajectories produced by both models predicted a clear seasonal pattern characterized by sustained low abundance of *An. funestus* throughout the dry season, which rose to a peak within several weeks after the onset of rains (Figure 5.1).

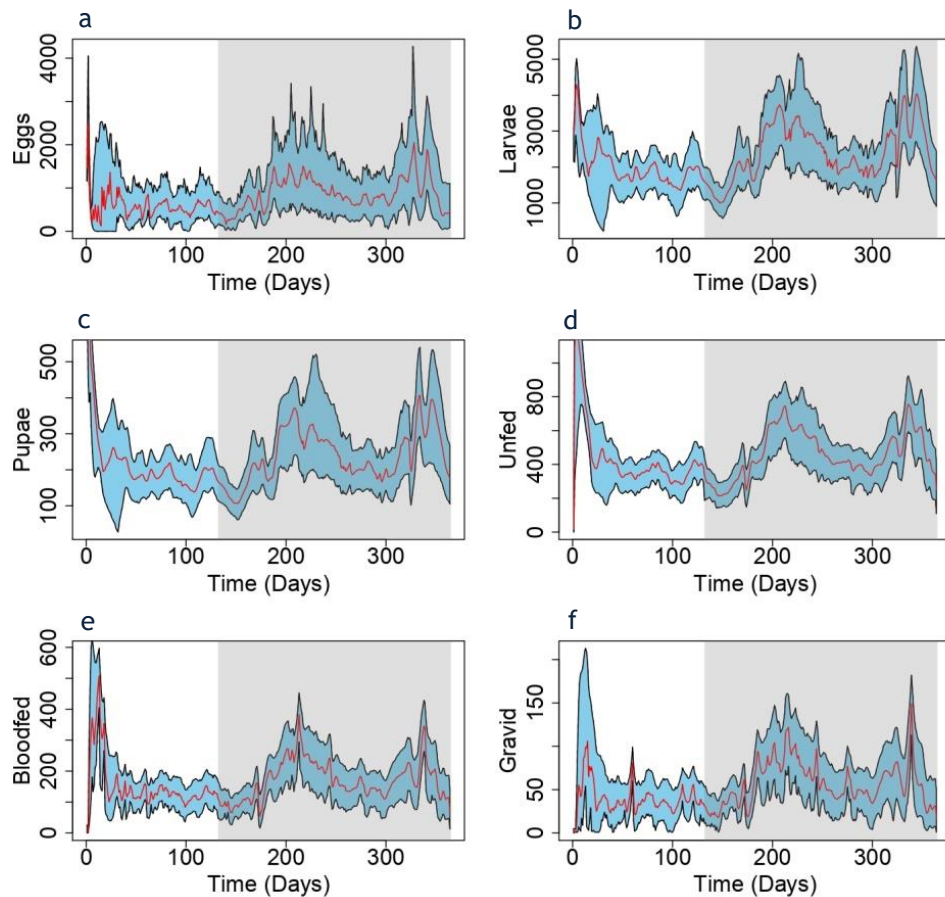


Figure 5.1: Reconstruction of the abundance trajectories of the six mosquito life-stages; a) eggs, b) larvae, c) pupae, d) unfed, e) bloodfed and f) gravid from the SSM fitted to a single population. The red line indicates the mean posterior values and the respective 95% credible intervals are shown in “sky-blue”. The grey-shaded region indicates periods with rainfall. Time step “0” refers to the start of data collection June 2018 and ending May 2019.

In the single population model, demographic parameters such as adult survival (all gonotrophic stages) were highly sensitive to temperature; with values dropping notably outside the optimum value (27°C) (Figure 5.3). In contrast, adult survival was estimated to be less temperature-dependent in the

hierarchical model, and hence removed from the final model during model selection.

To highlight these differences, in the hierarchical model (before model selection), the daily survival of adults (all stages) was estimated to vary no more than 2% across a range from 20°C - 32°C. In contrast, the single population model estimated a 4.5-fold difference in adult daily survival across the range from 20°C - 32 °C (Figure 5.3); with a low of 0.21 at 20°C; compared to 0.937 at the 27°C optimal.

Table 5.1: Posterior means for the intrinsic and extrinsic drivers of the population dynamic as estimated by the state space model in [153] and the refitted single population model for *Anopheles funestus* and their respective means and 95% credible intervals.

Parameter		Multiple population		Single population	
Notation [‡]	Description	Mean	95-percentiles	Mean	95-percentiles
β_1	Linear coefficient for rainfall on larvae survival	0.01681	[0.00604, 0.0308]	0.07634*	[0.04172, 0.10681]
β_2	Density dependent coefficient for larvae on larvae survival	0.0001028	[1.0e-4, 1.1205e-4]	0.000123	[1.0e-4 4.990e-4]
β_3	Coefficient of interaction between larvae and rainfall on larvae survival	0.9601	[0.80810, 0.99999]	0.9468	[0.7309, 1.00]
β_4	Linear coefficient for temperature on larvae survival	0.487	[0.203, 0.806]	0.3157	[0.11703, 0.5941]
β_5	Quadratic coefficient for temperature on larvae survival	-0.00902	[-0.01492, -0.00376]	-0.00585	[-0.0110, -0.00217]
C_1	Linear coefficient for temperature on larvae development period	5.362e-4	[2.51e-8, 2.311e-3]	4.9724e-4	[5.097e-8, 2.16e-3]
φ_1	Linear coefficient for temperature on unfed, survival	0.074	[0.068, 0.081]	4.1033*	[1.8274, 5.0408]
φ_2	Quadratic coefficient for temperature on unfed survival	-0.00138	[-0.0015, -0.00126]	-0.07598*	[-0.0933, -0.0338]
θ_1	Linear coefficient for temperature on bloodfed survival	0.074	[0.068, 0.081]	4.1033*	[1.8274, 5.0408]
θ_2	Quadratic coefficient for temperature on bloodfed survival	-0.00138	[-0.0015, -0.00126]	-0.07598*	[-0.0933, -0.0338]
α_1	Linear coefficient for temperature on gravid survival	0.074	[0.068, 0.081]	4.1033*	[1.8274, 5.0408]
α_2	Quadratic coefficient for temperature on gravid survival	-0.00138	[-0.0015, -0.00126]	-0.07598*	[-0.0933, -0.0338]

* Coefficients of environmental covariates that differ between the two types of model structure highlighted in orange (Bayesian t-test was used)

[‡] Notations' meaning and the modelling equations should be referred to in the previous chapter (Chapter 4).

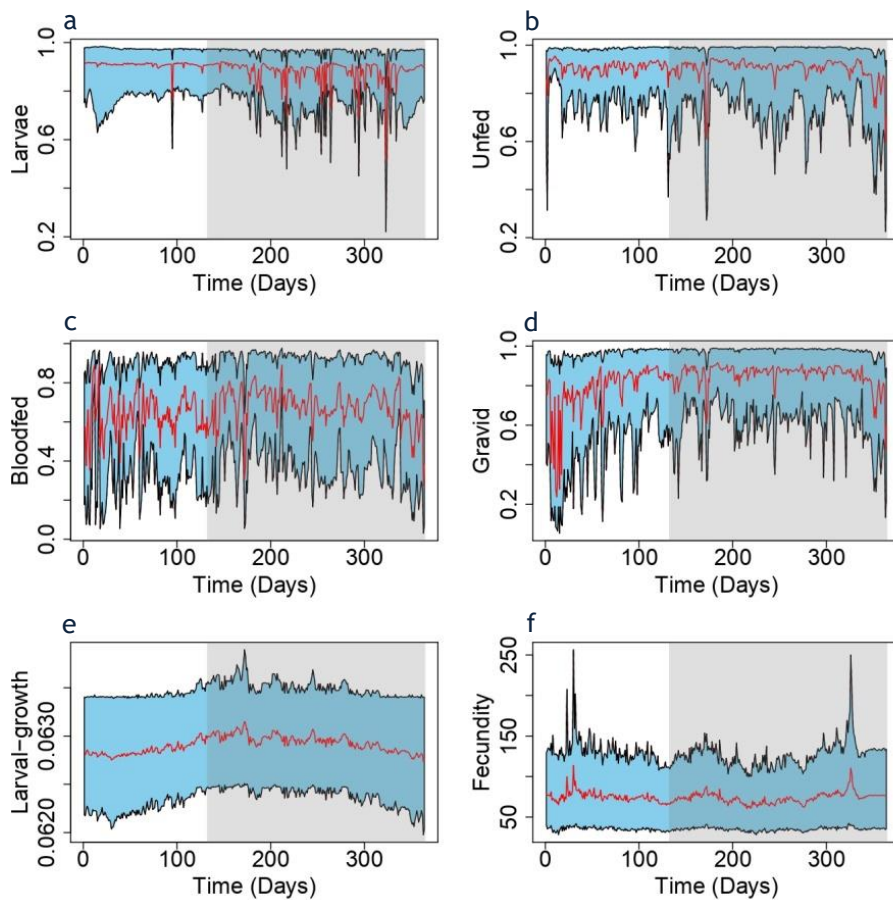


Figure 5.2: The survival trajectories of *An. funestus* from a wild population in Tanzania as estimated by the SSM model for the four life stages; a) larvae, b) unfed, c) blood-fed and d) gravid mosquitoes. The bottom row shows; e) larval development rate and f) fecundity trends over time. The red line indicates the mean posterior values and the respective 95% credible intervals are shown in “sky-blue”. The grey shaded region indicates periods with rainfall. Time step “0” refers to the start of data collection June 2018 and ending May 2019.

Larval survival was not strongly associated with temperature or cumulative weekly rainfall in either the single or hierarchical model (Figure 5.3). However, larval survival was estimated to be strongly negatively associated with daily rainfall in the single population but not in the hierarchical model. In the single population model, daily larval survival was estimated to be less than 5% when daily rainfall reaches >50mm (Figure 5.3); compared to ~ 85% in the hierarchical model (Figure 4.6).

The importance of microclimatic variables was emphasized in this single-population model, indicating that there were stark differences between the two populations that the hierarchical parameters were not enough to capture; hence a muted response was estimated (Figure 5.3). Much of the goodness of fit of the single population model was due to the ability of the observation part of the model to assign variation in the data to noise, rather than signal.

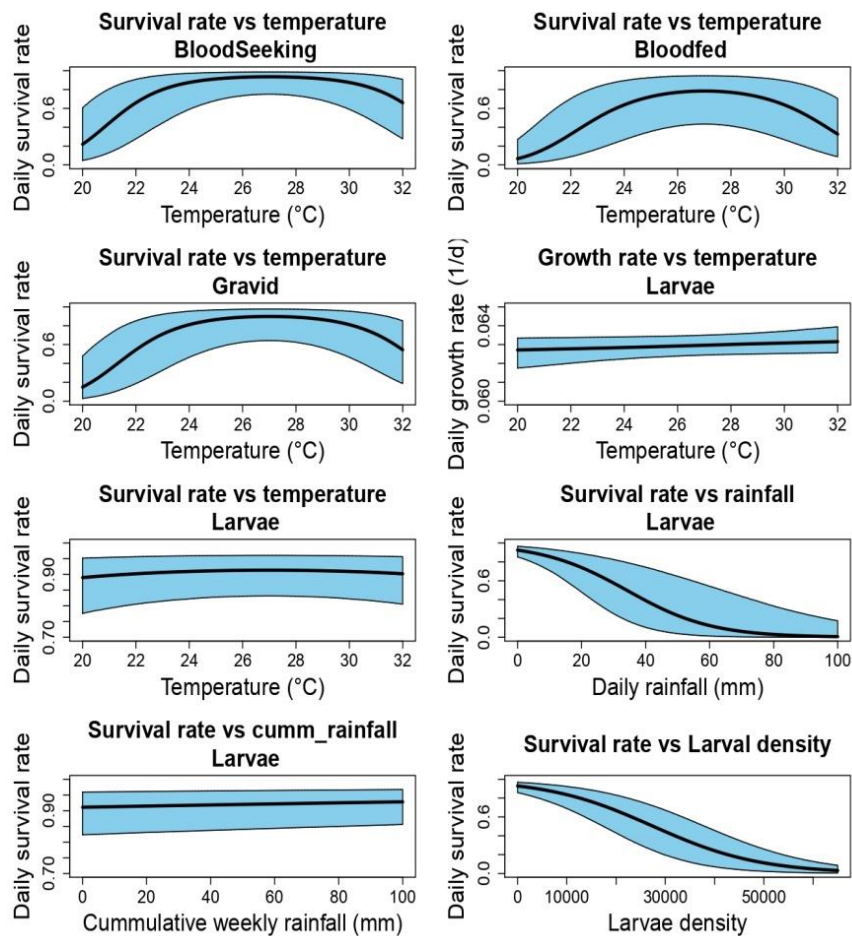


Figure 5.3: The influence of environmental covariates on the demographic parameters as estimated from the single population dynamics model of wild *An. funestus*.

5.3.2 Unexplained drivers of population dynamics

By constraining the density dependence parameter, it was possible to explore hidden mechanism which might contributes to population growth beyond density dependence and demographic parameters. In both models (single vs. hierarchical), the density dependence parameters were being reduced to low values which

suggests that observation uncertainty during data collection might be creating additional instability in the system. Also, there was evidence of hidden processes accelerating population growth that the model was only able to account for by diminishing density dependence. Both models (Figure 5.1 and Figure 4.3) show a slight increase in the abundance of the adult (unfed, bloodfed, gravid) mosquitos several weeks after the first rain event after a long period of dryness. The single population model suggests that density dependence was unable to explain the persistently low values and the rapid explosive increases simultaneously (Table 5.1). This is similar to the findings of the original hierarchical model, with no difference in the density dependence values from the original hierarchical model even after constraining the prior values for the density dependence parameters.

5.3.3 Ability of the model to predict missing seasonal data

Here, I assessed the ability of the single population model to predict a portion of missing seasonal data through visual inspection of the credible intervals of the population abundance trajectories. This indicated that the model with constrained density dependence can reliably reconstruct up to 25% of missing time series data (spanning wet and dry season) with sensible credible intervals (Figure 5.4). However, when the proportion of missing data was increased from 25% to 50% (incorporating largely dry season); the model lost its prediction capability as evidenced by increasing levels of uncertainty around predicted abundance trajectories (Figure 5.5). The high level of uncertainty in the 50% part of the missing data was mainly driven by the low value of the density dependence parameter which was unable to keep the population from exploding.

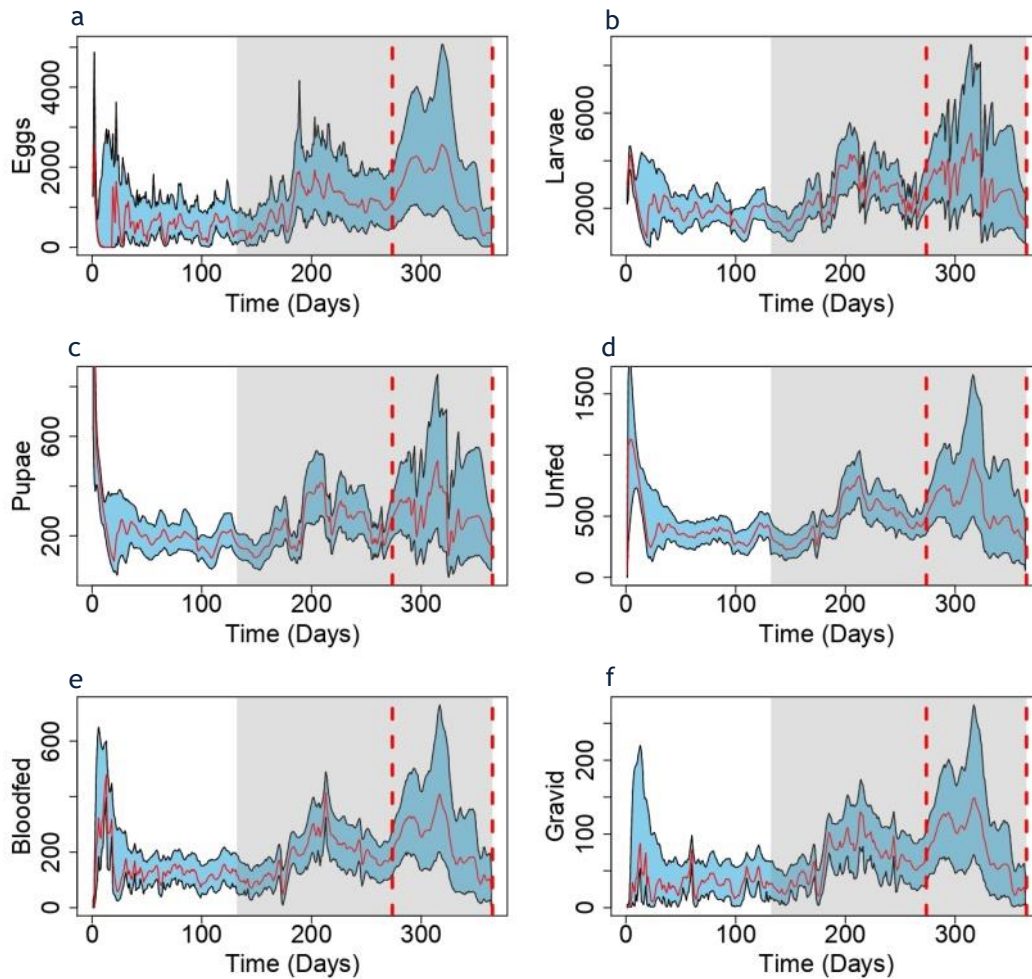


Figure 5.4: Abundance trajectories showing the prediction of the 25% missing data at the end. The vertical red dotted lines corresponds to missing data (25%) which were removed during model fitting and allow the model to predict. The red line indicates the mean posterior values and the respective 95% credible intervals are shown in “sky-blue”. The grey shaded region indicates periods with rainfall. Time step “0” refers to the start of data collection June 2018 and ending May 2019.

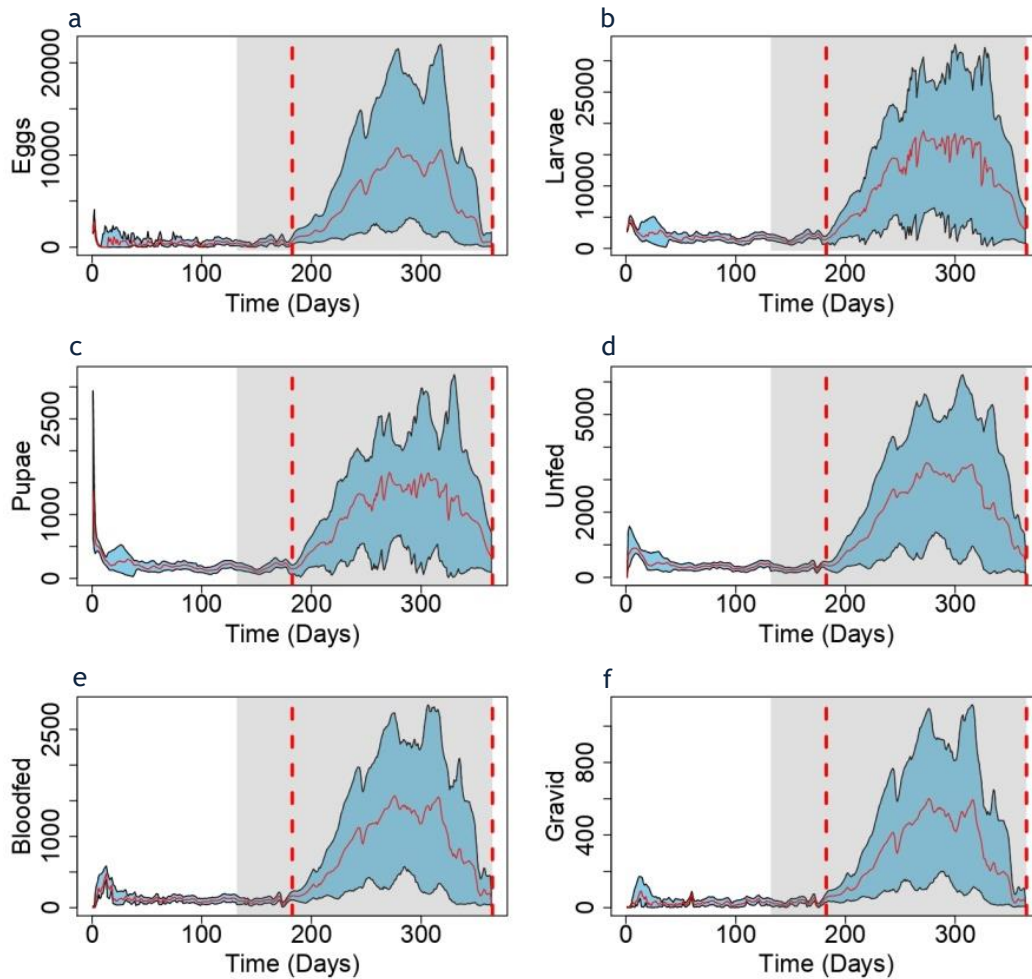


Figure 5.5: Abundance trajectories showing the prediction of the 50% missing data at the end. The vertical red dotted lines corresponds to missing data (50%) which were removed during model fitting and allow the model to predict. The red line indicates the mean posterior values and the respective 95% credible intervals are shown in “sky-blue”. The grey shaded region indicates period with rainfall. Time step “0” refers to the start of data collection June 2018 and ending May 2019.

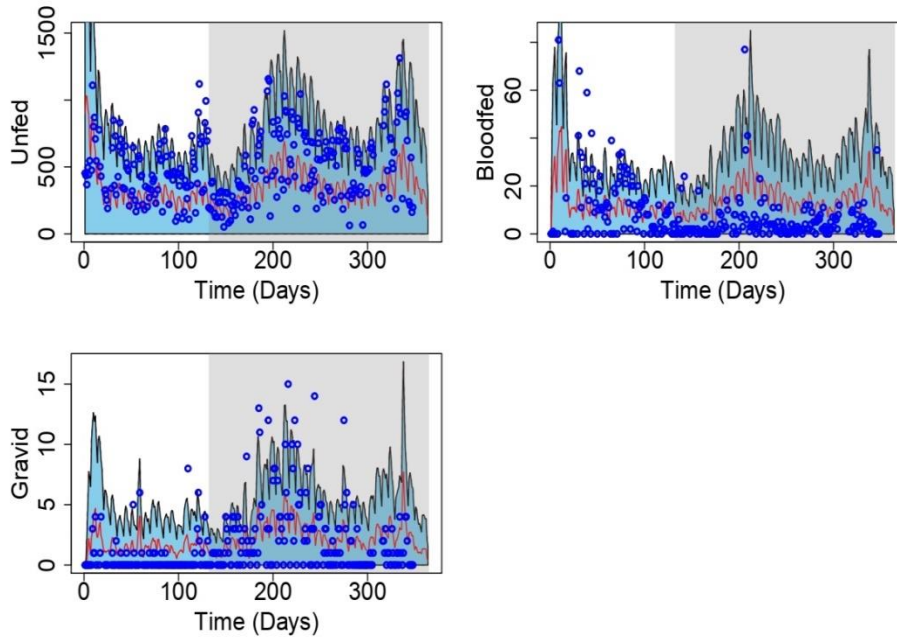


Figure 5.6: Observed vs. model estimated values for the three adult stages with data collected using CDC light trap both in June 2018 -May 2019. Red lines are the model estimated trajectories with “sky-blue” showing their 95% credible intervals. The blue circles are the observed values from the Light trap catches. Grey areas are the periods with rainfalls episodes. Time step “0” refers to the start of data collection June 2018 and ending May 2019.

5.4 Discussion

I re-examined the previously developed SSM model for the population dynamics of the wild population of *An. funestus* (Chapter 4, [153]) by fitting it to a single population. This analysis suggests that the reconstructed seasonal population trajectories of *An. funestus* were broadly similar in main features in hierarchical and single population model. In both cases, *An. funestus* were predicted to remain stable at low densities across the dry season, and start to rise several weeks after the first rains, with a peak occurring at the start of the dry season. The contribution of density dependence remained minimal in the single population model, but was sufficient to be retained by the model. I had to constrain the density dependency parameter in all the models. This requirement to constrain density dependence in the model suggests the existence of observation uncertainty during data collection which creates additional volatility in the system, and/or the

presence of a missing regulatory process that was accelerating population growth; which the model was only able to account for by diminishing density dependence.

In contrast to findings obtained for the Hierarchical model, *An. funestus* demographic parameters in the single population model were more responsive to environmental covariates. Demographic effects of covariates were much stronger in the single population model compared to hierarchical model. The hierarchical model assumed that parameters describing the response of demographic variables to micro-climatic conditions were the same in all populations. Releasing the model to fit to only one population resulted in a shift from muted to strong responses of environmental covariates. This implies that the response of *An. funestus* demography to environmental conditions may be diverse and vary between populations. For example, larval survival varied by 78% and 85% respectively along the range of variation in temperature and rainfall covariates considered in simulations. The SSMs are great in modelling population dynamics models but can be used with caution as may underestimate the role of environmental drivers when fitted over multiple populations.

This model was able to predict seasonal abundance trends relatively well when 25% of data were missing, but struggled when this was increased to 50%. The single population model was thus quite robust to missing data as long as the data included in fitting contained some representation from the dry and wet seasons. This indicates that the model can predict only if it learns from both wet and dry seasons. This model can be expanded to include other aspects of human malaria dynamics, or it can be used to simulate the efficacy and effectiveness of various interventions individually or in combination. This would allow more sophisticated evaluation of *An. funestus* specific intervention in different target areas.

In general, most of the population dynamics models previously developed for African malaria vectors have not accounted for biological processes beyond traditionally life history processes of births and death. Other processes such as aestivation, diapause or mosquito migration (e.g. [351,352]) could lead to changes in vector population abundance beyond what can be attributed to these life history processes. For example, aestivation is a process through which mosquitoes may become temporarily ‘dormant’ by concealing and restricting their flight activities

until the onset of first rain [151,353,354]. In the current *An. funestus* population dynamic model, I speculate that such additional factors could play an important role in population regulation beyond the current minimal role of density dependence. This hypothesis is based on the observation that in the absence of explicit incorporation of processes like aestivation/diapause into this model, the density dependency parameter was penalised by having its value reduced to account for the missing factors.

A successful mosquito dynamics model should be able to satisfactorily capture key features of population trajectories as a result of known life history and development processes. For example, in a closed population, changes in adult mosquito abundance are expected to follow those of larval abundance, with a lag period characteristic of typical larval development periods. If unexplained rises and declines are evident, this may suggest additional biological processes are missing from the model; including deviation from the assumption of a closed population. For example, some studies have shown that seasonal aestivation and migration of adult mosquitoes has a strong influence on the overall dynamics of *An. arabiensis* [351,354]. This was detected through a signature in a population model that showed vector densities rose far quicker at the start of the wet season than could be explained by the time required for egg-larval-adult transition [351]. Study on non Anopheline species shows that, *Aedes aegypti* species eggs can survive the dry soil for more than two months [355-357] contrary to *Anopheles* eggs which survive less than 15 days [358]. With the dry period of more than two months in most of African countries which are malaria endemic, the only possible survival mechanism for adult mosquitoes is through aestivation [45]. Similar unexpected changes in population size beyond what can be explained by reproduction and mortality could be due to pulses in dispersal into or out of populations [100,359]. Additionally, it is possible for habitat composition to affect one demographic rate in one place but a different one in another. For example, the two time series data used in the hierarchical model contain differed in mean population abundance suggesting that abundance varies with geographical location. A life history-based model that fails to capture key feature of population dynamics can serve a useful purpose in highlighting the existence of additional regulatory factors. With additional data on aestivation, mosquito migration or

diapause this model can be further extended to incorporate all these environmentally driven aspects of the mosquito ecology. This may further increase the predictive accuracy of this SSM and generalizability in the assessment of stage-specific impact expected from different vector control measures.

5.5 Conclusion:

Using a novel parsimonious framework, the effect of rainfall, temperature, and density-dependence was investigated on more geographically restricted population of *An. funestus* s.l. (considered as 'one population') from southern Tanzania. The single population framework developed here could allow for a more robust analysis and evaluation of various vector control interventions, as well as their integration into malaria transmission models, in the future. This model's ability to explain the response of demographic parameters to environmental covariates indicates its value in simulating the response of this *An. funestus* population to vector control measures used individually or in combination. In this regard, the developed paradigm is a significant step forward; however it also identifies critical research gaps beyond demographic processes (i.e. aestivation or diapause) that must be addressed if we are to gain a better understanding of the ecology and population dynamics of this vector species. Furthermore, future models should include spatial elements to capture the diversity and presence of any source of heterogeneity in multiple populations.

6.0 Chapter 6: General Discussion

6.1 Overview of the main findings

The overall goal of this thesis was to contribute to a general foundation of improving knowledge on the ecology and surveillance of *Anopheles funestus*, a major vector of residual malaria transmission in many settings in Africa. It is hoped that information gained through this work will aid the campaign against malaria by improving vector control strategies in Tanzania and other settings where *An. funestus* is the major source of transmission. Malaria transmission remains high in Tanzania; hence this work will contribute important knowledge on how to exploit the ecology of *An. funestus* to further progress towards elimination. This general discussion will provide a brief summary of key findings from each of my specific objectives, discuss relevant challenges and limitations of this study, and highlight key implications for vector control and malaria elimination.

6.1.1 Fitness characteristics and colonization barriers

Extensive investigation and characterization of the biology of any malaria vector requires a stable laboratory colony. The lack of colonies from locally representative *An. funestus* populations creates a gap in terms of how to tackle transmission mediated by this vector in Tanzania. For example, assessment and monitoring of insecticide-based interventions requires carrying out bioassays on mosquitoes. Semi-field systems are often been used as the first step to study the behavior and response to intervention for any malaria vectors before the field trials. Most phase 1 intervention trials on *An. gambiae* were conducted in controlled laboratory settings, enabled by the existence of stable insectary colonies [196,360]. However, similar evaluations for *An. funestus* have been limited by the difficulty of establishing stable colonies under lab or semi-field settings. Consequently although *An. funestus* is a major vector in Tanzania, it has not been possible to evaluate the efficacy of different vector control intervention or trapping methods for local populations of this species under standardized (lab or semi-field) conditions.

Here, I evaluated key barriers associated with the colonization of this malaria vector species in the laboratory environment. I attempted to colonize this species by collecting wild mosquitos (F_0) from three villages in the rural part of south-eastern Tanzania and rearing them in the laboratory. This showed that the fitness characteristics (i.e. mating, fecundity) of F_1 offspring in the laboratory were impaired relative to that of a stable *An. funestus* colony (FUM0Z). Mating was the biggest barrier to establishing further filial generations; with <10% of F_1 females were able to mate in the laboratory whereas 92% of wild F_0 were mated. This resulted in very few viable eggs being produced despite the relatively large number of F_1 females, which were insufficient to generate a further filial generation. This low mating success is consistent with the known eurygamy of this species [38,39]. Other aspects of *An. funestus* development and fitness in the laboratory were also impaired. Notably, the very long larval development period (2-3 weeks) observed for *An. funestus* in the laboratory led to a low probability of survival to adulthood. The larval development period for *An. funestus* in the lab was considerably longer than reported for other African vector species (e.g. *An. gambiae* sl. 9-11days). Although my attempts to colonize a Tanzanian *An. funestus* population were not successful, they provided general knowledge on the major barriers to colonization (e.g. mating) and help focus investigation on how to overcome them.

6.1.2 Surveillance methods of outdoor vectors of malaria transmission

Surveillance of vector populations is of great importance for assessing the effectiveness of interventions and monitoring the behavior of mosquito species in a given setting. The most important entomological indicator of malaria transmission is the entomological inoculation rate (EIR) [361]; calculated as the product of mosquito biting and infection rates. Human landing catches (HLCs) are the gold standard for estimating biting rates and the EIR in both indoor and outdoor environments. However, this method is increasingly restricted due to ethical concerns arising from the exposure of collectors to potentially infected mosquito bites. Whereas several exposure-free alternatives to the HLC have been evaluated for *An. gambiae* s.l. (HLC); there is less understanding of which methods are best

for *An. funestus*; particularly in outdoor settings. A trap evaluation study comparing the performance of HLC and six exposure-free alternative traps for outdoor settings was conducted in places where both *An. gambiae s.l.* and *An. funestus* are found. Here, I analyse the data and generate associations between the alternative traps and HLC. These associations were later used to develop a calibration tool for predicting the number of mosquitoes collected by HLC if someone were to use one of the alternative trap evaluated.

Relationships between collections made by the HLC and alternative methods may not accurately reflect their association across more diverse ecological contexts. If we wish to not only evaluate how an exposure-free trap performs relative to the HLC, but allow the 'HLC'-equivalent exposure rate to be predicted from it, it is necessary to identify which type of mathematical relationship (linear or non-linear) best describes their association. Here, a statistical calibration tool was developed under a Bayesian framework in the form of a *Shiny App* interface for its interrogation. The tool developed here provides predicted mean values for each alternative traps and their credible intervals which can be used to obtain estimates relative to HLC. Results suggest that trap performance is less affected by population baseline density (intra-specific) for all the species, though these findings tend to differ when the same alternative traps are evaluated in a different environment [124,288].

This analysis provided little evidence that the relative performance of mosquito traps is modified by the density of the target vector or other mosquito species in the environment. Trap catches varied between species and between model configurations, so no specific model or trap is 'best' for all vector species. The tool developed here warrants further evaluation of different alternative traps to consider how representative and consistent they are compared to the HLC or other collection methods.

6.1.3 Drivers of population dynamics of wild *Anopheles funestus*

Chapter 4 describes an innovative state-space population dynamics model of wild *An. funestus* in Tanzania. Population dynamics model have been frequently used to

understand the dynamics of the African malaria vectors in the *An. gambiae* complex [150,158,362]. Similar models have been difficult to develop and parameterize for *An. funestus* due to the limited knowledge of their fitness and demography. Consequently, the response of *An. funestus* to environmental factors and interventions is often inferred from population dynamics models derived for *An. gambiae* s.l.

Here, I used data collected during attempts to colonize *An. funestus* (Chapter 2) and additional data from the literature as the prior information to develop a biological process model of *An. funestus* population dynamics. The specification of this model allowed *An. funestus* dynamics to be influenced by both intrinsic (density dependence) and extrinsic drivers (environmental covariates). Population abundance time-series data were used to inform the observation process model (collections from CDC light trap). CDC light traps are designed to capture mosquitoes that are looking for a blood meal (host seeking), but also occasionally catch gravid and bloodfed mosquitoes. Consequently the observation model attempted to account for trap bias in collections of bloodfed and gravid mosquitoes. Further work is needed to assess the proportion of the population; whether unfed, gravid and bloodfed, that is sampled in CDC and other trapping methods. Such information will refine the observation model and accuracy of resultant demographic predictions.

In examining environmental covariates of *An. funestus* dynamics, I focused on temperature and rainfalls given these are known to be key drivers of mosquito fitness and demography. Additionally, the impact of intrinsic drivers was addressed through consideration of density dependence arising at the larval stage. The potential contribution of environmental covariates to vector dynamics was assessed through a removal strategy and see what the model would predict. The resultant model was able to reconstruct the abundance trajectories for all *An. funestus* life stages and gonotrophic stages. Notably, the relatively low uncertainties around these trajectories indicate the model was a reasonable fit to the data. These trajectories show that *An. funestus* densities are generally higher during the rainy period; with numbers peaking towards the end of the wet season. Notably, although *An. funestus* densities were low during the dry season, they

persisted throughout the full duration of this period. In contrast, *An. gambiae* s.s. and *An. arabiensis* had almost no captures during the driest period. During the dry season, the estimated mean values for *An. funestus* were quite low but sufficient to keep the population going until the first rain. The survival trajectories of larvae and adult stages were similar across seasons; indicating this species is relatively resilient to temperature and rainfall extremes. The ability of this vector to survive the driest part of the year indicates it plays a crucial role in sustaining malaria transmission throughout the rest of the year. Targeting *An. funestus* during the dry season could thus be a key to disrupting transmission during its most vulnerable point.

This modelling framework suggests that density dependence may be present in *An. funestus* populations, but makes a relatively minimal contribution to their dynamics. I hypothesised that there is an additional feature in the dynamics that regulates the population by lowering density dependence parameters. This was further evaluated in Chapter 5. Whether this is due to the nature of the breeding habitat or not, it warrants further investigation in the laboratory or semi-field systems. This species depends much on the presence of large and semi/permanent larval habitats such as rivers and large water reservoirs [54,341]. Rainfall (one week lagged cumulative) plays a crucial role in creating these habitats, and was positively associated with larval survival when the density dependence was taken into consideration.

6.1.4 Generalizability of population dynamics models

Chapter 5 describes a series of simulation exercises performed with the novel SSM model developed in Chapter 4; to explore its generalizability and ability to predict missing data. A key focus was on examining the generalizability of inferences drawn about the drivers of *An. funestus* dynamics from the original hierarchical model, by re-fitting it to a single population. Environmental covariates are key drivers of many mosquito populations, but if these are not well captured during the model development it might result in model misspecifications. The density dependence parameters were estimated to be small in both types of models fitted. Most of the demographic parameters were the same for both the hierarchical and

single population model except for the adult survival. Specifically, the survival of all the gonotrophic stages was very sensitive to changes in environmental covariates (i.e. temperature) in the single population model but not the hierarchical one.

In a further step, I evaluated the model's ability to reconstruct annual *An. funestus* population dynamics when different proportions of data from the annual time series were missing (25% and 50%). When model predictions were tested under a data removal strategy, the model was able to reconstruct up to 25% of the missing data with sensible credible intervals. However when half of the data (50%) was removed, the model's ability to reconstruct *An. funestus* dynamics was highly reduced by increasing the level of uncertainty around the predicted mean abundance. The model was able to predict the missing segment in the trajectories if it learns from both wet and dry seasons. Finally, I was able to test various features other than density dependence parameters that could be contributing to population regulation by increasing or decreasing the flexibility of the density dependence priors in the single population model. Even with high level of flexibility in density dependence priors, the model was suggesting small contribution of this parameter in regulating the dynamics. Given that the density dependence parameter was minimized regardless of the flexibility in the prior values, this implies that additional features might be driving the dynamic by reducing the density dependence's contribution to the overall dynamics. The difficulty of capturing sustained troughs and peaks purely via flexible density dependence indicates the need for additional currently missing biological processes (i.e. aestivation, diapause or migration) in the life-history of the mosquitoes.

6.2 Questions arising

This work generated several questions which warrant further investigation. First, why is the mating success of *An. funestus* so poor in the laboratory? This biological process is poorly understood in eurygamic species. Stable colonies will only be achieved through a significant improvement in the mating process under laboratory conditions. How could this be achieved? One option would be to facilitate

swarming behavior in more natural semi-field setups where wild adult mosquitos could be released and thoroughly examined. Establishment of colonies could also be assisted by modelling to predict the initial size of wild populations to achieve successive filial generations, and set targets for the required mating percentage to reach the first filial and the subsequent generation. Future research on mating can look at these issues in order to have a better understanding of the colonization process. While I was unable to establish *An. funestus* colony in this study, colleagues at IHI have subsequently had success in rearing a Tanzanian *An. funestus* strain up to 26 (F_{26}) generations in the laboratory (Hape *et al*, in prep).

This work has evaluated the performance of a number of exposure-free traps for measuring host seeking *An. funestus* in outdoor settings. Notably, all of these gave an underestimation of biting density relative to the HLC gold standard. Unfortunately, *An. funestus* abundance is quite low in the current study site; hence, calibrating any additional trap against *An. funestus* will need more extensive sampling to reach over longer periods of time to generate sufficient sample sizes and statistical power to robustly characterize their relationships with the HLC. Regarding the statistical technique developed in this study, considerable effort should be invested into designing sensitive traps which can work in areas of low density vector populations. More investigation into how to improve the luring mechanism is recommended.

Modelling malaria vectors like *An. funestus* requires detailed understanding of how environmental covariates drive their dynamics. Several environmental variables expected to be of importance (temperature, rainfall) were explored during the model development process to assess their association with *An. funestus* dynamics. This produced some counterintuitive results. For example, demographic parameters (adult and larval survival) did not appear to be very sensitive to varying temperatures and rainfall in the hierarchical model; despite the well-known impact of these covariates on vector population dynamics and fitness [40,363]. The apparent low sensitivity to these environmental variables may be a genuine ecological property of these populations within this particular study site, or the result of high stochasticity in the mosquito data used to inform the model; generating too much noise to detect clear signals of these parameters. This raises

further questions about the sources of stochasticity in mosquito catch data. For example, how much impact does the presence or movement of human in the sample houses have on *An. funestus* catch rates? It is known that this species is highly endophagic and anthropophilic in nature. Thus the presence of humans will ultimately attract mosquitoes into houses for feeding. Previous work on the same study area shows that the number of people in the sampled houses was positively correlated with the number of mosquitoes sampled [295]. In this work, I did not consider the variations in the number of occupancy in each sampled houses.

Another unexplained feature of the mosquito surveillance data used in modelling was its apparent periodicity. The model developed here made use of daily time series data from mosquito surveillance that was made from Monday to Friday over one year period skipping weekends. The unexpected feature of this data was an apparent weekly periodicity; with catches appearing to decrease throughout the sampling week. The possible biological or environmental reason for this is unknown. One possibility is that *An. funestus* population within a household is limited, and gets progressively depleted by trapping with daily catches replenishing over weekend break. There is evidence which suggests “mass trapping” in houses can reduce the size of mosquitoes population and maybe malaria transmission [364]. In this case, a potential concern that would arise is whether mosquito populations might keep decreasing even if there was no weekend break. Would this be a potential mechanism to estimate the population size via removal sampling as previously documented by Service [365]?

6.3 Implications of the findings

6.3.1 *Anopheles funestus* colonization bottlenecks

To address ongoing residual malaria transmission, a comprehensive ecological understanding of all vectors that play a role in transmission is required. This study provides the first documentation of attempts to colonise *An. funestus* in Tanzania. It laid a foundation for continuing efforts in Tanzania to colonise this species, which have recently been successful (Hape *et al*, in prep). By studying all the barriers to colonization outlined in the second chapter, another team of scientists

at IHI has managed to reach 26 (F_{26}) laboratory generations of *An. funestus* from a local population (Hape *et al*, in prep). Learning from my experience, this team changed strategy to not just collect maternal population (F_0) at a single point; instead they repeatedly collect wild females over several weeks and months and cumulatively add them into the same laboratory founder population cages. This meant that much larger numbers of females (>2000) were present in each of multiple laboratory cages. This generated substantially larger founder populations than available for my experiments (Chapter 2 [24]). Similar to my observation, the initial mating success in these larger laboratory population was very low over first few generations. However, the larger size of these founder populations proved sufficient to generate enough offspring even with low mating success to seed further generations. Eventually, this strain started to adapt to the laboratory conditions, leading to a rise in mating success after 4-5 generations and establishment of a stable line (Hape *et al*, in prep).

6.3.2 Reliability of the mosquito sampling tools

The trapping evaluation I conducted has several implications for improving the surveillance of *An. funestus*, particularly in outdoor settings. I found that trap catches for *An. funestus* were independent of the abundance of other mosquito species in the area. This implies that there is no saturation effect in trap performance; at least across the range of densities surveyed here. In general, the relationship between the HLC and other trapping methods could be described by a simple linear relationship. Also this work demonstrated that there can be a considerable number of *An. funestus* host seeking in outdoor environments. While these *An. funestus* populations were relatively low density (compared to other vectors), the high infection rates of this vector (e.g. ~85%, [88]) means that the number host seeking outdoors contribute to residual transmission. Outdoor exposure to *An. funestus* is usually ignored in conventional surveillance activities, with only indoor sampling conducted. This focus on indoor sampling must change if we want to better quantify and tackle residual transmission. Given that people in this study area are clearly exposed to *An. funestus*, trapping methods are required that can reflect outdoor exposure as estimated by the HLC. Here, no trap was

extremely highly correlated with the HLC for *An. funestus* outdoors; however the two best candidates were the M-Trap (MTR) and M-trap with additional CDC (MTRC) inside. Therefore, if someone were to use either of these traps to sample outside biting mosquitos, the predicted mean values from this calibration method could be used to calculate the human biting rate as estimated by the HLC. Before making a decision on which outdoor trap to use, the *Shinny App* interface may be used to explore the possible range of values and how wide the credible intervals for different methods.

6.3.3 Model parameterization and validation

When modelling mosquito population dynamics, not all data or parameter uncertainty can be accounted for in the model development process. In general, population dynamic models address only four aspects of population change (i.e., mortality, birth, immigration and emigration). In mosquitoes, all these demographic process could be influenced either by vector control intervention currently in place or changes in environmental conditions [40,363]. Malaria vector species vary in their response to environmental variability [363], thus necessitating development of species-specific models.

A wider insight from this work is into application of stochastic State-Space Models for analyzing the dynamics and demography of wild vector populations. SSMs have been used in many fields of ecology but rarely used to study the dynamics of malaria vectors [332,366]. These SSMs account for two distinct types of stochasticity: sampling imprecision and biological variation. In general, combining these two stochastic processes yields better estimates of ecological quantities of interest than modelling only one stochastic source directly. An advantage of this approach is its ability to indirectly estimate the otherwise hidden demographic rates and processes that could plausibly generate the observed dynamics. Many of these demographic rates are very difficult to directly estimate in the field (fecundity, daily survival etc.), thus this approach provides a useful alternative. Population trajectories reconstructed by these models could be used to identify seasonality in abundance and the underlying demographic rates that give rise to it (survival, fecundity, and larval development rates). However, the mosquito

collection devices used (i.e., traps) and human errors during processing (i.e. counting) can have a significant impact on the quality of observation data. Careful consideration and adjustment of trapping methodology and processing thus may improve the general applicability and reliability of these types of dynamic models.

6.3.4 Selection of optimal vector control package

The potential impact of vector control intervention can be estimated from its impacts on vector demography and fitness parameters. A realistic population dynamics model enables the impacts of these intervention effects on the size and stability of a vector species to be predicted. With further development, the modelling framework developed here can be used to evaluate the anticipated response of *An. funestus* to various vector control interventions, either individually or in combination. Uniquely, this framework could enable identification of optimal environmental conditions or times of the year to deploy interventions for maximum impact. Rainfall patterns play a big role in intervention deployment strategies like IRS and LSM. For example LSM is applied during the driest period when the habitats are fixed and few [95,137,163] unlike IRS which is applied during the transmission seasons [367,368]. This framework can be used to simulate standard and variable seasonal implementation of these and other interventions, to identify which optimal package can generate the maximum negative impact on *An. funestus* survival. Despite its complexity, this framework may be expanded in the future to accommodate additional ecological and behavioral processes that may impact *An. funestus* dynamics such as host choice, oviposition behavior, and processes such as migration, diapause or aestivation.

6.4 Limitations of the study

This study provides a detailed understanding of the ecology and the drivers of the dynamics of *An. funestus* in the wild population. As described in the previous chapters, there are several limitations associated with different parts of this work; of which a few general ones will be highlighted here. Firstly, several of the direct estimates of *An. funestus* fitness and demography used in my modeling work were

derived from an unstable population. Specifically, many of the fitness parameters that served as prior values for my population dynamics model were derived from unsuccessful attempts to colonize *An. funestus* in the lab (Chapter 2). Here, detailed individual measurements of larval development time, larval and adult survival, and fecundity were measured from cohorts of F_0 females brought into the lab and their F_1 offspring. Given these individuals were not maintained past the second filial generations in the lab, their fitness values may have been impaired and thus unrepresentative of likely values in the wild. Additionally, F_0 were fed on the blood of an unnatural host in the insectary (chickens) to produce eggs for the next generation. The subsequent fecundity and survival of *An. funestus* after feeding on this host may not be reflective of their fitness after human feeding. Lyimo et al have shown that, fecundity and survival are not impaired when *An. arabiensis* is not fed on their natural host [78,81]. Also the age and mating status of the F_0 *An. funestus* females could not be estimated at capture, and may have introduced another source of variability. It is known that mosquitoes need several generations to adapt to insectary conditions [58,170], whereas I only had data for the first two generations due to poor mating success. This does not necessarily mean that all the fitness estimates derived from these adapting mosquitoes are unrealistic. For example their survival rates were relatively high and consistent with values estimated by Okoye et al [222,330]. The mean values generated here, were later used in the Bayesian framework with a wider prior range to make sure the model priors were not unnecessary precise and influential. Certainly, further model development using either fitness parameters from a stable *An. funestus* colony, or as directly estimated in the field, would be useful.

Secondly, the calibration tool developed here to predict human landing catch (HLC) - equivalent values from alternative exposure-free traps was only done for outdoor collections. Thus, we do not yet have a similar tool for calibration of indoor traps. Given that the majority of *An. funestus* bites still occur indoors, expanding this framework to indoor settings is a priority. Human landing catches are the gold standard for sampling host seeking mosquito both indoors and outdoors. In my analysis of outdoor sampling, some traps provided estimates with very wide credible intervals; with this not being due to poor fitting but rather very low numbers of *An. funestus* at the time of sampling. *Anopheles funestus* are

found at relatively low abundance in the study area. Further evaluation of this type of calibration approach in areas with higher *An. funestus* densities is needed to refine the calibration tool and make it more generalizable to data from different settings.

In addition to the previous issues mentioned, another important limitation of the population dynamics modelling work was its reliance on data from one sampling method, the CDC light trap, which is specifically targeted host seeking mosquitoes (unfed). This method is not effective for sampling other adult female life stages (i.e. blood-fed and gravid), but since sampling effort needs to be standardized for this type of modelling, I had to introduce a parameter in the observation model to account for trap bias. This meant that estimates of the abundance of blood fed and gravid females were derived from an inefficient method, and are likely to be less robust than those for unfed. Additionally, there are limitations with using CDC light traps to infer population abundance trends, even of unfed females. It is uncertain what proportion of the mosquito population, whether unfed, blood fed or gravid, and are sampled in a single CDC trap. This could potentially be explored in semi-field experiments where the number of individuals caught in a CDC trap from a population of known size could be estimated.

6.5 Further work

Ecological studies of *An. funestus* must continue if we are to control residual malaria transmission in African countries where the disease stills a public health problem. The barriers to colonization and possible solutions are described in Chapter 2, which also offers a full overview of the mating process in captivity. Currently there is an ongoing colonization process which started after my work was completed. Several generations have been maintained in Tanzania's ongoing effort, in addition to the one filial generation created through this work. When the colony is stable, this will aid in the estimation of demographic parameters and used in testing new traps, different insecticides formulation, spatial repellents to genetically modified mosquitoes.

The use of modelling to understand the dynamics of the local population of *An. funestus* species in Tanzania was demonstrated in Chapters 4 and 5. The role of modelling can change to address different questions at each step of its development process. The population model established here, for example, was first used to illustrate how environmental variables and intrinsic factors (density dependence) influence *An. funestus* dynamics and to estimate their demographic and fitness parameters in the wild. The next step will be to utilize the same model to look into the effects of different vector control interventions on adult survival and reproduction, and the resultant impact on population size and stability. As I have access to the whole range of posterior means generated by this model (i.e., 100,000 samples), I will be able to minimize the degree of uncertainty while simulating multiple intervention options. With additional data, this population dynamic model will be expanded to include other potential regulatory processes that I hypothesized could be present in Chapter 5 (i.e. mosquito aestivation, diapause, and migration). I will also explore developing this SSM into a meta-populations model which could be used to describe different, connected subpopulations of *An. funestus* across a landscape. Technically, the modelling framework's computational efficiency will have to be optimized to allow for low uncertainty in observational data collection, which will eventually lead to more robust prediction. At the same time, regular high quality data collection is critical for both decision-making and the validation of the population model used to select optimal intervention packages.

6.6 Conclusions

The work presented here covers several aspects of *An. funestus* ecology that are critical to understanding the species' stability and response to interventions. This work covers the colonisation process, vector surveillance, and modelling of population dynamics of *An. funestus* in Tanzania. The findings here will greatly contribute to a general understanding of *An. funestus* ecology, how this vector responds to environmental covariates, and colonisation barriers. Knowledge on *An. funestus* biology will continue to be impeded until the barriers with getting them to mate in the lab are overcome. The role of outdoor biting is often neglected in

An. funestus, but could be a key component of residual transmission. Until recently, we did not have a reliable alternative to HLC that is effective for sampling *An. funestus* outdoors. Population dynamics model confirms relative stability of demographic rates throughout the seasonal cycle of extreme temperature and rainfalls. The findings will also help future modelling efforts which aim at selecting the optimal vector control intervention package which can disrupt the survival of *An. funestus*. As a result, any additional efforts in Tanzania aimed at *An. funestus* could result in the eradication of malaria.

7.0 Chapter 7: Addendum of Chapter 3

7.1 Rationale

The main aim of this addendum is to correct for the error found in chapter 3. In the original chapter 3, I modelled the mosquito catches by alternative traps using a mixture of gamma-Poisson distribution with a log-link function. The choice of “log” violates the linearity assumption as “log” tends to plateau at high numbers. This means the simple linear model assumption is violated because the “log” function will not hold a linear relationship when there is a high number of mosquito catches.

In order to address this issue, I have restructured the negative binomial model by using an “identity-link” function instead of the “log-link” function. This will allow me to accurately assess the relationship between HLC and alternative traps catches, as the “identity-link” function does not violate the linearity assumption. In addition to this, I have also changed the prior specification to match the current model structure and assumptions.

This modification to the original model will help to provide more accurate and reliable results, and will allow for a better understanding of the relationship between HLC and different alternative traps catches. The use of the identity-link function in place of the log-link function will ensure that the model is able to capture full range of possible outcomes as hypothesized in chapter 3 (i.e. intra-specific or inter-specific density dependencies). By carefully considering the choice of link functions and adjusting the model structure, updating all tables and figures as needed, I am confident that the revised model will be able to provide more accurate and reliable results.

7.2 Model fitting

The main goal of the analyses was to create a calibration tool to evaluate outdoor mosquito traps and to validate the tool by comparing the performance of candidate trapping methods relative to HLC, the “gold standard”. In particular, I

wanted to test the shape of the association curve linking the numbers of mosquitoes collected by each trap type with those collected by the HLC. First, I pooled all the hourly collections into a single collection cup per trap per night. Then, for each of the focus mosquito groups (*Culex* genera, *Anopheles funestus* s.l and *Anopheles arabiensis*), I modelled nightly HLC catches as a function of the catching rate of each alternative trap.

Four linear models were developed within a Bayesian model fitting framework to allow me to test for linear and non-linear associations through increasing levels of complexity. The Bayesian approach allowed specific constraints on parameters based on biological plausibility, in the form of priors and uncertainty when converting the counts from alternative traps into HLC equivalent values in the form of full posteriors.

For any given trap and mosquito group, I defined the response variable (N_i) as the number of female mosquitoes on every i^{th} sampling night. The final model did not account for other environmental covariates at specific trap location (e.g. temperature, humidity). Initial analyses suggest that, environmental covariates did not improve model fitting. I fitted the model following a negative binomial distribution using “identity-link” function with parameter p_i and r such that;

$$N_i \sim NegBin(p_i, r)$$

$$p_i = \frac{r}{r + \lambda_i}$$

Where λ_i is defined by the shape of the relationship between N_i and the number of mosquitoes collected with the alternative trap n_i (Table 7.1). Since the algebraic form of this relationship is not known, I made three assumptions with specific mathematical definitions, as follows; 1) that the relationship must start at the origin (i.e. when HLC catches zero mosquitoes, the alternative traps will, on average also collect zero mosquitoes), 2) that the relationship is positive (i.e., no negative relationships between trap catches), and 3) that any given trap could potentially suffer from a density effect (i.e., the slope of the relationship is not constant and it can change according to the abundance of mosquitoes, either just of the same mosquito group or of all mosquitoes).

To define λ_i , I therefore formulated four possible scenarios to describe the relationship between HLCs and other trapping methods as summarized in Table 6.1. In model 1, I considered a simple linear relationship between N_i and n_i (Table 6.1). In model 2, I tested if the efficiency of the alternative trap was dependent on the density of the focal mosquito (e.g. intra-specific density dependence) by adding a quadratic term n_i^2 (Table 6.1). In model 3, I tested if the captures of a given group by a given trap were dependent on the abundance of the other taxonomic group (e.g. “inter-specific” density dependence) by adding, an interaction term between n_i and the number of all the females from other mosquito groups collected with the same trap (m_i) (Table 6.1). Model 4 was similar to Model 3, but I considered all the other K_i taxonomic groups separately. Therefore it included all the pair wise interaction terms between n_i and the number of females of each k^{th} mosquito group (s_{k_i}) (Table 7.1). My analysis mainly focused on three mosquito groups, but I collected a higher number of species hence $K > 3$).

Table 7.1: Description of models used to investigate the relationships between female mosquito catches by human landing catch and alternative traps.

Model	Structure
Model 1	$\lambda_i = \beta_1 n_i$
Model 2	$\lambda_i = \beta_1 n_i + \beta_2 n_i^2$
Model 3	$\lambda_i = \beta_1 n_i + \beta_2 n_i m_i$
Model 4	$\lambda_i = \beta_1 n_i + \sum_{k=1}^K \beta_k n_i s_{k_i}$

This analysis was performed in the statistical environment R, version 4.0 [246], with Bayesian model fitting to the data done using the program JAGS [301] interfaced within R via the package *rjags* [302]. For parameters β_1, β_2 and β_k I used gamma prior (shape = 0.1, rate = 0.1). The prior for the size r was defined from uniform distribution (min = 0, max = 10^5). The prior for β_1 was chosen to ensure a positive relationship between n_i and N_i and a positive effect of the quadratic and

the interaction terms for β_2 and β_k . To achieve convergence, the models were run for up to 3×10^4 iterations. Means of posterior distributions with corresponding credible intervals were obtained for each model coefficient β . I compared different models by their Deviance Information Criteria (DIC). To further validate the results, the data was randomly divided into two sets: training set (75%) and a test set (25%). The root-mean-square error (RMSE) was then calculated for each model as the average prediction error on the test set. This allowed us to assess the performance of each model on unseen data and determine which model was the most accurate and reliable

7.3 Interactive calibration tool

I designed a look-up table (Table 7.3) containing means of posterior predictions for different combinations of mosquito taxa, trap types and models. This allowed me to predict the expected number of a given mosquito taxa from an HLC (with credible intervals) based on the number caught in the alternative traps. I also developed an interactive online tool, in the form of an *R Shiny* App [303] to facilitate these evaluations. This tool provides users with an interactive graphical user interface (GUI) to select the number of captured mosquitoes for a group of interest by trap type, and to explore the predicted number of mosquitoes caught in an HLC by method.

7.4. Results summary

Following the reanalysis of the data using the negative binomial distribution with identity-link function rather than the Poisson with log-link as was previously done in chapter 3, we have made the following key observations:

- Out of the four models that were fitted to the six different traps used for the development of the calibration tool, the simple linear model is still the one that was the most preferred. Among all the models, as previously mentioned in Chapter 3, there were no big differences in deviance explained for *Anopheles funestus* and *Anopheles arabiensis* (Table 7.3).

- Across the range of mosquito catches, there is no saturation effect or non-linearity as it was hypothesized in model 2 (Table 7.2). This means there is no evidence of intra-specific density dependence. This is similar with model 3 which assess the effect of other females mosquitoes caught by specific trap. There was no clear evidence of inter-specific density dependence for all the six alternative traps and all the three species (Table 7.3). This was also clearly shown by the β_2 coefficient which is very small for all the models.
- *Anopheles funestus* poor calibrations were mainly affected by the very low catches for all the alternative traps. The wider credible intervals were mainly driven by very low catches of this mosquito species.
- All figures (Figure 7.1, Figure 7.2 and Figure 7.3) and the lock-up tables (Table 7.4) were produced based on the simplest linear model (Mode 1).

Table 7.2: Coefficients of each parameter (β_1, β_2) used to explain the relationship between HLC catches and alternative traps for all the four models.

Species	β	SUN	BGS	ITT-C	MMX	MTRC	MTR
a) <i>Culex</i> spp.							
Model 1	β_1	4.34 [3.54, 5.37]	4.78 [3.85, 5.94]	2.97 [2.33, 3.75]	10.95 [8.93, 13.47]	2.26 [1.92, 2.67]	2.00 [1.68, 2.37]
Model 2	β_1	4.35 [3.54, 5.34]	4.79 [3.83, 5.91]	2.98 [2.32, 3.76]	10.97 [8.91, 13.47]	2.25 [1.90, 2.67]	1.99 [1.68, 2.38]
	β_2	2.3e-4 [0.0, 0.002]	1.8e-4 [0.0, 0.002]	1.3e04 [0.0, 0.001]	1.3e-3 [0.0, 0.01]	4.8e-5 [0.0, 5.1e-5]	2.8e-5 [0.0, 2.6e-4]
Model 3	β_1	4.32 [3.54, 5.33]	4.78 [3.86, 5.92]	2.98 [2.32, 3.81]	10.96 [8.80, 13.61]	2.26 [1.90, 2.68]	1.99 [1.67, 2.34]
	β_2	2.1e-4 [0.0, 0.002]	8.4e-4 [0.0, 0.01]	5.5e-4 [0.0, 0.05]	3.5e-3 [0.0, 0.023]	8.7e-4 [0.0, 8.8e-4]	6.0e-4 [0.0, 0.01]
Model 4	β_1	4.22 [3.39, 5.19]	4.56 [3.68, 5.66]	2.95 [2.31, 3.79]	10.78 [8.81, 13.35]	2.12 [1.73, 2.57]	1.93 [1.63, 2.30]
	β_2	NA	NA	NA	NA	NA	NA
b) <i>An. arabiensis</i>							
Model 1	β_1	9.97 [7.92, 12.52]	12.98 [9.89, 16.77]	12.25 [9.43, 16.13]	13.83 [9.88, 19.31]	6.65 [5.39, 8.26]	7.41 [6.25, 8.88]
Model 2	β_1	10.01 [7.90, 12.59]	12.97 [9.97, 17.06]	12.27 [9.27, 16.12]	13.76 [10.05, 19.03]	6.67 [5.42, 8.19]	7.41 [6.23, 8.79]
	β_2	0.004 [0.0, 0.04]	2.5e-4 [0.0, 0.002]	6.2e-4 [0.00, 0.007]	0.004 [0.0, 0.04]	8.2e-4 [0.0, 0.006]	3.2e-4 [0.0, 0.003]
Model 3	β_1	9.98 [7.89, 12.45]	12.98 [9.93, 17.14]	11.59 [7.70, 15.85]	13.73 [9.59, 19.03]	6.66 [5.34, 8.19]	7.39 [6.02, 8.83]
	β_2	2.4e-4 [0.0, 0.002]	3.7e-4 [0.0, 0.003]	0.02 [0.00, 0.14]	4.3e-3 [0.0, 0.04]	1.41e-4 [0.0, 0.001]	2.8e-4 [0.0, 0.03]
Model 4	β_1	9.97 [7.81, 12.49]	10.96 [7.48, 15.35]	11.47 [7.65, 15.79]	11.07 [7.09, 16.58]	5.97 [3.91, 7.96]	7.30 [6.04, 8.82]
	β_2	NA	NA	NA	NA	NA	NA
c) <i>An. funestus</i>							
Model 1	β_1	4.83 [2.44, 9.36]	2.23 [1.56, 2.99]	1.66 [1.04, 2.59]	2.73 [1.28, 5.45]	2.20 [1.54, 3.19]	1.99 [1.21, 3.08]
Model 2	β_1	4.77 [2.38, 9.01]	2.23 [1.57, 2.99]	1.62 [0.99, 2.56]	2.72 [1.25, 5.57]	2.21 [1.52, 3.14]	1.99 [1.25, 3.13]
	β_2	0.007 [0.0, 0.08]	0.009 [0.0, 0.09]	0.03 [0.0, 0.19]	0.006 [0.0, 0.06]	0.003 [0.0, 0.03]	0.003 [0.0, 0.03]
Model 3	β_1	4.85 [2.40, 9.16]	2.23 [1.59, 3.02]	1.64 [1.03, 2.52]	2.71 [1.25, 5.46]	2.19 [1.50, 3.14]	1.97 [1.25, 3.10]
	β_2	2.1e-4 [0.0, 0.002]	1.3e-4 [0.0, 0.001]	1.6e-4 [0.0, 0.002]	6.2e-4 [0.0, 0.01]	1.3e-4 [0.0, 0.001]	6.4e-5 [0.0, 8.5e-4]
Model 4	β_1	4.27 [1.43, 9.46]	2.01 [1.17, 2.90]	0.94 [0.69, 1.22]	0.11 [0.0, 0.79]	2.15 [1.42, 3.22]	1.59 [0.001, 2.96]
	β_2	NA	NA	NA	NA	NA	NA

*NA = Individual interaction between species of interest (i.e. *An. funestus*, *An. arabiensis* and *Culex* spp.) and each of 8 females species captured during the study period. This generates 8 different values of β_2 for the most complex model (model 4)

Table 7.3: Summary (DIC and RMSE values) of models used to investigate the relationship between the numbers of female mosquitoes collected with human landing catch (HLC) and the six alternative outdoor traps. See Table 6.1 for description and models formulation.

Species and Model	SUN			BGS			ITT-C			MMX			MTRC			MTR		
	DIC	Δ DIC	RMSE	DIC	Δ DIC	RMSE	DIC	Δ DIC	RMSE	DIC	Δ DIC	RMSE	DIC	Δ DIC	RMSE	DIC	Δ DIC	RMSE
a) <i>Culex</i>																		
Model 1	1437.9	0.12	129.2	1490.2	1.65	150.4	1099.5	0.04	203.3	1167.9	0.00	120.6	1699.4	0.10	107.7	1612.9	2.22	81.6
Model 2	1438.2	0.44	130.3	1490.6	2.03	150.8	1099.6	0.22	207.6	1168.2	0.29	122.1	1699.3	0.03	109.6	1612.9	2.29	86.4
Model 3	1437.7	0.00	129.4	1490.2	1.61	151.4	1099.5	0.08	202.6	1168.4	0.51	122.5	1699.3	0.00	108.0	1612.7	1.99	84.7
Model 4	1437.9	0.18	138.6	1488.6	0.00	177.1	1099.4	0.00	205.9	1168.7	0.79	121.7	1699.5	0.20	117.7	1610.7	0.00	86.5
b) <i>An. arabiensis</i>																		
Model 1	1009.1	0.00	174.0	767.8	0.00	153.9	757.6	0.00	158.1	544.7	0.67	178.7	1415.3	0.00	140.1	1437.6	0.09	99.6
Model 2	1100.1	1.06	177.1	768.0	0.22	155.7	757.9	0.25	159.4	544.4	0.38	178.2	1415.7	0.37	140.2	1437.6	0.14	100.6
Model 3	1099.6	0.54	177.0	768.1	0.28	155.3	757.8	0.22	153.8	544.8	0.77	180.8	1415.6	0.31	141.3	1437.5	0.00	100.1
Model 4	1101.4	2.35	184.1	768.1	0.33	156.3	758.1	0.48	150.8	543.9	0.00	275.9	1417.4	2.11	154.4	1438.3	0.86	101.2
c) <i>An. funestus</i>																		
Model 1	90.1	0.00	9.41	61.6	0.21	3.83	118.3	11.9	2.41	44.6	0.00	4.15	155.0	0.00	7.63	132.7	0.27	4.47
Model 2	90.5	0.39	10.25	61.8	0.38	3.85	119.3	12.8	2.43	44.6	0.01	4.22	155.1	0.08	7.69	132.6	0.18	4.61
Model 3	90.4	0.24	10.67	61.4	0.00	3.83	118.4	11.9	2.41	45.9	1.29	4.14	155.3	0.33	7.65	132.5	0.00	4.58
Model 4	91.8	1.69	10.86	62.7	1.26	2.87	106.5	0.00	2.41	56.6	12.0	1.33	156.9	1.86	12.9	134.6	2.18	11.21

SUN: Suna trap, BGS: BG-Sentinel trap, ITT-C: Ifakara Tent Trap version C, MMX: Mosquito Magnet trap, MTRC: M-trap combined with CDC Light, MTR: M-trap;

Table 7.4: Predicted values for estimating the expected mosquito catches by human landing catch and alternative traps, according to the linear model (Model 1). Numbers in the first column refer to the mosquitoes collected with a given trap. To obtain the estimate of the equivalent number that one would collect with HLC, refer to the column corresponding to the trap itself. Numbers in brackets are (95% credible intervals).

	Collected	Expected HLC					
		SUN	BGS	ITT-C	MMX	MTRC	MTR
a) <i>Culex</i> spp.	10	43 (35-54)	48 (39-59)	30 (23-37)	110 (89-134)	23 (19-27)	20 (17-24)
	20	87 (71-107)	96 (77-119)	59 (47-75)	219 (179-269)	45 (38-53)	40 (34-47)
	30	130 (106-161)	143 (116-178)	89 (70-112)	329 (268-403)	68 (57-80)	60 (51-71)
	40	174 (142-215)	191 (154-238)	119 (93-150)	438 (357-538)	90 (77-107)	80 (67-95)
	50	217 (177-269)	239 (193-297)	149 (116-187)	548 (446-672)	113 (96-134)	100 (84-119)
	60	260 (213-322)	287 (231-356)	178 (140-225)	657 (536-806)	136 (115-160)	120 (101-142)
	70	304 (248-376)	335 (270-416)	208 (163-262)	767 (625-941)	158 (134-187)	140 (118-166)
	80	347 (284-430)	382 (308-475)	238 (186-300)	876 (714-1075)	181 (153-214)	160 (135-190)
	90	391 (319-484)	430 (347-535)	267 (210-337)	986 (804-1209)	204 (172-241)	180 (152-213)
100	434 (354-537)	478 (385-594)	297 (233-375)	1095 (893-1344)	226 (192-267)	200 (168-237)	
b) <i>An. arabiensis</i>	10	100 (79-125)	130 (99-168)	122 (94-161)	138 (99-193)	67 (54-83)	74 (62-89)
	20	199 (158-250)	260 (198-335)	245 (189-323)	277 (198-386)	133 (108-165)	148 (125-178)
	30	299 (237-376)	390 (297-503)	367 (283-484)	415 (296-579)	200 (162-248)	222 (187-266)
	40	399 (317-501)	519 (396-671)	490 (377-645)	553 (395-773)	266 (215-331)	297 (250-355)
	50	498 (396-626)	649 (495-839)	612 (471-807)	691 (494-966)	333 (269-413)	371 (312-444)
	60	598 (475-751)	779 (594-1006)	735 (566-968)	830 (593-1159)	399 (323-496)	445 (375-533)

	70	698 (554-877)	909 (693-1174)	857 (660-1129)	968 (692-1352)	466 (377-579)	519 (437-621)
	80	798 (633-1002)	1039 (792-1342)	980 (754-1291)	1106 (791-1545)	532 (431-661)	593 (500-710)
	90	897 (712-1127)	1169 (891-1510)	1102 (848-1452)	1244 (889-1738)	599 (485-744)	667 (562-799)
	100	997 (792-1252)	1298 (990-1677)	1225 (943-1613)	1383 (988-1931)	665 (539-826)	741 (625-888)
c) <i>An. funestus</i>	10	48 (24-94)	22 (16-30)	17 (10-26)	27 (13-54)	22 (15-32)	20 (12-31)
	20	97 (49-187)	45 (31-60)	33 (21-52)	55 (26-109)	44 (31-64)	40 (24-62)
	30	145 (73-281)	67 (47-90)	50 (31-78)	82 (38-163)	66 (46-96)	60 (36-93)
	40	193 (98-374)	89 (62-120)	66 (41-104)	109 (51-218)	88 (62-128)	79 (49-123)
	50	241 (122-468)	112 (78-150)	83 (52-130)	136 (64-272)	110 (77-160)	99 (61-154)
	60	290 (146-561)	134 (94-180)	100 (62-156)	164 (77-327)	132 (93-191)	119 (73-185)
	70	338 (171-655)	156 (109-210)	116 (73-182)	191 (90-381)	154 (108-223)	139 (85-216)
	80	386 (195-748)	178 (125-240)	133 (83-208)	218 (103-436)	176 (123-255)	159 (97-247)
	90	434 (220-842)	201 (140-269)	149 (93-234)	246 (115-490)	198 (139-287)	179 (109-278)
	100	483 (244-936)	223 (156-299)	166 (104-260)	273 (128-545)	220 (154-319)	199 (121-308)

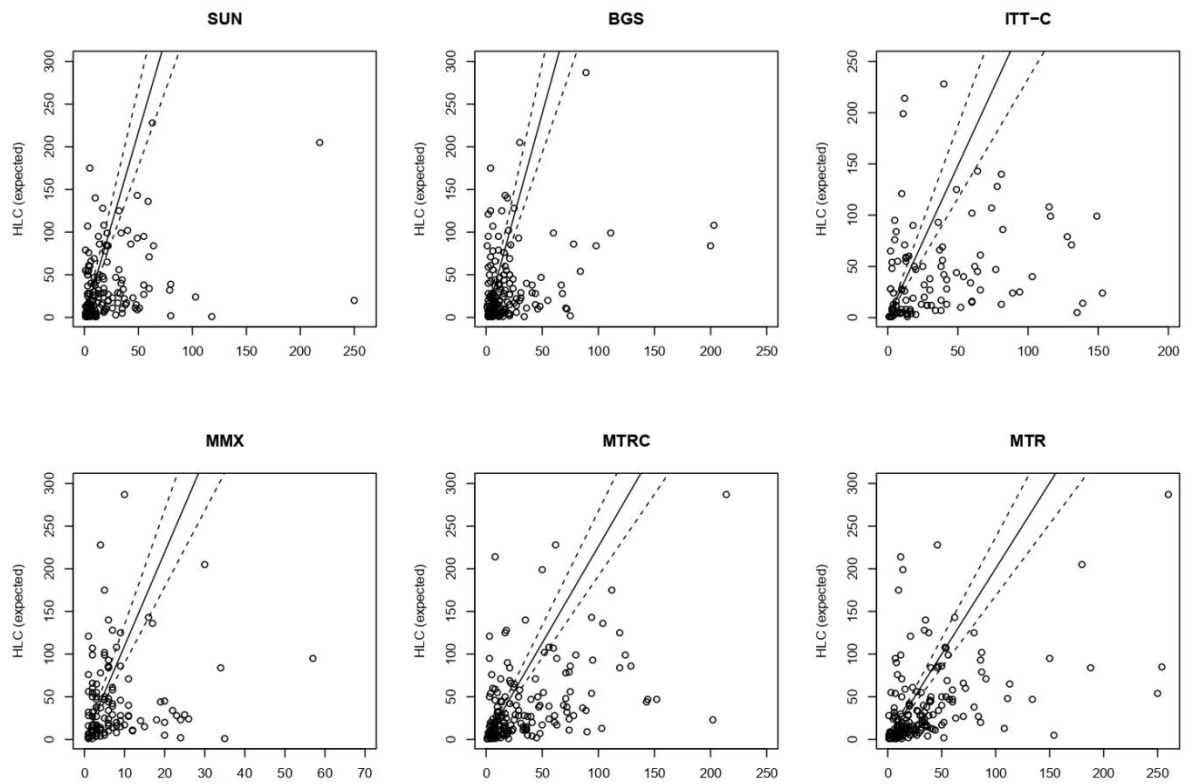


Figure 7.1: Expected number of female *Culex* spp. mosquitoes collected with HLC (y-axis), given the number of females collected with alternative traps (x-axis). Continuous line is the prediction of a normal distribution model assuming a linear relationship; dashed lines are 95% credible intervals and black circles are the actual observed values.

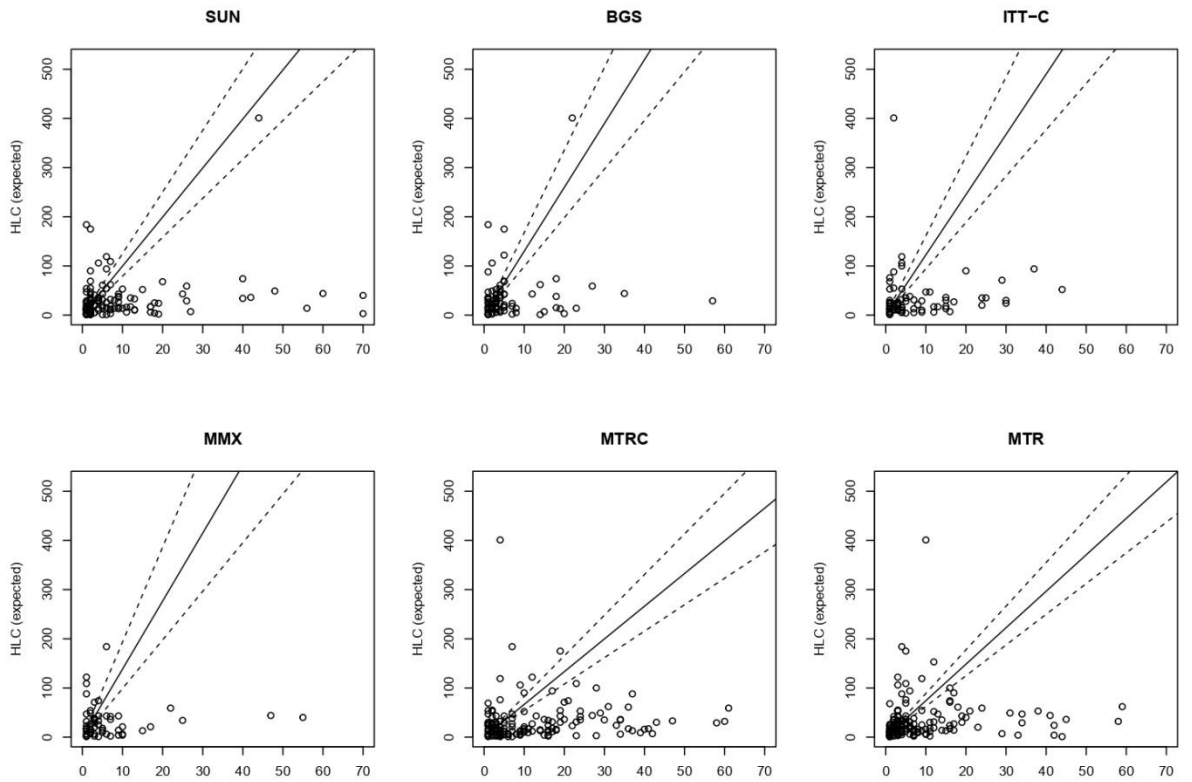


Figure 7.2: Expected number of female *Anopheles arabiensis* mosquitoes collected with HLC (y-axis), given the number of females collected with alternative traps (x-axis). Continuous line is the prediction of a normal distribution model assuming a linear relationship; dashed lines are 95% credible intervals and black circles are the actual observed values.

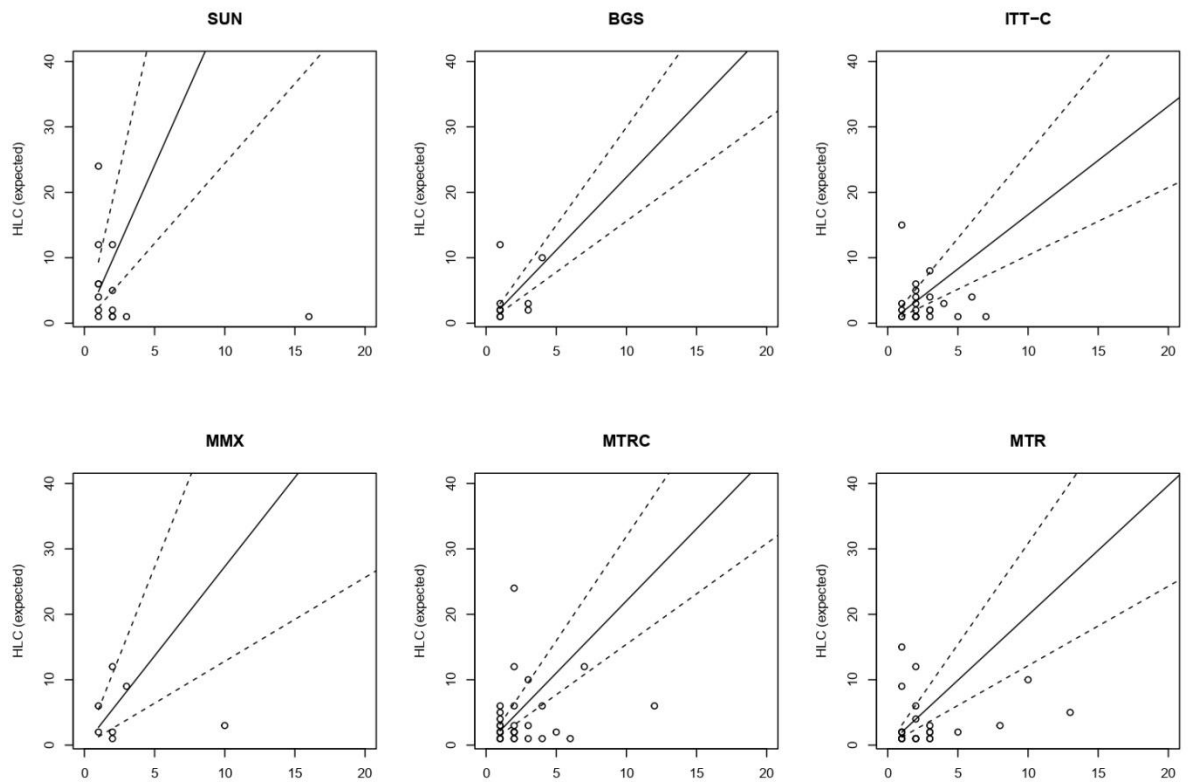


Figure 7.3: Expected number of female *Anopheles funestus* mosquitoes collected with HLC (y-axis), given the number of females collected with alternative traps (x-axis). Continuous line is the prediction of a normal distribution model assuming a linear relationship; dashed lines are 95% credible intervals and black circles are the actual observed values.

7.5 Conclusion

After reanalyzing the data, it became clear that there were no substantial differences between the two model fitting techniques within the catch range values. The current approach remains valid, as it was primarily implemented to address errors in the previous one. It was not possible to identify a single model which performs better for all the species and all the alternative traps. As a result, I selected the most parsimonious model (i.e. model 1) which is the simple linear model. All figures and tables were created based on the simple linear model. Overall, I believe that the revised version of the work represent a significant improvement over the original chapter 3.

8.0 Appendices

8.1 Appendix 1: Shiny App Interfaces

8.1.1 Shiny App dashboard showing one example of a linear relationship (model 1) between HLC and an alternative trap (i.e., MTC) for *Culex* spp



Calibration tool for outdoor-biting mosquitoes sampling

What mosquitoes are you collecting?

culex
 gambiae
 funestus

Which trap are you using?

MTC
 BGS
 IFT
 MMX
 MTRC
 SUN

How many mosquitoes did you catch?

30

What model? (please see paper for details)

1 (linear effect)
 2 (saturation effect)
 3 (effect of other species)

Run

INSTRUCTIONS

This tool can be used to explore the output of the models for mosquito trap calibration presented in Ngowo et al (2022) (<https://www.researchsquare.com/article/rs-1494460/v1>) and to estimate the HLC-equivalent number of mosquitoes collected with exposure-free alternative traps.

On the input panel you can select the species of interest, the trap and the model (see 'Ngowo et al. for details).

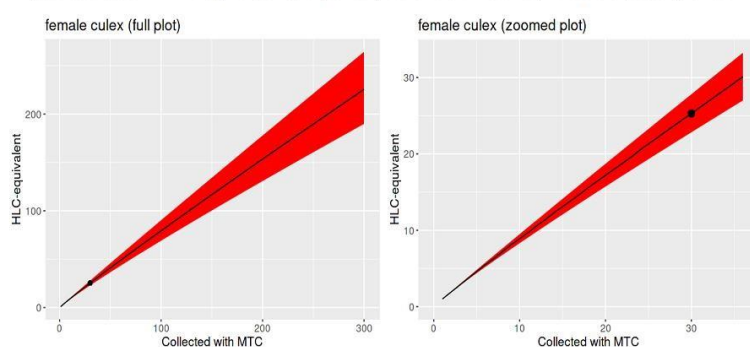
By clicking on 'Run' you will generate the plot of predicted HLC-equivalent catches.

Please note that coefficients of the models generating the prediction will be updated regularly as additional data are gathered (see above mentioned paper for more details).

To report a bug, or for any question, please write to luca.nelli@glasgow.ac.uk (mailto:luca.nelli@glasgow.ac.uk)

Results

If you collected 30 culex with MTC trap, then you might expect 25.3 (credible intervals: 22.83/27.81) HLC-equivalent, according to model 1.



8.1.2 Shiny App dashboard showing one example of a saturation effect (model 2) between HLC and an alternative trap (i.e., MTC) for *Culex* spp



Calibration tool for outdoor-biting mosquitoes sampling

What mosquitoes are you collecting?

culx
 gambiae
 funestus

Which trap are you using?

MTC
 BGS
 IFT
 MMX
 MTRC
 SUN

How many mosquitoes did you catch?

What model? (please see paper for details)

1 (linear effect)
 2 (saturation effect)
 3 (effect of other species)

INSTRUCTIONS

This tool can be used to explore the output of the models for mosquito trap calibration presented in Ngowo et al (2022) (<https://www.researchsquare.com/article/rs-1494460/v1>) and to estimate the HLC-equivalent number of mosquitoes collected with exposure-free alternative traps.

On the input panel you can select the species of interest, the trap and the model (see 'Ngowo et al. for details).

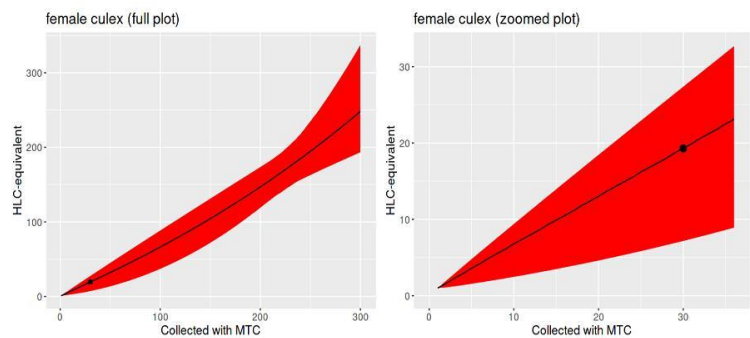
By clicking on 'Run' you will generate the plot of predicted HLC-equivalent catches.

Please note that coefficients of the models generating the prediction will be updated regularly as additional data are gathered (see above mentioned paper for more details).

To report a bug, or for any question, please write to luca.nelli@glasgow.ac.uk (mailto:luca.nelli@glasgow.ac.uk)

Results

If you collected 30culx with MTC trap, then you might expect 19.3 (credible intervals: 7.17/27.37) HLC-equivalent, according to model 2.



8.1.3 Shiny App dashboard showing one example of a model which account for other species (model 3) between HLC and an alternative trap (i.e., MTC) for *Culex* spp



Calibration tool for outdoor-biting mosquitoes sampling

What mosquitoes are you collecting?

culex
 gambiae
 funestus

Which trap are you using?

MTC
 BGS
 IFT
 MMX
 MTRC
 SUN

How many mosquitoes did you catch?

What model? (please see paper for details)

1 (linear effect)
 2 (saturation effect)
 3 (effect of other species)

How many females of other unidentified species did you catch?

INSTRUCTIONS

This tool can be used to explore the output of the models for mosquito trap calibration presented in Ngowo et al (2022) (<https://www.researchsquare.com/article/rs-1494460/v1>) and to estimate the HLC-equivalent number of mosquitoes collected with exposure-free alternative traps.

On the input panel you can select the species of interest, the trap and the model (see 'Ngowo et al. for details).

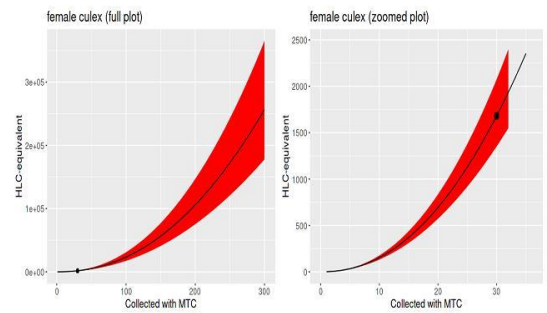
By clicking on 'Run' you will generate the plot of predicted HLC-equivalent catches.

Please note that coefficients of the models generating the prediction will be updated regularly as additional data are gathered (see above mentioned paper for more details).

To report a bug, or for any question, please write to luca.nelli@glasgow.ac.uk (mailto:luca.nelli@glasgow.ac.uk)

Results

If you collected 30 culex with MTC trap, then you might expect 1681 (credible intervals: 1351.17/2075.44) HLC-equivalent, according to model 3.



9 References

1. WHO. WHO Malaria Report 2021. Geneva: World Health Organization; 2021.
2. Bhatt S, Weiss DJ, Cameron E, Bisanzio D, Mappin B, Dalrymple U, et al. The effect of malaria control on *Plasmodium falciparum* in Africa between 2000 and 2015. *Nature*. 2015;526: 1-9. doi:10.1038/nature15535 <http://www.nature.com/nature/journal/v526/n7572/abs/nature15535.html#supplementary-information>
3. WHO. World malaria report. World malaria report. 2020. doi:<http://www.who.int/malaria/publications/world-malaria-report-2017/en/>
4. Pigott DM, Atun R, Moyes CL, Hay SI, Gething PW. Funding for malaria control 2006-2010: A comprehensive global assessment. *Malaria Journal*. BioMed Central; 2012. pp. 1-11. doi:10.1186/1475-2875-11-246
5. Alonso PL, Tanner M. Public health challenges and prospects for malaria control and elimination. *Nat Med*. 2013;19: 150-5. doi:10.1038/nm.3077
6. Cohen AJM, Okumu F, Moonen B. The malaria fight's diminishing gains and growing challenges. *Sci Transl Med*. 2021;14. doi:10.1126/SCITRANSLMED.ABN3256
7. The Lancet. Malaria vaccine approval: a step change for global health. *The Lancet*. 2021. p. 1381. doi:10.1016/S0140-6736(21)02235-2
8. PATH. Malaria parasite life cycle | PATH's Malaria Vaccine Initiative. In: Malaria Vaccine Initiative [Internet]. 2021 [cited 16 May 2022]. Available: <https://www.malariavaccine.org/malaria-and-vaccines/vaccine-development/life-cycle-malaria-parasite>
9. Griffin JT, Hollingsworth TD, Okell LC, Churcher TS, White M, Hinsley W, et al. Reducing *Plasmodium falciparum* malaria transmission in Africa: A model-based evaluation of intervention strategies. *PLoS Med*. 2010;7. doi:10.1371/journal.pmed.1000324
10. Kokwaro G, Mwai L, Nzila A. Artemether/lumefantrine in the treatment of uncomplicated *falciparum* malaria. *Expert Opin Pharmacother*. 2007;8: 75-94. doi:10.1517/14656566.8.1.75
11. Balikagala B, Fukuda N, Ikeda M, Katuro OT, Tachibana S-I, Yamauchi M, et al. Evidence of Artemisinin-Resistant Malaria in Africa. *N Engl J Med*.

2021;385: 1163-1171. doi:10.1056/nejmoa2101746

12. Woolhouse MEJ, Dye C, Etard J-F, Smith T, Charlwood JD, Garnett GP, et al. Heterogeneities in the transmission of infectious agents: Implications for the design of control programs. *Proc Natl Acad Sci U S A*. 1997.
13. Sabbatani S, Fiorino S, Manfredi R. The emerging of the fifth malaria parasite (*Plasmodium knowlesi*): a public health concern? *Brazilian J Infect Dis*. 2010. doi:10.1590/s1413-86702010000300019
14. Sinka ME, Bangs MJ, Manguin S, Coetzee M, Mbogo CM, Hemingway J, et al. The dominant *Anopheles* vectors of human malaria in Africa, Europe and the Middle East: occurrence data, distribution maps and bionomic précis. *Parasit Vectors*. 2010;3: 117. doi:10.1186/1756-3305-3-117
15. Gillies M, Coetzee M. A Supplement to the *Anophelinae* of Africa South of the Sahara. *Publ South African Inst Med Res*. 1987;55: 63.
16. Takken W, Verhulst NO. Host Preferences of Blood-Feeding Mosquitoes. *Annu Rev Entomol*. 2011;58: 120928130709004. doi:10.1146/annurev-ento-120811-153618
17. Cox FE. History of the discovery of the malaria parasites and their vectors. *Parasites and Vectors*. BioMed Central; 2010. pp. 1-9. doi:10.1186/1756-3305-3-5
18. Trampuz A, Jereb M, Muzlovic I, Prabhu RM. Clinical review: Severe malaria. *Crit Care*. 2003;7: 315. doi:10.1186/cc2183
19. Strickland GT, Hill DR. Hunter's tropical medicine and emerging infectious diseases. WB Saunders company; 2000.
20. Genton B, D'Acremont V. Clinical features of malaria in returning travelers and migrants. *Travel malaria Hamilt BC, Ontario, Canada, Decker*. 2001; 371-392.
21. Service MW. Introduction to the mosquitoes (Order Diptera: Family Culicidae): classification, morphology, life cycle and control principles. *A Guide to Medical Entomology*. London: Macmillan Education UK; 1980. pp. 22-43. doi:10.1007/978-1-349-16334-2_4
22. Porretta D, Mastrantonio V, Crasta G, Bellini R, Comandatore F, Rossi P, et al. Intra-instar larval cannibalism in *Anopheles gambiae* (s.s.) and *Anopheles stephensi* (Diptera: Culicidae). *Parasites and Vectors*. 2016;9: 1-9. doi:10.1186/s13071-016-1850-5
23. Lyons CL, Coetzee M, Chown SL. Stable and fluctuating temperature

- effects on the development rate and survival of two malaria vectors, *Anopheles arabiensis* and *Anopheles funestus*. *Parasit Vectors*. 2013;6: 104. doi:10.1186/1756-3305-6-104
24. Ngowo HS, Hape EE, Matthiopoulos J, Okumu FO. Fitness Characteristics of the Malaria Vector, *Anopheles Funestus*, During an Attempted Laboratory Colonization. *Malar J*. 2020;20: 148. doi:https://doi.org/10.21203/rs.3.rs-104896/v1
 25. Lyimo., Takken W, Koella JC. Effect of rearing temperature and larval density on larval survival, age at pupation and adult size of *Anopheles gambiae*. *Entomol Exp Appl*. 1992;63: 265-271. doi:10.1007/BF00192775
 26. Sciences B, Laboratories S, Bayoh MN, Lindsay SW. Temperature-related duration of aquatic stages of the Afrotropical malaria vector mosquito *Anopheles gambiae* in the laboratory. *Med Vet Entomol*. 2004;18: 174-179. doi:10.1111/j.0269-283X.2004.00495.x
 27. Lyons CL, Coetzee M, Terblanche JS, Chown SL. Thermal limits of wild and laboratory strains of two African malaria vector species, *Anopheles arabiensis* and *Anopheles funestus*. *Malar J*. 2012;11: 226. doi:10.1186/1475-2875-11-226
 28. Kelly-Hope, A L, Hemingway J, McKenzie FE. Environmental factors associated with the malaria vectors *Anopheles gambiae* and *Anopheles funestus* in Kenya. *Malar J*. 2009;8: 268. doi:10.1186/1475-2875-8-268
 29. Afrane YA, Githeko AK, Yan G. The ecology of *Anopheles* mosquitoes under climate change: Case studies from the effects of deforestation in East African highlands. *Ann N Y Acad Sci*. 2012;1249: 204-210. doi:10.1111/j.1749-6632.2011.06432.x
 30. Hii JL, Chew M, Sang VY, Munstermann LE, Tan SG, Panyim S, et al. Population genetic analysis of host seeking and resting behaviors in the malaria vector, *Anopheles balabacensis* (Diptera: Culicidae). *J Med Entomol*. 1991;28: 675-84. doi:10.1093/jmedent/28.5.675
 31. Gillies MT. The duration of the gonotrophic cycle in *Anopheles gambiae* and *Anopheles funestus*, with a note on the efficiency of hand catching. *East Afr Med J*. 1953;30: 129-135.
 32. Olayemi IK, Ande AT. Life table analysis of *Anopheles gambiae* (Diptera: Culicidae) in relation to malaria transmission. *J Vector Borne Dis*. 2009;46: 295-298.

33. Kaindoa EW, Ngowo HS, Limwagu AJ, Tchouakui M, Hape E, Abbasi S, et al. Swarms of the malaria vector *Anopheles funestus* in Tanzania. *Malar J*. 2019. doi:10.1186/s12936-019-2660-y
34. Sawadogo PS, Namountougou M, Toé KH, Rouamba J, Maïga H, Ouédraogo KR, et al. Swarming behaviour in natural populations of *Anopheles gambiae* and *An. coluzzii*: Review of 4 years survey in rural areas of sympatry, Burkina Faso (West Africa). *Acta Trop*. 2014;130: 24-34. doi:10.1016/j.actatropica.2013.10.015
35. Dao A, Adamou A, Yaro AS, Maïga M, Kassogue Y, Traoré SF, et al. Assessment of Alternative Mating Strategies in *Anopheles gambiae*: Does Mating Occur Indoors? *Assessment of Alternative Mating Strategies in Anopheles gambiae : Does Mating Occur Indoors?* 2008;45: 643-652.
36. Nambunga IH, Msugupakulya BJ, Hape EE, Mshani IH, Kahamba NF, Mkandawile G, et al. Wild populations of malaria vectors can mate both inside and outside human dwellings. *Parasites and Vectors*. 2021;14: 1-14. doi:10.1186/s13071-021-04989-8
37. Wijit A, Taai K, Dedkhad W, Hempolchom C, Thongsahuan S, Srisuka W, et al. Comparative Studies on the Stenogamous and Eurygamous Behavior of Eight *Anopheles* Species of the Hyrcanus Group (Diptera: Culicidae) in Thailand. *Insects*. 2016;7: 11. doi:10.3390/insects7020011
38. Kim S, Trocke S, Sim C. Comparative studies of stenogamous behaviour in the mosquito *Culex pipiens* complex. *Med Vet Entomol*. 2018;32: 427-435. doi:10.1111/mve.12309
39. Lardeux F, Quispe V, Tejerina R, Rodríguez R, Torrez L, Bouchité B, et al. Laboratory colonization of *Anopheles pseudopunctipennis* (Diptera: Culicidae) without forced mating. *Comptes Rendus - Biol*. 2007;330: 571-575. doi:10.1016/j.crv.2007.04.002
40. Agyekum TP, Botwe PK, Arko-Mensah J, Issah I, Acquah AA, Hogarh JN, et al. A Systematic Review of the Effects of Temperature on *Anopheles* Mosquito Development and Survival: Implications for Malaria Control in a Future Warmer Climate. *Int J Environ Res Public Heal* 2021, Vol 18, Page 7255. 2021;18: 7255. doi:10.3390/IJERPH18147255
41. Gillies MT, Wilkes TJ. A study of the age-composition of populations of *Anopheles gambiae* Giles and *A. funestus* Giles in North-Eastern Tanzania. *Bull Entomol Res*. 1965;56: 237-262. doi:10.1017/S0007485300056339

42. Onori E, Grab B. Indicators for the forecasting of malaria epidemics. *Bull World Health Organ.* 1980.
43. Smith DL, McKenzie FE. Statics and dynamics of malaria infection in *Anopheles* mosquitoes. *Malar J.* 2004;3: 1-14. doi:10.1186/1475-2875-3-13/TABLES/2
44. Smith DL, Battle KE, Hay SI, Barker CM, Scott TW, McKenzie FE. Ross, Macdonald, and a theory for the dynamics and control of mosquito-transmitted pathogens. *PLoS Pathog.* 2012;8. doi:10.1371/journal.ppat.1002588
45. Depinay J-MOMO, Mbogo CM, Killeen G, Knols B, Beier J, Carlson J, et al. A simulation model of African *Anopheles* ecology and population dynamics for the analysis of malaria transmission. *Malar J.* 2004;3: 29. doi:10.1186/1475-2875-3-29
46. Gimnig JE, Ombok M, Kamau L, Hawley WA. Characteristics of Larval *Anopheline* (*Diptera* : *Culicidae*) Habitats in Western Kenya. 1999.
47. Paaijmans KP, Imbahale SS, Thomas MB, Takken W. Relevant microclimate for determining the development rate of malaria mosquitoes and possible implications of climate change. *Malar J.* 2010;9: 196. doi:10.1186/1475-2875-9-196
48. Paaijmans KP, Huijben S, Githeko AK, Takken W. Competitive interactions between larvae of the malaria mosquitoes *Anopheles arabiensis* and *Anopheles gambiae* under semi-field conditions in western Kenya. *Acta Trop.* 2009;109: 124-130. doi:10.1016/j.actatropica.2008.07.010
49. Kweka EJ, Zhou G, Gilbreath TM, Afrane Y, Nyindo M, Githeko AK, et al. Predation efficiency of *Anopheles gambiae* larvae by aquatic predators in western Kenya highlands. *Parasites and Vectors.* 2011;4: 1-7. doi:10.1186/1756-3305-4-128
50. Woodley SK, Mattes BM, Yates EK, Relyea RA. Exposure to sublethal concentrations of a pesticide or predator cues induces changes in brain architecture in larval amphibians. *Oecologia.* 2015;179: 655-665. doi:10.1007/s00442-015-3386-3
51. Service MW. Mortalities of the larvae of the *Anopheles gambiae* Giles complex and detection of predators by the precipitin test. *Bull Entomol Res.* 1973. doi:10.1017/S0007485300003862
52. Service MW. Mortalities of the immature stages of species b of the

- Anopheles gambiae complex in Kenya: Comparison between rice fields and temporary pools, identification of predators, and effects of insecticidal spraying. *J Med Entomol.* 1977. doi:10.1093/jmedent/13.4-5.535
53. Koenraadt CJM, Majambere S, Hemerik L, Takken W. The effects of food and space on the occurrence of cannibalism and predation among larvae of *Anopheles gambiae* s.l. *Entomol Exp Appl.* 2004;112: 125-134. doi:10.1111/j.0013-8703.2004.00186.x
 54. Gimnig JE, Ombok M, Kamau L, Hawley WA. Characteristics of Larval Anopheline (Diptera: Culicidae) Habitats in Western Kenya. *Source J Med Entomol J Med Entomol.* 2001;38: 282-288. doi:10.1603/0022-2585-38.2.282
 55. Ye-Ebiyo Y, Pollack RJ, Kiszewski A, Spielman A. Enhancement of development of larval *Anopheles arabiensis* by proximity to flowering maize (*Zea mays*) in turbid water and when crowded. *Am J Trop Med Hyg.* 2003.
 56. Hawley WA. The Effect of Larval Density on Adult Longevity of a Mosquito, *Aedes sierrensis*: Epidemiological Consequences. *J Anim Ecol.* 2006. doi:10.2307/4389
 57. Gimnig JE, Ombok M, Otieno S, Michael G, Vulule JM, Walker ED, et al. Density-Dependent Development of *Anopheles gambiae* (Diptera: Culicidae) Larvae in Artificial Habitats. *J Med Entomol.* 2002.
 58. Ng'habi KR, Lee Y, Knols BGJ, Mwasheshi D, Lanzaro GC, Ferguson HM. Colonization of malaria vectors under semi-field conditions as a strategy for maintaining genetic and phenotypic similarity with wild populations. *Malar J.* 2015;14: 1-11. doi:10.1186/s12936-014-0523-0
 59. Russell TL, Lwetoijera DW, Knols BGJ, Takken W, Killeen GF, Ferguson HM. Linking individual phenotype to density-dependent population growth: the influence of body size on the population dynamics of malaria vectors. *Proc R Soc B Biol Sci.* 2011;278: 3142-3151. doi:10.1098/rspb.2011.0153
 60. Lyimo EO, Takken W, Koella JC. Effect of rearing temperature and larval density on larval survival, age at pupation and adult size of *Anopheles gambiae*. *Entomol Exp Appl.* 1992;63: 265-271. doi:10.1111/j.1570-7458.1992.tb01583.x
 61. Ng'habi, John B, Nkwengulila G, Knols BGJ, Killeen GF, Ferguson HM. Effect of larval crowding on mating competitiveness of *Anopheles gambiae*

- mosquitoes. *Malar J.* 2005;4: 1-9. doi:10.1186/1475-2875-4-49
62. Fillinger U, Sonye G, Killeen GF, Knols BGJ, Becker N. The practical importance of permanent and semipermanent habitats for controlling aquatic stages of *Anopheles gambiae* sensu lato mosquitoes: Operational observations from a rural town in western Kenya. *Trop Med Int Heal.* 2004. doi:10.1111/j.1365-3156.2004.01335.x
 63. Koenraadt CJM, Majambere S, Hemerik L, Takken W. Cannibalism and predation among larvae of *Anopheles gambiae* s.l. *Entomol Exp Appl.* 2004;112: 125-134.
 64. Krebs C. *The Experimental Analysis of Distribution and Abundance.* Ecol New York Harper Row. 1972.
 65. Macdonald G. The epidemiology and control of malaria. *Epidemiol Control Malaria.* 1957;7: 577-578.
 66. Gillies M, Meillon D. *The Anophelinae of Africa south of the Sahara (Ethiopian zoogeographical region).* Sahara Ethiop Zoogeographical. 1968; 343 pp.
 67. Gillies MT, Coetzee M. *A Supplement to the Anophelinae of the South of the Sahara (Afrotropical Region).* Publications of the South African Institute for Medical Research. 1987. pp. 1-143.
 68. Sinka ME, Bangs MJ, Manguin S, Rubio-Palis Y, Chareonviriyaphap T, Coetzee M, et al. A global map of dominant malaria vectors. *Parasit Vectors.* 2012;5: 69. doi:10.1186/1756-3305-5-69
 69. Coetzee M, Hunt RH, Wilkerson R, Torre A Della, Coulibaly MB, Besansky NJ. *Anopheles coluzzii* and *anopheles amharicus*, new members of the *anopheles gambiae* complex. *Zootaxa.* 2013;3619: 246-274. doi:10.11646/zootaxa.3619.3.2
 70. Coetzee M, Craig M, Le Sueur D. Distribution of African malaria mosquitoes belonging to the *Anopheles gambiae* complex. *Parasitology Today. Elsevier Current Trends;* 2000. pp. 74-77. doi:10.1016/S0169-4758(99)01563-X
 71. Scott JA, Brogdon WG, Collins FH. Identification of single specimens of the *Anopheles gambiae* complex by the polymerase chain reaction. *Am J Trop Med Hyg.* 1993;49: 520-529.
 72. Lemasson J, Fontenille D, Lochouart L, Dia I, Simard F, Ba K, et al. Comparison of Behavior and Vector Efficiency of *Anopheles gambiae* and *An . arabiensis* (*Diptera : Culicidae*) in Barkedji , a Sahelian Area of

Senegal. 1997; 396-403.

73. Bigoga JD, Nanfack FM, Awono-Ambene PH, Patchoké S, Atangana J, Otia VS, et al. Seasonal prevalence of malaria vectors and entomological inoculation rates in the rubber cultivated area of Niete, South Region of Cameroon. *Parasit Vectors*. 2012;5: 197. doi:10.1186/1756-3305-5-197
74. Lindsay SW, Parson L, Thomas CJ. Mapping the ranges and relative abundance of the two principal African malaria vectors, *Anopheles gambiae sensu stricto* and *An. arabiensis*, using climate data. *Proc R Soc B Biol Sci*. 1998;265: 847-854. doi:10.1098/rspb.1998.0369
75. Mutuku FM, King CH, Mungai P, Mbogo C, Mwangangi J, Muchiri EM, et al. Impact of insecticide-treated bed nets on malaria transmission indices on the south coast of Kenya. *Malar J*. 2011;10: 356. doi:10.1186/1475-2875-10-356
76. Bayoh MN, Mathias DK, Odiere MR, Mutuku FM, Kamau L, Gimnig JE, et al. *Anopheles gambiae*: historical population decline associated with regional distribution of insecticide-treated bed nets in western Nyanza Province, Kenya. *Malar J*. 2010;9: 62. doi:10.1186/1475-2875-9-62
77. Russell TL, Govella NJ, Azizi S, Drakeley CJ, Kachur SP, Killeen GF. Increased proportions of outdoor feeding among residual malaria vector populations following increased use of insecticide-treated nets in rural Tanzania. *Malar J*. 2011;10: 80. doi:10.1186/1475-2875-10-80
78. Lyimo IN, Haydon DT, Mbina KF, Daraja AA, Mbehela EM, Reeve R, et al. The fitness of African malaria vectors in the presence and limitation of host behaviour. *Malar J*. 2012;11: 1-12. doi:10.1186/1475-2875-11-425
79. Kreppel KS, Viana M, Main BJ, Johnson PCD, Govella NJ, Lee Y, et al. Emergence of behavioural avoidance strategies of malaria vectors in areas of high LLIN coverage in Tanzania. *Sci Rep*. 2020;10: 1-11. doi:10.1038/s41598-020-71187-4
80. Maia MF, Robinson A, John A, Mgando J, Simfukwe E, Moore SJ. Comparison of the CDC Backpack aspirator and the Prokopack aspirator for sampling indoor- and outdoor-resting mosquitoes in southern Tanzania. *Parasit Vectors*. 2011;4: 124. doi:10.1186/1756-3305-4-124
81. Lyimo IN, Haydon DT, Russell TL, Mbina KF, Daraja AA, Mbehela EM, et al. The impact of host species and vector control measures on the fitness of African malaria vectors. *Proc Biol Sci*. 2013;280: 20122823.

doi:10.1098/rspb.2012.2823

82. Chaves LF, Harrington LC, Keogh CL, Nguyen AM, Kitron UD. Blood feeding patterns of mosquitoes: random or structured? *Front Zool.* 2010;7: 3. doi:10.1186/1742-9994-7-3
83. Briët OJT, Chitnis N. Effects of changing mosquito host searching behaviour on the cost effectiveness of a mass distribution of long-lasting, insecticidal nets: a modelling study. *Malar J.* 2013;12: 215. doi:10.1186/1475-2875-12-215
84. Vezenegho SB, Chiphwanya J, Hunt RH, Coetzee M, Bass C, Koekemoer LL. Characterization of the *Anopheles funestus* group, including *Anopheles funestus*-like, from Northern Malawi. *Trans R Soc Trop Med Hyg.* 2013;107: 753-762. doi:10.1093/trstmh/trt089
85. Mouatcho J, Cornel AJ, Dahan-Moss Y, Koekemoer LL, Coetzee M, Braack L. Detection of *Anopheles rivulorum*-like, a member of the *Anopheles funestus* group, in South Africa. *Malar J.* 2018;17: 1-7. doi:10.1186/s12936-018-2353-y
86. Dia I, Guelbeogo MW, Ayala D. Advances and Perspectives in the Study of the Malaria Mosquito *Anopheles funestus*. *Anopheles mosquitoes - New insights into malaria vectors.* InTech; 2013. doi:10.5772/55389
87. Coetzee M, Fontenille D. Advances in the study of *Anopheles funestus*, a major vector of malaria in Africa. *Insect Biochemistry and Molecular Biology.* 2004. pp. 599-605. doi:10.1016/j.ibmb.2004.03.012
88. Kaindoa EW, Matowo NS, Ngowo HS, Mkandawile G, Mmbando A, Finda M, et al. Interventions that effectively target *Anopheles funestus* mosquitoes could significantly improve control of persistent malaria transmission in south-eastern Tanzania. *PLoS One.* 2017;12. doi:10.1371/journal.pone.0177807
89. Lwetoijera D, Harris C, Kiware SS, Dongus S, Devine GJ, McCall PJ, et al. Increasing role of *Anopheles funestus* and *Anopheles arabiensis* in malaria transmission in the Kilombero Valley, Tanzania. *Malar J.* 2014;13: 331. doi:10.1186/1475-2875-13-331
90. Mendis C, Jacobsen JL, Gamage-Mendis A, Bule E, Dgedge M, Thompson R, et al. *Anopheles arabiensis* and *An. funestus* are equally important vectors of malaria in Matola coastal suburb of Maputo, southern Mozambique. *Med Vet Entomol.* 2000;14: 171-180. doi:10.1046/j.1365-2915.2000.00228.x

91. Okumu F, Finda M. Key Characteristics of Residual Malaria Transmission in Two Districts in South-Eastern Tanzania-Implications for Improved Control. *J Infect Dis.* 2021;223: S143-S154. doi:10.1093/infdis/jiaa653
92. Hargreaves K, Koekemoer LL, Brooke BD, Hunt RH, Mthembu J, Coetzee M. *Anopheles funestus* resistant to pyrethroid insecticides in South Africa. *Med Vet Entomol.* 2000;14: 181-189. doi:10.1046/j.1365-2915.2000.00234.x
93. Killeen GF. Characterizing, controlling and eliminating residual malaria transmission. *Malar J.* 2014;13: 330. doi:10.1186/1475-2875-13-330
94. Koenraadt CJ, Githeko AK, Takken W. The effects of rainfall and evapotranspiration on the temporal dynamics of *Anopheles gambiae* s.s. and *Anopheles arabiensis* in a Kenyan village. *Acta Trop.* 2004;90: 141-153. Available:
http://www.ncbi.nlm.nih.gov/entrez/query.fcgi?cmd=Retrieve&db=PubMed&dopt=Citation&list_uids=15177140
95. Nambunga IH, Ngowo HS, Mapua SA, Hape EE, Msugupakulya BJ, Msaky DS, et al. Aquatic habitats of the malaria vector *Anopheles funestus* in rural south-eastern Tanzania. *Malar J.* 2020;19: 1-11. doi:10.1186/s12936-020-03295-5
96. Kabbale FG, Akol AM, Kaddu JB, Onapa AW. Biting patterns and seasonality of *Anopheles gambiae* sensu lato and *Anopheles funestus* mosquitoes in Kamuli District, Uganda. *Parasit Vectors.* 2013;6: 340. doi:10.1186/1756-3305-6-340
97. Minakawa N, Dida GO, Sonye GO, Futami K, Njenga SM. Malaria vectors in Lake Victoria and adjacent habitats in Western Kenya. *PLoS One.* 2012. doi:10.1371/journal.pone.0032725
98. Cooke MK, Kahindi SC, Oriango RM, Owaga C, Ayoma E, Mabuka D, et al. “A bite before bed”: exposure to malaria vectors outside the times of net use in the highlands of western Kenya. *Malar J.* 2015;14: 259. doi:10.1186/s12936-015-0766-4
99. Kent RJ, Thuma PE, Mharakurwa S, Norris DE. Seasonality, blood feeding behavior, and transmission of *Plasmodium falciparum* by *Anopheles arabiensis* after an extended drought in southern Zambia. *Am J Trop Med Hyg.* 2007;76: 267-74. doi:76/2/267 [pii]
100. Takken W, Charlwood JD, Billingsley PF, Gort G. Dispersal and survival of

- Anopheles funestus and *A. gambiae* s.l. (Diptera: Culicidae) during the rainy season in southeast Tanzania. Bull Entomol Res. 1998;88: 561. doi:10.1017/S0007485300026080
101. Moiroux N, Damien GB, Egrot M, Djenontin A, Chandre F, Corbel V, et al. Human exposure to early morning Anopheles funestus biting behavior and personal protection provided by long-lasting insecticidal nets. PLoS One. 2014;9: 8-11. doi:10.1371/journal.pone.0104967
 102. Moiroux N, Gomez MB, Pennetier C, Elanga E, Djènontin A, Chandre F, et al. Changes in Anopheles funestus Biting Behavior Following Universal Coverage of Long-Lasting Insecticidal Nets in Benin. J Infect Dis. 2012;206: 1622-1629. doi:10.1093/infdis/jis565
 103. Ngowo HS, Kaindoa EW, Matthiopoulos J, Ferguson HM, Okumu FO. Variations in household microclimate affect outdoor-biting behaviour of malaria vectors. Wellcome Open Res. 2017;2: 102. doi:10.12688/wellcomeopenres.12928.1
 104. Hunt RH, Brooke BD, Pillay C, Koekemoer LL, Coetzee M. Laboratory selection for and characteristics of pyrethroid resistance in the malaria vector Anopheles funestus. Med Vet Entomol. 2005;19: 271-275. doi:10.1111/j.1365-2915.2005.00574.x
 105. WHO. Guidelines for Malaria Vector Control. Guidelines for Malaria Vector Control. 2019. p. 161. Available: <http://www.ncbi.nlm.nih.gov/pubmed/30844152>
 106. Costa-Neta BM, Lima-Neto AR, da Silva AA, Brito JM, Aguiar JVC, Ponte IS, et al. Centers for Disease Control-type light traps equipped with high-intensity light-emitting diodes as light sources for monitoring Anopheles mosquitoes. Acta Trop. 2018;183: 61-63. doi:10.1016/j.actatropica.2018.04.013
 107. Beier JC, Perkins P V., Koros JK, Onyango FK, Gargan TP, Wirtz RA, et al. Malaria Sporozoite Detection by Dissection and Elisa to Assess Infectivity of Afrotropical Anopheles (Diptera: Culicidae). J Med Entomol. 1990;27: 377-384. doi:10.1093/jmedent/27.3.377
 108. Huho B, Briët O, Seyoum A, Sikaala C, Bayoh N, Gimnig J, et al. Consistently high estimates for the proportion of human exposure to malaria vector populations occurring indoors in rural Africa. Int J Epidemiol. 2013;42: 235-247. doi:10.1093/ije/dys214

109. Seyoum A, Sikaala CH, Chanda J, Chinula D, Ntamatungiro AJ, Hawela M, et al. Human exposure to anopheline mosquitoes occurs primarily indoors, even for users of insecticide-treated nets in Luangwa Valley, South-east Zambia. *Parasit Vectors*. 2012;5: 101. doi:10.1186/1756-3305-5-101
110. Monroe A, Moore S, Koenker H, Lynch M, Ricotta E. Measuring and characterizing night time human behaviour as it relates to residual malaria transmission in sub-Saharan Africa: A review of the published literature. *Malar J*. 2019;18: 1-12. doi:10.1186/s12936-019-2638-9
111. Bacaër N, Bacaër N. Ross and malaria (1911). *A Short History of Mathematical Population Dynamics*. Springer London; 2011. pp. 65-69. doi:10.1007/978-0-85729-115-8_12
112. Wotodjo AN, Trape JF, Richard V, Doucouré S, Diagne N, Tall A, et al. No difference in the incidence of malaria in human-landing mosquito catch collectors and non-collectors in a Senegalese village with endemic malaria. *PLoS One*. 2015;10: e0126187. doi:10.1371/journal.pone.0126187
113. Costantini C, Sagnon NF, Sanogo E, Merzagora L, Coluzzi M. Relationship to human biting collections and influence of light and bednet in CDC light-trap catches of West African malaria vectors. *Bull Entomol Res*. 1998;88: 503-511. doi:10.1017/s000748530002602x
114. Briët OJT, Huho BJ, Gimnig JE, Bayoh N, Seyoum A, Sikaala CH, et al. Applications and limitations of Centers for Disease Control and Prevention miniature light traps for measuring biting densities of African malaria vector populations: a pooled-analysis of 13 comparisons with human landing catches. *Malar J*. 2015;14: 247. doi:10.1186/s12936-015-0761-9
115. Tangena J-AA, Thammavong P, Hiscox A, Lindsay SW, Brey PT. The Human-Baited Double Net Trap: An Alternative to Human Landing Catches for Collecting Outdoor Biting Mosquitoes in Lao PDR. *PLoS One*. 2015;10: e0138735. doi:10.1371/journal.pone.0138735
116. Okumu FO, Kotas ME, Kihonda J, Mathenge E, Killeen GF, Moore SJ. Comparative Evaluation of Methods Used for Sampling Malaria Vectors in the Kilombero Valley, South Eastern Tanzania. *Open Trop Med J*. 2008;1: 51-55. doi:10.2174/1874315300801010051
117. Gimnig JE, Walker ED, Otieno P, Kosgei J, Olang G, Ombok M, et al. Incidence of malaria among mosquito collectors conducting human landing catches in western kenya. *Am J Trop Med Hyg*. 2013;88: 301-308.

doi:10.4269/ajtmh.2012.12-0209

118. Achee NL, Youngblood L, Bangs MJ, Lavery J V., James S. Considerations for the Use of Human Participants in Vector Biology Research: A Tool for Investigators and Regulators. *Vector-Borne Zoonotic Dis.* 2015;15: 89-102. doi:10.1089/vbz.2014.1628
119. Ndebele P, Musesengwa R. View point: Ethical dilemmas in malaria vector research in Africa: Making the difficult choice between mosquito, science and humans. *Malawi Med J.* 2012;24: 65-68.
120. Sumaye RD, Abatih EN, Thiry E, Amuri M, Berkvens D, Geubbels E. Inter-epidemic Acquisition of Rift Valley Fever Virus in Humans in Tanzania. Sang RC, editor. *PLoS Negl Trop Dis.* 2015;9: e0003536. doi:10.1371/journal.pntd.0003536
121. Okumu F, Biswaro L, Mbeleyela E, Killeen GF, Mukabana R, Moore SJ. Using nylon strips to dispense mosquito attractants for sampling the malaria vector *Anopheles gambiae* s.s. *J Med Entomol.* 2010;47: 274-82. doi:10.1603/ME09114
122. Abong'O B, Yu X, Donnelly MJ, Geier M, Gibson G, Gimnig J, et al. Host Decoy Trap (HDT) with cattle odour is highly effective for collection of exophagic malaria vectors. *Parasit Vectors.* 2018;11: 533. doi:10.1186/s13071-018-3099-7
123. Hiscox A, Otieno B, Kibet A, Mweresa CK, Omusula P, Geier M, et al. Development and optimization of the Suna trap as a tool for mosquito monitoring and control. *Malar J.* 2014;13: 257. doi:10.1186/1475-2875-13-257
124. Maliti D V, Govella NJ, Killeen GF, Mirzai N, Johnson PCD, Kreppel K, et al. Development and evaluation of mosquito-electrocuting traps as alternatives to the human landing catch technique for sampling host-seeking malaria vectors. *Malar J.* 2015;14: 502. doi:10.1186/s12936-015-1025-4
125. Kreppel KS, Johnson PCD, Govella NJ, Pombi M, Maliti D, Ferguson HM. Comparative evaluation of the Sticky-Resting-Box-Trap, the standardised resting-bucket-trap and indoor aspiration for sampling malaria vectors. *Parasit Vectors.* 2015;8: 462. doi:10.1186/s13071-015-1066-0
126. Zembere K, Chirombo J, Nasoni P, McDermott DP, Tchongwe-Divala L, Hawkes FM, et al. The human-baited host decoy trap (HDT) is an efficient

- sampling device for exophagic *Anopheles arabiensis* within irrigated lands in southern Malawi. *Sci Rep.* 2022;12: 1-10. doi:10.1038/s41598-022-07422-x
127. Sudia WD, Chamberlain RW. Classic paper: Battery-operated light trap, an improved model. *J Am Mosq Control Assoc.* 1988.
 128. Sikaala CH, Killeen GF, Chanda J, Chinula D, Miller JM, Russell TL, et al. Evaluation of alternative mosquito sampling methods for malaria vectors in Lowland South-East Zambia. *Parasit Vectors.* 2013;6: 91. doi:10.1186/1756-3305-6-91
 129. Mboera L. Sampling techniques for adult Afrotropical malaria vectors and their reliability in the estimation of entomological inoculation rate. *Tanzan J Health Res.* 2006;7: 117-124. doi:10.4314/thrb.v7i3.14248
 130. Sherrard-Smith E, Skarp JE, Beale AD, Fornadel C, Norris LC, Moore SJ, et al. Mosquito feeding behavior and how it influences residual malaria transmission across Africa. *Proc Natl Acad Sci U S A.* 2019;116: 15086-15096. doi:10.1073/pnas.1820646116
 131. Killeen GF, Govella NJ, Lwetoijera DW, Okumu FO. Most outdoor malaria transmission by behaviourally-resistant *Anopheles arabiensis* is mediated by mosquitoes that have previously been inside houses. *Malar J.* 2016;15: 225. doi:10.1186/s12936-016-1280-z
 132. Moshi IR, Ngowo H, Dillip A, Msellemu D, Madumla EP, Okumu FO, et al. Community perceptions on outdoor malaria transmission in Kilombero Valley, Southern Tanzania. *Malar J.* 2017;16: 1-8. doi:10.1186/s12936-017-1924-7
 133. Eckhoff PA. A malaria transmission-directed model of mosquito life cycle and ecology. *Malar J.* 2011;10: 1-17. doi:10.1186/1475-2875-10-303/FIGURES/8
 134. Aron JL, May RM. The population dynamics of malaria. *The Population Dynamics of Infectious Diseases: Theory and Applications.* Springer, Boston, MA; 1982. pp. 139-179. doi:10.1007/978-1-4899-2901-3_5
 135. Viana M, Ng'habi K, Lyimo I, Ferguson HM, Matthiopoulos J, Killeen G. Mesocosm experiments reveal the impact of mosquito control measures on malaria vector life history and population dynamics. *Sci Rep.* 2018;8: 1-12. doi:10.1038/s41598-018-31805-8
 136. Reiner RC, Perkins TA, Barker CM, Niu T, Chaves LF, Ellis AM, et al. A

- systematic review of mathematical models of mosquito-borne pathogen transmission: 1970-2010. *J R Soc Interface.* 2013;10. doi:10.1098/rsif.2012.0921
137. Smith DL, Perkins TA, Tusting LS, Scott TW, Lindsay SW. Mosquito Population Regulation and Larval Source Management in Heterogeneous Environments. 2013;8. Available: <https://journals.plos.org/plosone/article?id=10.1371/journal.pone.0071247>
 138. Yakob L, Yan G. A network population model of the dynamics and control of African malaria vectors. *Trans R Soc Trop Med Hyg.* 2010;104: 669-675. doi:10.1016/j.trstmh.2010.07.014
 139. Barbosa S, Kay K, Chitnis N, Hastings IM. Modelling the impact of insecticide-based control interventions on the evolution of insecticide resistance and disease transmission. *Parasites and Vectors.* 2018;11: 1-21. doi:10.1186/s13071-018-3025-z
 140. Ermert V, Fink AH, Jones AE, Morse AP. Development of a new version of the Liverpool malaria model. II. Calibration and validation for West Africa. *Malar J.* 2011;10: 1-17. doi:10.1186/1475-2875-10-62
 141. White MT, Griffin JT, Churcher TS, Ferguson NM, Basáñez MG, Ghani AC. Modelling the impact of vector control interventions on *Anopheles gambiae* population dynamics. *Parasites and Vectors.* 2011;4: 1-14. doi:10.1186/1756-3305-4-153
 142. Hamilton M, Mahiane G, Werst E, Sanders R, Briët O, Smith T, et al. Spectrum-Malaria: A user-friendly projection tool for health impact assessment and strategic planning by malaria control programmes in sub-Saharan Africa. *Malar J.* 2017;16: 1-15. doi:10.1186/s12936-017-1705-3
 143. Yé Y, Louis VR, Simboro S, Sauerborn R. Effect of meteorological factors on clinical malaria risk among children: an assessment using village-based meteorological stations and community-based parasitological survey. *BMC Public Health.* 2007;7: 101. doi:10.1186/1471-2458-7-101
 144. Grosbois V, Gimenez O, Gaillard JM, Pradel R, Barbraud C, Clobert J, et al. Assessing the impact of climate variation on survival in vertebrate populations. *Biol Rev.* 2008;83: 357-399. doi:10.1111/j.1469-185X.2008.00047.x
 145. Paaijmans KP, Read AF, Thomas MB. Understanding the link between

- malaria risk and climate. *Proc Natl Acad Sci U S A*. 2009;106: 13844-9. doi:10.1073/pnas.0903423106
146. Lindsay SW, Birley MH. Climate change and malaria transmission. *Ann Trop Med Parasitol*. 1996;90: 573-88. Available: <http://www.ncbi.nlm.nih.gov/pubmed/9039269>
 147. Chalvet-Monfray K, Sabatier P, Bicout DJ. Downscaling modeling of the aggressiveness of mosquitoes vectors of diseases. 2007 [cited 17 Apr 2022]. doi:10.1016/j.ecolmodel.2007.01.024
 148. Abiodun GJ, Maharaj R, Witbooi P, Okosun KO. Modelling the influence of temperature and rainfall on the population dynamics of *Anopheles arabiensis*. *Malar J*. 2016;15: 1-15. doi:10.1186/S12936-016-1411-6/FIGURES/12
 149. Degaetano AT. Meteorological effects on adult mosquito (*Culex*) populations in metropolitan New Jersey. 2005; 345-353. doi:10.1007/s00484-004-0242-2
 150. Parham PE, Michael E. Modeling the effects of weather and climate change on malaria transmission. *Environ Health Perspect*. 2010;118: 620-626. doi:10.1289/ehp.0901256
 151. Charlwood JD. Some like it hot: A differential response to changing temperatures by the malaria vectors *Anopheles funestus* and *An. gambiae* s.l. *PeerJ*. 2017;2017. doi:10.7717/peerj.3099
 152. Brie OJT. A simple method for calculating mosquito mortality rates , correcting for seasonal variations in recruitment. 2002; 22-27.
 153. Ngowo HS, Okumu FO, Hape EE, Mshani IH, Ferguson HM, Matthiopoulos J. Using Bayesian state-space models to understand the population dynamics of the dominant malaria vector, *Anopheles funestus* in rural Tanzania. *Malar J*. 2022;21: 1-17. doi:10.1186/s12936-022-04189-4
 154. Afrane YAWA, Lawson BW, Githeko AK, Yan G. Effects of microclimatic changes caused by land use and land cover on duration of gonotrophic cycles of *Anopheles gambiae* (Diptera: Culicidae) in western Kenya highlands. *J Med Entomol*. 2005;42: 974-980. doi:10.1603/0022-2585(2005)042[0974:EOMCCB]2.0.CO;2
 155. Beck-Johnson LM, Nelson WA, Paaijmans KP, Read AF, Thomas MB, Bjørnstad ON. The effect of temperature on *Anopheles* mosquito population dynamics and the potential for malaria transmission. *PLoS One*.

- 2013;8: e79276. doi:10.1371/journal.pone.0079276
156. Paaijmans KP, Wandago MO, Githeko AK, Takken W. Unexpected high losses of *Anopheles gambiae* larvae due to rainfall. *PLoS One*. 2007;2: 1146. doi:10.1371/journal.pone.0001146
 157. Rúa GL, Quiñones ML, Vélez ID, Zuluaga JS, Rojas W, Poveda G, et al. Laboratory estimation of the effects of increasing temperatures on the duration of gonotrophic cycle of *Anopheles albimanus* (Diptera: Culicidae). *Mem Inst Oswaldo Cruz*. 2005;100: 515-520. doi:10.1590/S0074-02762005000500011
 158. Whittaker C, Winskill P, Sinka M, Pironon S, Massey C, Weiss DJ, et al. A novel statistical framework for exploring the population dynamics and seasonality of mosquito populations. 2022. doi:10.1098/rspb.2022.0089
 159. Newman KB, Buckland ST, Lindley ST, Thomas L, Fernández C. Hidden process models for animal population dynamics. *Ecol Appl*. 2006;16: 74-86. doi:10.1890/04-0592
 160. Ewing DA, Cobbold CA, Purse B V., Nunn MA, White SM. Modelling the effect of temperature on the seasonal population dynamics of temperate mosquitoes. *J Theor Biol*. 2016;400: 65-79. doi:10.1016/j.jtbi.2016.04.008
 161. Brady OJ, Godfray HCJ, Tatem AJ, Gething PW, Cohen JM, McKenzie FE, et al. Adult vector control, mosquito ecology and malaria transmission. *Int Health*. 2015;7: 121-129. doi:10.1093/inthealth/ihv010
 162. Eckhoff PA, Bever CA, Gerardin J, Wenger EA. Fun with maths: Exploring implications of mathematical models for malaria eradication. *Malar J*. 2014;13: 1-6. doi:10.1186/1475-2875-13-486/FIGURES/4
 163. Runge M, Mapua S, Nambunga I, Smith TA, Chitnis N, Okumu FO, et al. Evaluation of different deployment strategies for larviciding to control malaria: a simulation study. *Malar J*. 2021;10: 1-13. doi:10.1186/s12936-021-03854-4
 164. Thawer SG, Chacky F, Runge M, Reaves E, Mandike R, Lazaro S, et al. Sub-national stratification of malaria risk in mainland Tanzania: A simplified assembly of survey and routine data. *Malar J*. 2020;19: 177. doi:10.1186/s12936-020-03250-4
 165. Runge M, Thawer SG, Molteni F, Chacky F, Mkude S, Mandike R, et al. Sub-national tailoring of malaria interventions in Mainland Tanzania: simulation of the impact of strata-specific intervention combinations using modelling.

- Malar J. 2022;21: 1-17. doi:10.1186/s12936-022-04099-5
166. Selvaraj P, Wenger EA, Gerardin J. Seasonality and heterogeneity of malaria transmission determine success of interventions in high-endemic settings: A modeling study. *BMC Infect Dis.* 2018;18: 1-14. doi:10.1186/s12879-018-3319-y
 167. Altizer S, Dobson A, Hosseini P, Hudson P, Pascual M, Rohani P. Seasonality and the dynamics of infectious diseases. *Ecol Lett.* 2006;9: 467-484. doi:10.1111/j.1461-0248.2005.00879.x
 168. Le Sueur D, Sharp BL, Sueur D le. The breeding requirements of three members of the *Anopheles gambiae* Giles complex (Diptera: Culicidae) in the endemic malaria area of Natal, South Africa. *Bull Entomol Res.* 1988;78: 549-560.
 169. Killeen GF, Chitnis N. Potential causes and consequences of behavioural resilience and resistance in malaria vector populations: a mathematical modelling analysis. *Malar J.* 2014;13: 97. doi:10.1186/1475-2875-13-97
 170. Service MW, Oguamah D. Colonization of anopheles funestus [43]. *Nature.* Nature Publishing Group; 1958. p. 1225. doi:10.1038/1811225b0
 171. Killeen GF, Smith TA. Exploring the contributions of bed nets, cattle, insecticides and excitorepellency to malaria control: a deterministic model of mosquito host-seeking behaviour and mortality. *Trans R Soc Trop Med Hyg.* 2007;101: 867-880. doi:10.1016/j.trstmh.2007.04.022
 172. Mishra S, Fisman DN, Boily MC. The ABC of terms used in mathematical models of infectious diseases. *J Epidemiol Community Heal.* 2011;65: 87-94. doi:10.1136/JECH.2009.097113
 173. Killeen GF, Fillinger U, Knols BG. Advantages of larval control for African malaria vectors: Low mobility and behavioural responsiveness of immature mosquito stages allow high effective coverage. *Malar J* 2002 11. 2002;1: 1-7. doi:10.1186/1475-2875-1-8
 174. Matthews J, Bethel A, Osei G. An overview of malarial Anopheles mosquito survival estimates in relation to methodology. *Parasites and Vectors.* 2020;13: 1-12. doi:10.1186/s13071-020-04092-4
 175. Millar R. Bayesian state-space modeling of age-structured data: fitting a model is just the beginning. *Can J Fish Aquat Sci.* 2000;50: 43-50.
 176. Viana M, Hughes A, Matthiopoulos J, Ranson H, Ferguson HM. Delayed mortality effects cut the malaria transmission potential of insecticide-

- resistant mosquitoes. *Proc Natl Acad Sci U S A*. 2016;113: 8975-8980. doi:10.1073/pnas.1603431113
177. Harrison PJ, Hanski I, Ovaskainen O. Bayesian state-space modeling of metapopulation dynamics in the Glanville fritillary butterfly. *Ecol Monogr*. 2011;81: 581-598. doi:10.1890/11-0192.1
 178. Flesch AD. Spatiotemporal trends and drivers of population dynamics in a declining Sonoran Desert predator. *Biol Conserv*. 2014;175: 110-118. doi:10.1016/j.biocon.2014.04.021
 179. Rivot E, Prévost E, Parent E, Baglinière JL. A Bayesian state-space modelling framework for fitting a salmon stage-structured population dynamic model to multiple time series of field data. *Ecol Modell*. 2004;179: 463-485. doi:10.1016/j.ecolmodel.2004.05.011
 180. Viana M, Cleaveland S, Matthiopoulos J, Halliday J, Packer C, Craft ME, et al. Dynamics of a morbillivirus at the domestic-wildlife interface: Canine distemper virus in domestic dogs and lions. *Proc Natl Acad Sci*. 2015;112: 1464-1469. doi:10.1073/pnas.1411623112
 181. Ogoma SB, Ngonyani H, Simfukwe ET, Mseka A, Moore J, Killeen GF. Spatial repellency of transfluthrin-treated hessian strips against laboratory-reared *Anopheles arabiensis* mosquitoes in a semi-field tunnel cage. *Parasites and Vectors*. 2012;5. doi:10.1186/1756-3305-5-54
 182. Russell TL, Beebe NW, Cooper RD, Lobo NF, Burkot TR. Successful malaria elimination strategies require interventions that target changing vector behaviours. *Malar J*. 2013;12: 56. doi:10.1186/1475-2875-12-56
 183. Pluess B, Fc T, Lengeler C, Bl S. Indoor residual spraying for preventing malaria (Review). 2010. doi:10.1002/14651858.CD006657.pub2.www.cochranelibrary.com
 184. Okumu FO, Govella NJ, Moore SJ, Chitnis N, Killeen GF. Potential benefits, limitations and target product-profiles of odor-baited mosquito traps for malaria control in Africa. *PLoS One*. 2010;5. doi:10.1371/journal.pone.0011573
 185. Killeen GF, Seyoum A, Sikaala C, Zomboko AS, Gimnig JE, Govella NJ, et al. Eliminating malaria vectors. *Parasit Vectors*. 2013;6: 172. doi:10.1186/1756-3305-6-172
 186. Tusting LS, Ippolito MM, Willey B a, Kleinschmidt I, Dorsey G, Gosling RD, et al. The evidence for improving housing to reduce malaria: a systematic

- review and meta-analysis. *Malar J.* 2015;14: 209. doi:10.1186/s12936-015-0724-1
187. Lwetoijera D, Harris C, Kiware S, Dongus S, Devine GJ, McCall PJ, et al. Effective autodissemination of pyriproxyfen to breeding sites by the exophilic malaria vector *Anopheles arabiensis* in semi-field settings in Tanzania. *Malar J.* 2014;13: 1-10. doi:10.1186/1475-2875-13-161
188. Carvalho DO, Nimmo D, Naish N, McKemey AR, Gray P, Wilke ABB, et al. Mass production of genetically modified *Aedes aegypti* for field releases in Brazil. *J Vis Exp.* 2014. doi:10.3791/3579
189. Fiorenzano JM, Koehler PG, Xue R De. Attractive Toxic Sugar Bait (ATSB) For Control of Mosquitoes and Its Impact on Non-Target Organisms: A Review. *Int J Environ Res Public Heal* 2017, Vol 14, Page 398. 2017;14: 398. doi:10.3390/IJERPH14040398
190. Killeen GF, Tami a, Kihonda J, Okumu FO, Kotas ME, Grundmann H, et al. Cost-sharing strategies combining targeted public subsidies with private-sector delivery achieve high bednet coverage and reduced malaria transmission in Kilombero Valley, southern Tanzania. *BMC Infect Dis.* 2007;7: 121. doi:10.1186/1471-2334-7-121
191. Lalji S, Ngondi JM, Thawer NG, Tembo A, Mandike R, Mohamed A, et al. School Distribution as Keep-Up Strategy to Maintain Universal Coverage of Long-Lasting Insecticidal Nets: Implementation and Results of a Program in Southern Tanzania. [cited 18 Apr 2022]. Available: www.ghspjournal.org
192. Renggli S, Mandike R, Kramer K, Patrick F, Brown NJ, McElroy PD, et al. Design, implementation and evaluation of a national campaign to deliver 18 million free long-lasting insecticidal nets to uncovered sleeping spaces in Tanzania. *Malar J.* 2013;12: 85. doi:10.1186/1475-2875-12-85
193. Massue DJ, Moore SJ, Mageni ZD, Moore JD, Bradley J, Pigeon O, et al. Durability of Olyset campaign nets distributed between 2009 and 2011 in eight districts of Tanzania. *Malar J.* 2016;15: 176. doi:10.1186/s12936-016-1225-6
194. Lorenz LM, Overgaard HJ, Massue DJ, Mageni ZD, Bradley J, Moore JD, et al. Investigating mosquito net durability for malaria control in Tanzania- attrition, bioefficacy, chemistry, degradation and insecticide resistance (ABC DR): study protocol. 2014 [cited 18 Apr 2022]. doi:10.1186/1471-2458-14-1266

195. Msugupakulya BJ, Kaindoa EW, Ngowo HS, Kihonda JM, Kahamba NF, Msaky DS, et al. Preferred resting surfaces of dominant malaria vectors inside different house types in rural south - eastern Tanzania. *Malar J.* 2020; 1-15. doi:10.1186/s12936-020-3108-0
196. Who. Guidelines for Efficacy Testing of Insecticides for Indoor and Outdoor Ground-Applied Space Spray Applications. World Heal Organ. 2009;2: 1-61. Available: <http://www.who.int/iris/handle/10665/70070>
197. Tanser FC, Pluess B, Lengeler C, Sharp BL. Indoor residual spraying for preventing malaria. *Cochrane Database of Systematic Reviews.* 2007. doi:10.1002/14651858.CD006657
198. Killeen GF, Chitnis N, Moore SJ, Okumu FO. Target product profile choices for intra-domiciliary malaria vector control pesticide products: Repel or kill? *Malar J.* 2011;10. doi:10.1186/1475-2875-10-207
199. Okumu FO, Kiware SS, Moore SJ, Killeen GF. Mathematical evaluation of community level impact of combining bed nets and indoor residual spraying upon malaria transmission in areas where the main vectors are *Anopheles arabiensis* mosquitoes. *Parasites & Vectors.* 16 Jan 2013: 17. doi:10.1186/1756-3305-6-17
200. Fillinger U, Lindsay SW. Larval source management for malaria control in Africa: Myths and reality. *Malar J.* 2011;10: 1-10. doi:10.1186/1475-2875-10-353/TABLES/1
201. Tusting LS, Thwing J, Sinclair D, Fillinger U, Gimnig J, Bonner KE, et al. Mosquito larval source management for controlling malaria. *Cochrane Database of Systematic Reviews.* John Wiley and Sons Ltd; 2013. doi:10.1002/14651858.CD008923.pub2
202. WHO (World Health Organization). Test procedures for insecticide resistance monitoring in malaria vector mosquitoes. *World Heal Organ Tech Rep Ser.* 2013; 22. doi:10.1007/978-3-642-10565-4
203. Tusting LS. Larval source management: A supplementary measure for malaria control. *Outlooks Pest Manag.* 2014;25: 41-43. doi:10.1564/v25_feb_13
204. Riveron JM, Chiumia M, Menze BD, Barnes KG, Irving H, Ibrahim SS, et al. Rise of multiple insecticide resistance in *Anopheles funestus* in Malawi: A major concern for malaria vector control. *Malar J.* 2015. doi:10.1186/s12936-015-0877-y

205. Stevenson JC, Pinchoff J, Muleba M, Lupiya J, Chilusu H, Mwelwa I, et al. Spatio-temporal heterogeneity of malaria vectors in northern Zambia: Implications for vector control. *Parasites and Vectors*. 2016. doi:10.1186/s13071-016-1786-9
206. Rumisha SF red, Smith T, Abdulla S, Masanja H, Vounatsou P. Modelling heterogeneity in malaria transmission using large sparse spatio-temporal entomological data. *Glob Health Action*. 2014;7: 22682. doi:10.3402/gha.v7.22682
207. Hunt RH, Edwardes M, Coetzee M. Pyrethroid resistance in southern African *Anopheles funestus* extends to Likoma Island in Lake Malawi. *Parasites and Vectors*. 2010;3. doi:10.1186/1756-3305-3-122
208. Choi KS, Christian R, Nardini L, Wood OR, Agubuzo E, Muleba M, et al. Insecticide resistance and role in malaria transmission of *Anopheles funestus* populations from Zambia and Zimbabwe. *Parasit Vectors*. 2014;7: 464. doi:10.1186/s13071-014-0464-z
209. Matowo NS, Munhenga G, Tanner M, Coetzee M, Feringa WF, Ngowo HS, et al. Fine-scale spatial and temporal heterogeneities in insecticide resistance profiles of the malaria vector, *Anopheles arabiensis* in rural south-eastern Tanzania. *Wellcome Open Res*. 2017;2: 96. doi:10.12688/wellcomeopenres.12617.1
210. Menze BD, Riveron JM, Ibrahim SS, Irving H, Antonio-Nkondjio C, Awono-Ambene PH, et al. Multiple insecticide resistance in the malaria vector *Anopheles funestus* from Northern Cameroon is mediated by metabolic resistance alongside potential target site insensitivity mutations. *PLoS One*. 2016;11. doi:10.1371/journal.pone.0163261
211. Kawada H, Dida GO, Ohashi K, Komagata O, Kasai S, Tomita T, et al. Multimodal pyrethroid resistance in malaria vectors, *anopheles gambiae* s.s., *anopheles arabiensis*, and *anopheles funestus* s.s. in western Kenya. *PLoS One*. 2011;6. doi:10.1371/journal.pone.0022574
212. Sanou A, Nelli L, Guelbéogo WM, Cissé F, Tapsoba M, Ouédraogo P, et al. Insecticide resistance and behavioural adaptation as a response to long-lasting insecticidal net deployment in malaria vectors in the Cascades region of Burkina Faso. *Sci Rep*. 2021;11: 1-14. doi:10.1038/s41598-021-96759-w
213. Matowo NS, Abbasi S, Munhenga G, Tanner M, Mapua SA, Oullo D, et al.

- Fine-scale spatial and temporal variations in insecticide resistance in *Culex pipiens* complex mosquitoes in rural south-eastern Tanzania. *Parasit Vectors*. 2019. doi:10.1186/s13071-019-3676-4
214. Wondji CS, Coleman M, Kleinschmidt I, Mzilahowa T, Irving H, Ndula M, et al. Impact of pyrethroid resistance on operational malaria control in Malawi. *Proc Natl Acad Sci*. 2012;109: 19063-19070. doi:10.1073/pnas.1217229109
 215. Griffin JT, Bhatt S, Sinka ME, Gething PW, Lynch M, Patouillard E, et al. Potential for reduction of burden and local elimination of malaria by reducing *Plasmodium falciparum* malaria transmission: A mathematical modelling study. *Lancet Infect Dis*. 2016;16: 465-472. doi:10.1016/S1473-3099(15)00423-5
 216. NBS NB of S. Tanzania 2007-08 HIV/AIDS and Malaria Indicator Survey Key Findings. Tanzania 2007-08 HIV/AIDS Malar Indic Surv Key Find. 2008; 16.
 217. TMIS. Tanzania Malaria Indicator Survey Key indicators 2017. *Decis Support Syst*. 2017. doi:10.1016/j.dss.2003.08.004
 218. Russell TL, Lwetoijera DW, Maliti D, Chipwaza B, Kihonda J, Charlwood JD, et al. Impact of promoting longer-lasting insecticide treatment of bed nets upon malaria transmission in a rural Tanzanian setting with pre-existing high coverage of untreated nets. *Malar J*. 2010;9: 187. doi:10.1186/1475-2875-9-187
 219. Schellenberg JR, Abdulla S, Nathan R, Mukasa O, Marchant TJ, Kikumbih N, et al. Effect of large-scale social marketing of insecticide-treated nets on child survival in rural Tanzania. *Lancet*. 2001;357: 1241-7. doi:10.1016/S0140-6736(00)04404-4
 220. Martin JL, Mosha FW, Lukole E, Rowland M, Todd J, Charlwood JD, et al. Personal protection with PBO-pyrethroid synergist-treated nets after 2 years of household use against pyrethroid-resistant *Anopheles* in Tanzania. *Parasites and Vectors*. 2021;14: 1-8. doi:10.1186/s13071-021-04641-5
 221. Pinda PG, Eichenberger C, Ngowo HS, Msaky DS, Abbasi S, Kihonda J, et al. Comparative assessment of insecticide resistance phenotypes in two major malaria vectors, *Anopheles funestus* and *Anopheles arabiensis* in south-eastern Tanzania. *Malar J*. 2020;19: 1-11. doi:10.1186/s12936-020-03483-3
 222. Okoye PN, Brooke BD, Hunt RH, Coetzee M. Relative developmental and reproductive fitness associated with pyrethroid resistance in the major

- southern African malaria vector, *Anopheles funestus*. *Bull Entomol Res.* 2007;97: 599-605. doi:10.1017/S0007485307005317
223. Charlwood JD, Vij R, Billingsley PF. Dry season refugia of malaria-transmitting mosquitoes in a dry savannah zone of east Africa. *Am J Trop Med Hyg.* 2000;62: 726-732.
224. Ngowo HS, Limwagu AJ, Ferguson HM, Matthiopoulos J, Okumu FO. A statistical calibration tool for methods used to sample outdoor-biting mosquitoes. 2022 [cited 15 May 2022]. doi:10.21203/RS.3.RS-1494460/V1
225. Ferguson HM, Ng'habi KR, Walder T, Kadungula D, Moore SJ, Lyimo I, et al. Establishment of a large semi-field system for experimental study of African malaria vector ecology and control in Tanzania. *Malar J.* 2008;7: 158. doi:10.1186/1475-2875-7-158
226. Minakawa N, Githure JI, Beier JC, Yan G. Anopheline mosquito survival strategies during the dry period in western Kenya. *J Med Entomol.* 2001;38: 388-392. doi:10.1603/0022-2585-38.3.388
227. Ranson H, Abdallah H, Badolo A, Guelbeogo W, Kera-Hinzoumbé C, Yangalbé-Kalnoné E, et al. Insecticide resistance in *Anopheles gambiae*: data from the first year of a multi-country study highlight the extent of the problem. *Malar J.* 2009;8: 299. doi:10.1186/1475-2875-8-299
228. Williams J, Flood L, Praulins G, Ingham VA, Morgan J, Lees RS, et al. Characterisation of *Anopheles* strains used for laboratory screening of new vector control products. *Parasit Vectors.* 2019; 1-14. doi:10.1186/s13071-019-3774-3
229. Tripet F, Touré YT, Taylor CE, Norris DE, Dolo G, Lanzaro GC. DNA analysis of transferred sperm reveals significant levels of gene flow between molecular forms of *Anopheles gambiae*. *Mol Ecol.* 2001;10: 1725-1732. doi:10.1046/j.0962-1083.2001.01301.x
230. Kyrou K, Hammond AM, Galizi R, Kranjc N, Burt A, Beaghton AK, et al. A CRISPR-Cas9 gene drive targeting doublesex causes complete population suppression in caged *Anopheles gambiae* mosquitoes. *Nat Biotechnol.* 2018;36: 1062-1071. doi:10.1038/nbt.4245
231. Christophides GK, Zdobnov E, Barillas-Mury C, Birney E, Blandin S, Blass C, et al. Immunity-related genes and gene families in *Anopheles gambiae*. *Science (80-).* 2002;298: 159-165. doi:10.1126/science.1077136
232. Waterhouse RM, Kriventseva E V., Meister S, Xi Z, Alvarez KS, Bartholomay

- LC, et al. Evolutionary dynamics of immune-related genes and pathways in disease-vector mosquitoes. *Science* (80-). 2007;316: 1738-1743. doi:10.1126/science.1139862
233. Maia MF, Kreppel K, Mbeyela E, Roman D, Mayagaya V, Lobo NF, et al. A crossover study to evaluate the diversion of malaria vectors in a community with incomplete coverage of spatial repellents in the Kilombero Valley , Tanzania. *Parasit Vectors*. 2016; 1-13. doi:10.1186/s13071-016-1738-4
234. Kawada H, Dida GO, Sonye G, Njenga SM, Mwandawiro C, Minakawa N. Reconsideration of *Anopheles rivulorum* as a vector of *Plasmodium falciparum* in western Kenya: some evidence from biting time, blood preference, sporozoite positive rate, and pyrethroid resistance. *Parasit Vectors*. 2012;5: 230. doi:10.1186/1756-3305-5-230
235. Wilkes TJ, Matola YG, Charlwood JD. *Anopheles rivulorum*, a vector of human malaria in Africa. *Med Vet Entomol*. 1996;10: 108-110. doi:10.1111/j.1365-2915.1996.tb00092.x
236. Burke A, Dandalo L, Munhenga G, Dahan-Moss Y, Mbokazi F, Ngxongo S, et al. A new malaria vector mosquito in South Africa. *Sci Rep*. 2017;7: 1-5. doi:10.1038/srep43779
237. Nepomichene TN, Andrianaivolambo L, Boyer S, Bourguin C. Efficient method for establishing F1 progeny from wild populations of *Anopheles* mosquitoes. *Malar J*. 2017; 1-8. doi:10.1186/s12936-017-1681-7
238. Lardeux F, Quispe V, Tejerina R, Rodríguez R. (*Diptera* : *Culicidae*) without forced mating. 2007;330: 571-575. doi:10.1016/j.crv.2007.04.002
239. Sallum MAM, Peyton EL, Wilkerson RC. Six new species of the *Anopheles leucosphyrus* group, reinterpretation of *An. elegans* and vector implications. *Med Vet Entomol*. 2005;19: 158-199. doi:10.1111/j.0269-283X.2005.00551.x
240. Phasomkusolsil S, Wongnet O, Pantuwatana K, Tawong J, Monkanna N, Kornkan T, et al. Comparison of *Anopheles cracens* (Stenogamous) and *Anopheles dirus* (Eurygamous) blood-feeding behaviors, survival rates and fecundity after first and second blood meals. *Int J Mosq Res*. 2019;6: 14-21.
241. Kaindoa EW, Ngowo HS, Limwagu A, Mkandawile G, Kihonda J, Masalu JP, et al. New evidence of mating swarms of the malaria vector, *Anopheles*

- arabiensis in Tanzania. Wellcome Open Res. 2017;2: 88. doi:10.12688/wellcomeopenres.12458.1
242. Odetoyinbo JA. Preliminary investigation on the use of a light-trap for sampling malaria vectors in the Gambia. Bull World Health Organ. 1969;40: 547-560.
 243. Koekemoer LL, Kamau L, Hunt RH, Coetzee M. A cocktail polymerase chain reaction assay to identify members of the *Anopheles funestus* (Diptera: Culicidae) group. Am J Trop Med Hyg. 2002;66: 804-811.
 244. Moorefield HH. Sexual dimorphism in mosquito pupae. British Mosquito Bulletin. 1951. p. 14.
 245. Nasci RS. Relationship of Wing Length to Adult Dry Weight in Several Mosquito Species (Diptera : Culicidae). 1990; 716-719.
 246. R Development Core Team. R: A language and environment for statistical computing. R Foundation for Statistical Computing. 2021. doi:10.1017/CBO9781107415324.004
 247. Lyimo EO, Takken W. Effects of adult body size on fecundity and the pre-gravid rate of *Anopheles gambiae* females in Tanzania. Med Vet Entomol. 1993;7: 328-332. doi:10.1111/j.1365-2915.1993.tb00700.x
 248. Armbruster P, Hutchinson RA. Pupal mass and wing length as indicators of fecundity in *aedes albopictus* and *aedes geniculatus* (diptera: Culicidae). J Med Entomol. 2002;39: 699-704. doi:10.1603/0022-2585-39.4.699
 249. Bates D, Maechler M, Bolker B, Walker S. lme4: linear mixed-effects models using S4 classes. R package version 1.1-6. R. 2014. doi:http://CRAN.R-project.org/package=lme4
 250. Lumley T, S- R, Elizabeth A, Cynthia C. Package “ survival ” for Survival Analysis. 2020.
 251. Hougaard P. Frailty models for survival data. Lifetime Data Anal. 1995;1: 255-273. doi:10.1007/BF00985760
 252. Balan TA, Putter H. A tutorial on frailty models. Statistical Methods in Medical Research. SAGE Publications Ltd; 2020. pp. 3424-3454. doi:10.1177/0962280220921889
 253. Wickham H. R Graphics Cookbook. Media. 2009;35: 211. doi:10.1007/978-0-387-98141-3
 254. Kassambara A, Kosinski M, Biecek P. Package survminer Type Package Title Drawing Survival Curves using “ggplot2.” MranMicrosoftCom. 2017.

255. Tchigossou GM, Akoton R, Yessoufou A, Djegbe I, Zeukeng F, Atoyebi SM, et al. Water source most suitable for rearing a sensitive malaria vector, *Anopheles funestus* in the laboratory. *Wellcome Open Res.* 2018;2: 109. doi:10.12688/wellcomeopenres.12942.2
256. Thailayil J, Magnusson K, Godfray HCJ, Crisanti A, Catteruccia F. Spermless males elicit large-scale female responses to mating in the malaria mosquito *Anopheles gambiae*. *Proc Natl Acad Sci U S A.* 2011;108: 13677-13681. doi:10.1073/pnas.1104738108
257. Impoinvil DE, Cardenas GA, Gihture JI, Mbogo CM, Beier JC. Constant temperature and time period effects on *Anopheles gambiae* egg hatching. *J Am Mosq Control Assoc.* 2007. doi:10.2987/8756-971X(2007)23[124:CTATPE]2.0.CO;2
258. Tchouakui M, Riveron JM, Djonabaye D, Tchapga W, Irving H, Takam PS, et al. Fitness costs of the glutathione S-transferase epsilon 2 (L119F-GSTe2) mediated metabolic resistance to insecticides in the major African malaria vector *Anopheles funestus*. *Genes (Basel).* 2018;9. doi:10.3390/genes9120645
259. Schneider P, Takken W, McCall PJ. Interspecific competition between sibling species larvae of *Anopheles arabiensis* and *An. gambiae*. *Med Vet Entomol.* 2000;14: 165-170. doi:10.1046/j.1365-2915.2000.00204.x
260. Awono-Ambéné H P, Robert V. survival and emergence of immature *Anopheles arabiensis* mosquitoes in market-gardener wells in Dakar, Senegal. *Parasite.* 1999;6: 179-184. doi:10.1051/parasite/1999062179
261. Ng'habi KRN, Mwasheshi D, Knols BGJ, Ferguson HM. Establishment of a self-propagating population of the African malaria vector *Anopheles arabiensis* under semi-field conditions. *Malar J.* 2010;9: 356. doi:10.1186/1475-2875-9-356
262. Clements AN. The biology of mosquitoes. *The Biology of Mosquitoes.* 2011. doi:10.1007/978-3-540-92874-4
263. Takken W, Klowden MJ, Chambers GM. Effect of body size on host seeking and blood meal utilization in *Anopheles gambiae* sensu stricto (Diptera: Culicidae): the disadvantage of being small. *J Med Entomol.* 1998;35: 639-645. doi:10.1093/jmedent/35.5.639
264. Huho BJ, Ng'habi KR, Killeen GF, Nkwengulila G, Knols BGJ, Ferguson HM. Nature beats nurture: A case study of the physiological fitness of free-

- living and laboratory-reared male *Anopheles gambiae* s.l. *J Exp Biol.* 2007;210: 2939-2947. doi:10.1242/jeb.005033
265. Charlwood JDJD, Thompson R, Madsen H. Observations on the swarming and mating behaviour of *Anopheles funestus* from southern Mozambique. *Malar J.* 2003;2.
266. Charlwood JD. Studies on the bionomics of male *Anopheles gambiae* Giles and male *Anopheles funestus* Giles from southern Mozambique. *J Vector Ecol.* 2011;36: 382-394. doi:10.1111/j.1948-7134.2011.00179.x
267. Ferguson HM, John B, Ng'habi K, Knols BGJ. Redressing the sex imbalance in knowledge of vector biology. *Trends in Ecology and Evolution.* 2005. pp. 202-209. doi:10.1016/j.tree.2005.02.003
268. Baker RH. Mating problems as related to the establishment and maintenance of laboratory colonies of mosquitos. *Bull World Health Organ.* 1964;31: 467.
269. Bryan JH, Southgate BA. Studies of forced mating techniques on anopheline mosquitoes. *Mosquito News.* 1978. pp. 871-876.
270. Villarreal C, Arredondo-Jimenez J, Rodrigueze MH, Ulloa A. Colonization of *Anopheles pseudopunctipennis* from Mexico. 1998;14: 369-372.
271. Baerg DC. Colonization of *Anopheles pseudopunctipennis* in Panama. *J Med Entomol.* 1971;8: 180-182. doi:10.1093/jmedent/8.2.180
272. Strategy GT. Achieving and maintaining universal coverage with long-lasting insecticidal nets for malaria control. 2017.
273. Hemingway J, Hawkes NJ, McCarroll L, Ranson H. The molecular basis of insecticide resistance in mosquitoes. *Insect Biochem Mol Biol.* 2004;34: 653-665. doi:10.1016/j.ibmb.2004.03.018
274. Monroe A, Mihayo K, Okumu F, Finda M, Moore S, Koenker H, et al. Human behaviour and residual malaria transmission in Zanzibar: Findings from in-depth interviews and direct observation of community events. *Malar J.* 2019;18: 220. doi:10.1186/s12936-019-2855-2
275. Finda MF, Moshi IR, Monroe A, Limwagu AJ, Nyoni AP, Swai JK, et al. Linking human behaviours and malaria vector biting risk in south-eastern Tanzania. Carvalho LH, editor. *PLoS One.* 2019;14: e0217414. doi:10.1371/journal.pone.0217414
276. Monroe A, Asamoah O, Lam Y, Koenker H, Psychas P, Lynch M, et al. Outdoor-sleeping and other night-time activities in northern Ghana:

- implications for residual transmission and malaria prevention. *Malar J.* 2015;14: 35. doi:10.1186/s12936-015-0543-4
277. Ogoma SB, Ngonyani H, Simfukwe ET, Mseka A, Moore J, Maia MF, et al. The Mode of Action of Spatial Repellents and Their Impact on Vectorial Capacity of *Anopheles gambiae sensu stricto*. *PLoS One.* 2014;9: e110433. doi:10.1371/journal.pone.0110433
 278. Health Organization W. *Malaria surveillance, Monitoring & Evaluation: A Reference Manual.*
 279. Killeen GF, McKenzie FE, Foy BD, Schieffelin C, Billingsley PF, Beier JC. A simplified model for predicting malaria entomologic inoculation rates based on entomologic and parasitologic parameters relevant to control. *Am J Trop Med Hyg.* 2000;62: 535-544.
 280. Tusting LS, Bousema T, Smith DL, Drakeley C. *Measuring changes in plasmodium falciparum transmission. Precision, accuracy and costs of metrics.* 1st ed. *Advances in Parasitology.* Elsevier Ltd.; 2014. doi:10.1016/B978-0-12-800099-1.00003-X
 281. Charlwood JD, Smith T, Billingsley PF, Takken W, Lyimo EOK, Meuwissen JHET. Survival and infection probabilities of anthropophagic anophelines from an area of high prevalence of *Plasmodium falciparum* in humans. *Bull Entomol Res.* 1997;87: 445. doi:10.1017/S0007485300041304
 282. Govella NJ, Maliti DF, Mlwale AT, Masallu JP, Mirzai N, Johnson PCD, et al. An improved mosquito electrocuting trap that safely reproduces epidemiologically relevant metrics of mosquito human-feeding behaviours as determined by human landing catch. *Malar J.* 2016;15: 465. doi:10.1186/s12936-016-1513-1
 283. Service MW. A critical review of procedures for sampling populations of adult mosquitoes. *Bull Entomol Res.* 1977;67: 343-382. doi:10.1017/S0007485300011184
 284. Knols BGJ, de Jong R, Takken W. Differential attractiveness of isolated humans to mosquitoes in Tanzania. *Trans R Soc Trop Med Hyg.* 1995;89: 604-606. doi:10.1016/0035-9203(95)90406-9
 285. Lindsay SW, Adiamah JH, Miller JE, Pleass RJ, Armstrong JR. Variation in attractiveness of human subjects to malaria mosquitoes (Diptera: Culicidae) in The Gambia. *J Med Entomol.* 1993;30: 368-373. doi:10.1093/jmedent/30.2.368

286. Meza FC, Kreppel KS, Maliti DF, Mwale AT, Mirzai N, Killeen GF, et al. Mosquito electrocuting traps for directly measuring biting rates and host-preferences of *Anopheles arabiensis* and *Anopheles funestus* outdoors. *Malar J.* 2019;18: 1-11. doi:10.1186/S12936-019-2726-X/FIGURES/4
287. Limwagu AJ, Kaindoa EW, Ngowo HS, Hape E, Finda M, Mkandawile G, et al. Using a miniaturized double-net trap (DN-Mini) to assess relationships between indoor-outdoor biting preferences and physiological ages of two malaria vectors, *Anopheles arabiensis* and *Anopheles funestus*. *Malar J.* 2019;18: 282. doi:10.1186/s12936-019-2913-9
288. Sanou A, Guelbéogo WM, Nelli L, Toé KH, Zongo S, Ouédraogo P, et al. Evaluation of mosquito electrocuting traps as a safe alternative to the human landing catch for measuring human exposure to malaria vectors in Burkina Faso. *Malar J.* 2019;18: 1-17. doi:10.1186/S12936-019-3030-5/FIGURES/8
289. Matowo NS, Moore J, Mapua S, Madumla EP, Moshi IR, Kaindoa EW, et al. Using a new odour-baited device to explore options for luring and killing outdoor-biting malaria vectors: a report on design and field evaluation of the Mosquito Landing Box. *Parasit Vectors.* 2013;6: 137. doi:10.1186/1756-3305-6-137
290. Mwanga EP, Ngowo HS, Mapua SA, Mmbando AS, Kaindoa EW, Kifungo K, et al. Evaluation of an ultraviolet LED trap for catching *Anopheles* and *Culex* mosquitoes in south-eastern Tanzania. *Parasites and Vectors.* 2019. doi:10.1186/s13071-019-3673-7
291. Govella NJ, Chaki PP, Geissbuhler Y, Kannady K, Okumu F, Charlwood JD, et al. A new tent trap for sampling exophagic and endophagic members of the *Anopheles gambiae* complex. *Malar J.* 2009;8: 157. doi:10.1186/1475-2875-8-157
292. Hawkes FM, Dabiré RK, Sawadogo SP, Torr SJ, Gibson G. Exploiting *Anopheles* responses to thermal, odour and visual stimuli to improve surveillance and control of malaria. *Sci Rep.* 2017;7: 17283. doi:10.1038/s41598-017-17632-3
293. Govella NJ, Chaki PP, Mpangile JM, Killeen GF. Monitoring mosquitoes in urban Dar es Salaam: evaluation of resting boxes, window exit traps, CDC light traps, Ifakara tent traps and human landing catches. *Parasit Vectors.* 2011;4: 40. doi:10.1186/1756-3305-4-40

294. Mathenge EM, Omweri GO, Irungu LW, Ndegwa PN, Walczak E, Smith T a., et al. Comparative field evaluation of the Mbita trap, the Centers for Disease Control light trap, and the human landing catch for sampling of malaria vectors in western Kenya. *Am J Trop Med Hyg.* 2004;70: 33-37.
295. Kaindoa EW, Mkandawile G, Ligamba G, Kelly-Hope LA, Okumu FO. Correlations between household occupancy and malaria vector biting risk in rural Tanzanian villages: implications for high-resolution spatial targeting of control interventions. *Malar J.* 2016;15: 199. doi:10.1186/s12936-016-1268-8
296. Sumaye RD, Geubbels E, Mbeyela E, Berkvens D. Inter-epidemic Transmission of Rift Valley Fever in Livestock in the Kilombero River Valley, Tanzania: A Cross-Sectional Survey. Bird B, editor. *PLoS Negl Trop Dis.* 2013;7: e2356. doi:10.1371/journal.pntd.0002356
297. Qiu YT, Smallegange RC, Braak CJF ter, Spitzen J, Van Loon JJA, Jawara M, et al. Attractiveness of MM-X Traps Baited with Human or Synthetic Odor to Mosquitoes (Diptera: Culicidae) in The Gambia. *J Med Entomol.* 2007. doi:10.1093/jmedent/44.6.970
298. Batista EPA, Ngowo HS, Opiyo M, Shubis GK, Meza FC, Okumu FO, et al. Semi-field assessment of the BG-Malaria trap for monitoring the African malaria vector, *Anopheles arabiensis*. *PLoS One.* 2017;12: 1-17. doi:10.1371/journal.pone.0186696
299. Mwangungulu SP, Sumaye RD, Limwagu AJ, Siria DJ, Kaindoa EW, Okumu FO. Crowdsourcing vector surveillance: Using community knowledge and experiences to predict densities and distribution of outdoor-biting mosquitoes in rural Tanzania. *PLoS One.* 2016;11. doi:10.1371/journal.pone.0156388
300. Greene W. Functional forms for the negative binomial model for count data. *Econ Lett.* 2008;99: 585-590. doi:10.1016/j.econlet.2007.10.015
301. Plummer M. JAGS : A Program for Analysis of Bayesian Graphical Models Using Gibbs Sampling JAGS : Just Another Gibbs Sampler. 2003.
302. Denwood MJ. runjags : An R Package Providing Interface Utilities, Model Templates, Parallel Computing Methods and Additional Distributions for MCMC Models in JAGS . *J Stat Softw.* 2016. doi:10.18637/jss.v071.i09
303. Winston Chang, Joe Cheng, JJ Allaire YX and JM. shiny: Web Application Framework for R. R package version 1.3.2. 2019.

304. Davis JR, Hall T, Chee E, Majala A, Minjas J, Shiff CJ. Comparison of sampling anopheline mosquitoes by light-trap and human-bait collections indoors at Bagamoyo, Tanzania. *Med Vet Entomol.* 1995;9: 249-255. doi:10.1111/j.1365-2915.1995.tb00130.x
305. Braack LE, Coetzee M, Hunt RH, Biggs H, Cornel A, Gericke A. Biting pattern and host-seeking behavior of *Anopheles arabiensis* (Diptera: Culicidae) in northeastern South Africa. *J Med Entomol.* 1994;31: 333-339. doi:10.1093/jmedent/31.3.333
306. Garrett-Jones C, Shidrawi GR. Malaria vectorial capacity of a population of *Anopheles gambiae*: an exercise in epidemiological entomology. *Bull World Health Organ.* 1969;40: 531-545.
307. McCann RS, Ochomo E, Bayoh MN, Vulule JM, Hamel MJ, Gimnig JE, et al. Reemergence of *Anopheles funestus* as a vector of *Plasmodium falciparum* in Western Kenya after long-term implementation of insecticide-treated bed nets. *Am J Trop Med Hyg.* 2014. doi:10.4269/ajtmh.13-0614
308. Fillinger U, Kannady K, William G, Vanek MJ, Dongus S, Nyika D, et al. A tool box for operational mosquito larval control: Preliminary results and early lessons from the Urban Malaria Control Programme in Dar es Salaam, Tanzania. *Malar J.* 2008;7: 1-25. doi:10.1186/1475-2875-7-20
309. Minakawa N, Sonye G, Mogi M, Yan G, Communication S. Habitat characteristics of *Anopheles gambiae* s . s . larvae in a Kenyan highland. *Med Vet Entomol.* 2004;18: 301-305. doi:10.1111/j.0269-283X.2004.00503.x
310. Nowicki P, Bonelli S, Barbero F, Balletto E. Relative importance of density-dependent regulation and environmental stochasticity for butterfly population dynamics. *Oecologia.* 2009;161: 227-239. doi:10.1007/s00442-009-1373-2
311. Charlwood JD. May the force be with you: measuring mosquito fitness in the field. *Ecol Asp Appl Genet Modif Mosquitoes.* 2003;2: 47-62.
312. Henderson PA, Magurran AE. Direct evidence that density-dependent regulation underpins the temporal stability of abundant species in a diverse animal community. *Proc R Soc B Biol Sci.* 2014;281. doi:10.1098/rspb.2014.1336
313. Mweresa CK, Omusula P, Otieno B, van Loon JJA, Takken W, Mukabana WR. Molasses as a source of carbon dioxide for attracting the malaria

- mosquitoes *Anopheles gambiae* and *Anopheles funestus*. *Malar J.* 2014;13: 160. doi:10.1186/1475-2875-13-160
314. Beier JC, Copeland R, Oyaró C, Masinya a, Odago WO, Oduor S, et al. *Anopheles gambiae* complex egg-stage survival in dry soil from larval development sites in western Kenya. *J Am Mosq Control Assoc.* 1990;6: 105-109.
315. Paaijmans KP, Heinig RL, Seliga RA, Blanford JI, Blanford S, Murdock CC, et al. Temperature variation makes ectotherms more sensitive to climate change. *Glob Chang Biol.* 2013;19: 2373-2380. doi:10.1111/gcb.12240
316. Blanford JI, Blanford S, Crane RG, Mann ME, Paaijmans KP, Schreiber K V, et al. Implications of temperature variation for malaria parasite development across Africa. *Sci Rep.* 2013;3: 1300. doi:10.1038/srep01300
317. Paaijmans KP, Thomas MB. The influence of mosquito resting behaviour and associated microclimate for malaria risk. *Malar J.* 2011;10: 183. doi:10.1186/1475-2875-10-183
318. Kirby MJ, Lindsay SW. Effect of temperature and inter-specific competition on the development and survival of *Anopheles gambiae sensu stricto* and *An. arabiensis* larvae. *Acta Trop.* 2009;109: 118-123. doi:10.1016/j.actatropica.2008.09.025
319. Paaijmans KP, Blanford S, Bell AS, Blanford JI, Read AF, Thomas MB. Influence of climate on malaria transmission depends on daily temperature variation. *Proc Natl Acad Sci U S A.* 2010;107: 15135-15139. doi:10.1073/pnas.1006422107
320. Gelman A, Jakulin A, Pittau MG, Su YS. A weakly informative default prior distribution for logistic and other regression models. *Ann Appl Stat.* 2008;2: 1360-1383. doi:10.1214/08-AOAS191
321. Plummer M, Best N, Cowles K, Vines K. CODA: Convergence Diagnosis and Output Analysis for MCMC. *R News.* 2006.
322. Gelman A, Rubin DB. Inference from iterative simulation using multiple sequences. *Stat Sci.* 1992. doi:10.1214/ss/1177011136
323. Spiegelhalter DJ, Best NG, Carlin BP, Linde A van der. Bayesian Measures of Model Complexity and Fit. *J R Stat Soc Ser C, Appl Stat.* 2002;64: 583-639.
324. Smith T, Charlwood JD, Takken W, Tanner M, Spiegelhalter DJ. Mapping the densities of malaria vectors within a single village. *Acta Trop.* 1995;59:

- 1-18. doi:10.1016/0001-706X(94)00082-C
325. Zhou G, Munga S, Minakawa N, Githeko AK, Yan G. Spatial relationship between adult malaria vector abundance and environmental factors in western Kenya highlands. *Am J Trop Med Hyg.* 2007;77: 29-35. doi:77/1/29 [pii]
326. Muriu SM, Coulson T, Mbogo CM, Godfray HCJ. Larval density dependence in *Anopheles gambiae* s.s., the major African vector of malaria. Boots M, editor. *J Anim Ecol.* 2013;82: 166-174. doi:10.1111/1365-2656.12002
327. Yang GJ, Brook BW, Whelan PI, Cleland S, Bradshaw CJA. Endogenous and exogenous factors controlling temporal abundance patterns of tropical mosquitoes. *Ecol Appl.* 2008;18: 2028-2040. doi:10.1890/07-1209.1
328. Hancock PA, White VL, Callahan AG, Godfray CHJ, Hoffmann AA, Ritchie SA. Density-dependent population dynamics in *Aedes aegypti* slow the spread of wMel Wolbachia. *J Appl Ecol.* 2016;53: 785-793. doi:10.1111/1365-2664.12620
329. Tuno N, Githeko A, Yan G, Takagi M. Interspecific variation in diving activity among *Anopheles gambiae* Giles, *An. arabiensis* Patton, and *An. funestus* Giles (Diptera: Culicidae) larvae. *J Vector Ecol.* 2007;32: 112-117. doi:10.3376/1081-1710(2007)32[112:ividaa]2.0.co;2
330. Zengenene MP, Munhenga G, Okumu F, Koekemoer LL. Effect of larval density and additional anchoring surface on the life-history traits of a laboratory colonized *Anopheles funestus* strain. *Med Vet Entomol.* 2022;36: 168-175. doi:10.1111/MVE.12563
331. Matthiopoulos J. How to be a Quantitative Ecologist: The “A to R” of Green Mathematics and Statistics. *How to be a Quantitative Ecologist: The “A to R” of Green Mathematics and Statistics.* Wiley; 2011. doi:10.1002/9781119991595
332. Newman KB, Buckland ST, Morgan BJT, King R, Borchers DL, Cole DJ, et al. *Modelling Population Dynamics.* New York, NY: Springer New York; 2014. doi:10.1007/978-1-4939-0977-3
333. Martens P, Kovats RS, Nijhof S, De Vries P, Livermore MTJ, Bradley DJ, et al. Climate change and future populations at risk of malaria. *Global Environmental Change.* Pergamon; 1999. pp. S89-S107. doi:10.1016/S0959-3780(99)00020-5
334. Lindsay SW, Birley MH. Climate change and malaria transmission. *Annals of*

- Tropical Medicine and Parasitology. Taylor & Francis; 1996. pp. 573-588. doi:10.1080/00034983.1996.11813087
335. Tian H, Li N, Li Y, Kraemer MUG, Tan H, Liu Y, et al. Malaria elimination on Hainan Island despite climate change. *Commun Med.* 2022;2. doi:10.1038/s43856-022-00073-z
 336. Lubinda J, Haque U, Bi Y, Hamainza B, Moore AJ. Near-term climate change impacts on sub-national malaria transmission. *Sci Rep.* 2021;11. doi:10.1038/s41598-020-80432-9
 337. Smith T, Maire N, Ross A, Penny M, Chitnis N, Schapira A, et al. Towards a comprehensive simulation model of malaria epidemiology and control. *Parasitology.* 2008;135: 1507-1516. doi:10.1017/S0031182008000371
 338. Kiware SS, Chitnis N, Moore SJ, Devine GJ, Majambere S, Merrill S, et al. Simplified Models of Vector Control Impact upon Malaria Transmission by Zoophagic Mosquitoes. [cited 13 May 2022]. doi:10.1371/journal.pone.0037661
 339. Smith DL, Dushoff J, McKenzie FE. The Risk of a Mosquito-Borne Infection in a Heterogeneous Environment. *PLOS Biol.* 2004;2: e368. doi:10.1371/JOURNAL.PBIO.0020368
 340. Kristan M, Abeku TA, Beard J, Okia M, Rapuoda B, Sang J, et al. Variations in entomological indices in relation to weather patterns and malaria incidence in East African highlands: implications for epidemic prevention and control. *Malar J.* 2008;7: 231. doi:10.1186/1475-2875-7-231
 341. Chirebvu E, Chimbari MJ. Characteristics of *Anopheles arabiensis* larval habitats in Tubu village, Botswana. *J Vector Ecol.* 2015;40: 129-138. doi:10.1111/jvec.12141
 342. Scheffer M, Carpenter S, Foley JA, Folke C, Walker B. Catastrophic shifts in ecosystems. *Nature.* 2001;413: 591-596.
 343. Gillies MT. Studies on the dispersion and survival of *Anopheles gambiae* Giles in East Africa, by means of marking and release experiments. *Bull Entomol Res.* 1961;52: 99-127. doi:10.1017/S0007485300055309
 344. Castañera MB, Aparicio JP, Gürtler RE. A stage-structured stochastic model of the population dynamics of *Triatoma infestans*, the main vector of Chagas disease. *Ecol Modell.* 2003;162: 33-53. doi:10.1016/S0304-3800(02)00388-5
 345. Schmidt FL, Oh IS, Hayes TL. Fixed- versus random-effects models in meta-

- analysis: Model properties and an empirical comparison of differences in results. *Br J Math Stat Psychol.* 2009;62: 97-128. doi:10.1348/000711007X255327
346. Kulkarni M a, Kweka E, Nyale E, Lyatuu E, Mosha FW, Chandramohan D, et al. Entomological evaluation of malaria vectors at different altitudes in Hai district, northeastern Tanzania. *J Med Entomol.* 2006;43: 580-588. doi:10.1603/0022-2585(2006)43[580:EEOMVA]2.0.CO;2
347. Smith T, Charlwood JD, Kihonda J, Mwankusye S, Billingsley P, Meuwissen J, et al. Absence of seasonal variation in malaria parasitaemia in an area of intense seasonal transmission. *Acta Trop.* 1993;54: 55-72. doi:10.1016/0001-706X(93)90068-M
348. Charlwood JD, Smith T, Kihonda J, Heiz B, Billingsley PF, Takken W. Density independent feeding success of malaria vectors (Diptera: Culicidae) in Tanzania. *Bull Entomol Res.* 1995;85: 29-35. doi:10.1017/S0007485300051981
349. Navarro D, Foxcroft D. Learning statistics with Jamovi: A tutorial for psychology students and other beginners (Version 0.75). *Gastronomía ecuatoriana y turismo local.* 2022. Available: <http://www.learnstatswithjasp.com>
350. Richard A, Morey D, Rouder JN, Jamil T, Forner K, Ly A, et al. Package “BayesFactor.” 2022. Available: <https://richarddmorey.github.io/BayesFactor/>
351. Lehmann T, Dao A, Yaro AS, Adamou A, Kassogue Y, Diallo M, et al. Aestivation of the African malaria mosquito, *Anopheles gambiae* in the Sahel. *Am J Trop Med Hyg.* 2010;83: 601-6. doi:10.4269/ajtmh.2010.09-0779
352. Taylor CE, Toure YT, Coluzzi M, Petrarca V. Effective population size and persistence of *Anopheles arabiensis* during the dry season in west Africa. *Med Vet Entomol.* 1993;7: 351-357. Available: <http://www.ncbi.nlm.nih.gov/pubmed/8268490>
353. Kaiser ML, Duncan FD, Brooke BD. Embryonic development and rates of metabolic activity in early and late hatching eggs of the major malaria vector *Anopheles gambiae*. *PLoS One.* 2014;9: 1-15. doi:10.1371/journal.pone.0114381
354. Dao A, Yaro AS, Diallo M, Timbine S, Huestis DL, Kassogue Y, et al.

- Signatures of aestivation and migration in Sahelian malaria mosquito populations. *Nature*. 2014;516: 387-390. doi:10.1038/nature13987
355. Focks DA, Haile DG, Daniels E, Mount GA. Dynamic life table model for *Aedes aegypti* (Diptera: Culicidae): Simulation and validation. *J Med Entomol*. 1993;30: 1018-1028. doi:10.1093/jmedent/30.6.1018
356. Focks DA, Daniels E, Haile DG, Keesling JE. A simulation model of the epidemiology of urban dengue fever: Literature analysis, model development, preliminary validation, and samples of simulation results. *Am J Trop Med Hyg*. 1995;53: 489-506. doi:10.4269/ajtmh.1995.53.489
357. Focks DA, Haile DG, Daniels E, Mount GA. Dynamic life table model for *Aedes aegypti* (Diptera: Culicidae): analysis of the literature and model development. *J Med Entomol*. 1993;30: 1003-1017. doi:10.1093/JMEDENT/30.6.1003
358. Koenraadt CJ, Paaijmans KP, Githeko AK, Knols BG, Takken W. Egg hatching, larval movement and larval survival of the malaria vector *Anopheles gambiae* in desiccating habitats. 2003 [cited 25 Apr 2022]. Available: <http://www.malariajournal.com/content/2/1/20>
359. Killeen G, Knols B, Gu W. Taking malaria transmission out of the bottle: Implications of mosquito dispersal for vector-control interventions. *Lancet Infect Dis*. 2003;3.
360. WHOPEP. Guidelines for laboratory and field testing of mosquito larvicides. World Heal Organ. 2005; 1-41.
361. Drakeley C, Schellenberg D, Kihonda J, Sousa C a., Arez a. P, Lopes D, et al. An estimation of the entomological inoculation rate for Ifakara: A semi-urban area in a region of intense malaria transmission in Tanzania. *Trop Med Int Heal*. 2003;8: 767-774. doi:10.1046/j.1365-3156.2003.01100.x
362. Christiansen-Jucht C, Erguler K, Shek CY, Basáñez MG, Parham PE. Modelling *Anopheles gambiae* s.s. Population Dynamics with Temperature- and Age-Dependent Survival. *Int J Environ Res Public Heal* 2015, Vol 12, Pages 5975-6005. 2015;12: 5975-6005. doi:10.3390/IJERPH120605975
363. Agyekum TP, Arko-Mensah J, Botwe PK, Hogarh JN, Issah I, Dwomoh D, et al. Effects of elevated temperatures on the development of immature stages of *Anopheles gambiae* (s.l.) mosquitoes. *Trop Med Int Heal*. 2022;27: 338-346. doi:10.1111/TMI.13732
364. Homan T, Hiscox A, Mweresa CK, Masiga D, Mukabana WR, Oria P, et al.

- The effect of mass mosquito trapping on malaria transmission and disease burden (SolarMal): a stepped-wedge cluster-randomised trial. *Lancet*. 2016;388: 1193-1201. doi:10.1016/S0140-6736(16)30445-7
365. Service MW. A critical review of procedures for sampling populations of adult mosquitoes. *Bull Entomol Res*. 1977;67: 343-382. doi:10.1017/S0007485300011184
366. Auger-méthé M, Newman K, Cole D, Empacher F, Gryba R, King AA, et al. A guide to state-space modeling of ecological time series. *Ecol Monogr*. 2021;91: e01470. doi:10.1002/ECM.1470
367. Okumu F, Moore S. Combining indoor residual spraying and insecticide-treated nets for malaria control in Africa: A review of possible outcomes and an outline of suggestions for the future. *Malaria Journal*. BioMed Central; 2011. pp. 1-13. doi:10.1186/1475-2875-10-208
368. Onyango S a, Kitron U, Mungai P, Muchiri EM, Kokwaro E, King CH, et al. Monitoring malaria vector control interventions: effectiveness of five different adult mosquito sampling methods. *J Med Entomol*. 2013;50: 1140-51. doi:10.1603/ME12206